

Molecular Mechanism of Actin Filament Elongation
by Ena/VASP Proteins

Von der Naturwissenschaftlichen Fakultät
der Gottfried Wilhelm Leibniz Universität Hannover
zur Erlangung des Grades
DOKTOR DER NATURWISSENSCHAFTEN
Dr. rer. nat.

genehmigte Dissertation
von

Dipl.-Biochem. Dennis Breitsprecher
geboren am 01.03.1981, in Einbeck

2010

Referent: PD Dr. Jan Faix
Korreferentin: Prof. Dr. Theresia Stradal
Tag der Promotion: 31.05.2010

Danksagung

Mein besonderer Dank gilt Herrn PD Dr. Jan 'Hans' Faix, der mir dieses anspruchsvolle und überaus interessante Projekt anvertraute und damit meine Faszination für die Vielfältigkeit der Zellbiologie und insbesondere für die Dynamik des Zytoskeletts entfachte. Dank ihm werde ich wohl auch in Zukunft so manche Stunde an diversen Mikroskopen verbringen und auch weiterhin der Erforschung des Zytoskeletts treu bleiben. Ich danke ihm für seine ständige Diskussionsbereitschaft und seine vorbildliche, unerschütterliche Motivation.

Frau Prof. Dr. Theresia Stradal danke ich herzlich für die Übernahme des Koreferats. Prof Dr. Bernard Huchzermeyer danke ich für die Übernahme des Prüfungsvorsitzes.

Besonderer Dank gebührt den Mitgliedern meiner Arbeitsgruppe, Antje Kiese Wetter, Jörn Linkner, Annette Breskott und Benjamin Nordholz, die stets durch Rat und Tat zu unterstützen wussten. Desweiteren danke ich Prof. Dr. Claus Urbanke und der Arbeitsgruppe von PD Dr. Ute Curth für hilfreiche Diskussionen zu biophysikalischen Fragen und viele kritische Denkanstöße, sowie Dr. Igor Chizhov für seine Hilfsbereitschaft und seinen großen Sachverstand wenn das TIRF-Mikroskop mal wieder nicht so wollte wie ich.

Außerdem danke ich Prof. Dr. Dietmar Manstein für die Möglichkeit, diese Arbeit in dem hervorragend ausgestatteten Institut für Biophysikalische Chemie anfertigen zu können.

Desweiteren möchte ich Dr. Klemens Rottner, Prof. Dr. Theresia Stradal, Dr. Nagendran Ramalingam, Prof. Dr. Michael Schleicher, Prof. Vic Small und Kai Schlüter für hervorragende, inspirierende Kollaborationen danken, ohne die die Wissenschaft nur halb so viel Freude bringen würde. In diesem Zuge möchte ich auch der Deutschen Forschungsgemeinschaft (DFG) danken, da erst deren Förderung diese Arbeit ermöglicht hat.

Weiterer Dank gilt auch den anderen Mitgliedern des Instituts für Biophysikalische Chemie, die ich nicht namentlich erwähnt habe, die jedoch auch ein Stück zum Erfolg beigetragen haben.

Meinen Eltern Sigrun und Hans-Jürgen gebührt besonderer Dank für ihre uneingeschränkte, bedingungslose Unterstützung in sämtlichen Lebenslagen.

Mein allergrößter Dank gilt meiner Frau Antje und meinem Sohn Mathis, denn welches Glück kann größer sein?

“If something is worth doing, it’s worth doing well.”
Annegret Domke

Zusammenfassung

Der dynamische Umbau des Aktin-Zytoskeletts ist für eine Vielzahl zellulärer Prozesse wie der Endozytose, der Zytokinese und der Zellbewegung verantwortlich. Proteine der *Enabled/vasodilator-stimulated phosphoprotein* (Ena/VASP) Familie werden in allen motilen eukaryotischen Zellen exprimiert und sind nachweislich wichtige Regulatoren der Aktinpolymerisation in Aktin-reichen Zellfortsätzen wie Lamellipodien und Filopodien. Obwohl Ena/VASP Proteine bereits vor mehr als 2 Jahrzehnten entdeckt wurden, wird die Wirkungsweise dieser Proteine auf die Aktinpolymerisation nach wie vor sehr kontrovers diskutiert.

In dieser Arbeit wurde durch Analyse des Wachstums einzelner Aktinfilamente durch *in vitro* TIRF-Mikroskopie und spektroskopische Methoden der molekulare Mechanismus von Ena/VASP Proteinen während der Filamentelongation entschlüsselt. Es konnte gezeigt werden, dass verschiedene Ena/VASP Proteine aus Säugern und *Dictyostelium* (hVASP, EVL, Mena und DdVASP) die Elongationsrate von Aktinfilamenten *in vitro* aktiv beschleunigen – dies allerdings in sehr unterschiedlichem Maße. Während dieses Prozesses sind Ena/VASP Proteine jedoch nicht wie Formine prozessiv mit dem schnell wachsenden Ende des Filaments verbunden. Stattdessen binden sie das Filamentende nur transient, transferieren ihre gebundenen Aktin Untereinheiten und bleiben anschließend an der Seite des Filaments haften während das Filamentende wieder spontan weiter elongiert werden kann. Aus diesem Grund kann das Wachstum der Aktinfilamente in Gegenwart von Ena/VASP effizient durch *Capping* Proteine (CP) terminiert werden. Besonders bemerkenswert war der Befund, dass das *Clustering* von VASP an Oberflächen zu prozessivem Filamentwachstum führt, welches dann seinerseits *de facto* nicht mehr durch CP inhibiert werden kann. Wir nehmen an, dass dieses Szenario den *in vivo* Zustand bei der Ausbildung von Lamellipodien und Filopodien widerspiegelt. Außerdem konnte in dieser Arbeit gezeigt werden, dass zwei WH2-ähnliche Aktin-Bindungsmotive, die G- und F-Aktin Bindestelle (GAB und FAB), für die beschleunigte Aktinpolymerisation verantwortlich sind, wobei die FAB darüber hinaus essentiell für die CP-Resistenz ist. Die detaillierte biochemische Analyse der GAB/Aktin Interaktion zeigte, dass dieses WH2-Bindungsmotiv aus dem schnell elongierenden DdVASP eine mehr als 1000-fach höhere Affinität zu G-Aktin als die GAB des langsam elongierenden hVASP besitzt, was auf einen direkten Zusammenhang zwischen der G-Aktin-Bindung und der Elongationsrate hindeutete. Zur Untermauerung dieser Hypothese wurde die GAB aus hVASP durch WH2-Motive anderer Proteine mit jeweils unterschiedlichen Aktin-Affinitäten ersetzt. Tatsächlich zeigten die Aktinfilament-Elongationsraten der konstruierten Proteinchimären eine direkte Korrelation mit der Aktin-Affinität ihrer WH2-Motive. Auf der Grundlage dieser Arbeit konnte so ein allgemeingültiger, auf G-Aktin-Rekrutierung beruhender Elongationsmechanismus der Ena/VASP-vermittelten Aktinpolymerisation formuliert werden, der voraussagt, dass Ena/VASP Proteine bei vorliegenden Aktinkonzentrationen von mehreren hundert μM in der Zelle effektive Filamentelongatoren sind, da unter diesen Bedingungen alle G-Aktin Bindestellen saturiert sind.

Schlagwörter: Aktin-Zytoskelett, TIRF-Mikroskopie, Elongationsfaktor.

Abstract

The dynamic rearrangement of the actin cytoskeleton triggers a plethora of cellular processes like endocytosis, cytokinesis and cell migration. Proteins of the Enabled/vasodilator-stimulated phosphoprotein family (Ena/VASP) are ubiquitously found in motile eukaryotic cells and are known to be critical regulators of actin assembly in actin-rich cell protrusions such as lamellipodia and filopodia. Although these proteins are already known for more than two decades, there is still considerable controversy regarding their precise effects on actin assembly.

We therefore analyzed the molecular mechanism by which Ena/VASP proteins from mammalian cells and *Dictyostelium discoideum* affect the assembly of single actin filaments using state-of-the-art *in vitro* TIRF microscopy and spectroscopic approaches to reconcile the long lasting inconsistencies in the field. We found that Ena/VASP members from mammals and *Dictyostelium* (hVASP, EVL, Mena and DdVASP) directly enhance the elongation rate of single actin filaments in polymerization assays, albeit to very different extents. During elongation, Ena/VASP is not processively associated with the growing end of the filament like a formin, but it only transiently binds to the end, transfers its bound actin subunits and subsequently stays attached to the side of the growing filament. Thus, this filament elongation process can be readily inhibited by capping proteins (CP) in solution. Most notably, clustering of Ena/VASP on a surface drastically changed its mode of action, now triggering processive filament elongation that became virtually resistant to CP, and hence possibly mimicking the role of Ena/VASP at the leading edge of migrating cells. We also found that the filament-elongation activity relies on two WH2 domain-related actin-binding sites within the C-terminal part of the protein, namely the G- and F-actin-binding sites (GAB and FAB), and showed that the FAB is crucial for CP resistance. Biochemical analysis of the actin/GAB interaction revealed that the actin affinity of the GAB from the fast elongating *Dictyostelium* orthologue is more than three orders of magnitude higher than that of the slow elongating mammalian counterpart, suggesting that the actin affinity of the GAB might determine the VASP-mediated elongation rate *in vitro*. Consistent with this hypothesis, replacement of the GAB motif of hVASP by related WH2 domains from other proteins with different actin affinities in fact showed a direct correlation between their affinity to G-actin and the mediated elongation rates. These results allow us to formulate a general, affinity-based mechanism for fast and processive Ena/VASP-mediated actin assembly, suggesting that all Ena/VASP family members are equally potent filament elongators at physiological actin concentrations in the range of hundreds of μM in the leading edge of the migrating cell since all actin-binding sites are saturated under these conditions.

Keywords: actin cytoskeleton, TIRF-microscopy, elongation factor.

| | |
|---|----|
| 1. Introduction | 1 |
| 1.1 The cytoskeleton | 1 |
| 1.1.1 Actin..... | 2 |
| 1.1.2. Actin structure..... | 2 |
| 1.1.3. Biochemical properties of actin..... | 4 |
| 1.1.4. Cellular actin structures | 5 |
| 1.1.5. Actin-binding proteins in the leading edge of the cell | 7 |
| 1.1.6. ADF/Cofilin | 10 |
| 1.1.6.1. Biochemical properties of ADF/cofilin..... | 10 |
| 1.1.6.2. Function and regulation of ADF/cofilin <i>in vivo</i> | 11 |
| 1.1.7. Formins..... | 12 |
| 1.1.7.1. Biochemical and structural properties of formins..... | 13 |
| 1.1.7.2. Cellular localization and regulation of formins | 15 |
| 1.1.8. The Thymosin β 4/WH2 motif | 16 |
| 1.1.9. Ena/VASP proteins..... | 20 |
| 1.1.9.1. Biochemical and structural properties of Ena/VASP proteins..... | 21 |
| 1.1.9.2. Cellular localization and function of Ena/VASP proteins | 23 |
| 1.1.10. Models of actin-based protrusion | 26 |
| 1.1.11. Biochemical approaches to study actin dynamics <i>in vitro</i> | 29 |
| 1.1.11.1. Pyrenyl-actin assays..... | 29 |
| 1.1.11.2. Biomimetic motility assays..... | 30 |
| 1.1.11.3. <i>In vitro</i> TIRF microscopy..... | 31 |
| 2. Results | 33 |
| 2.1. Manuscript 1: Analysis of Actin Assembly by <i>In vitro</i> TIRF Microscopy | 33 |
| 2.2. Manuscript 2: Arp2/3 complex interactions and actin network turnover in lamellipodia | 34 |
| 2.3. Manuscript 3: Clustering of VASP actively drives processive, WH2 domain-mediated actin assembly..... | 35 |
| 2.4. Manuscript 4: Filopodia: Complex models for simple rods | 36 |

| | |
|--|----|
| 2.5. Manuscript 5: Affinity-based mechanism of fast Ena/VASP-mediated actin filament elongation..... | 37 |
| 2.5.1. Introduction..... | 37 |
| 2.5.2. Results..... | 39 |
| 2.5.2.1. VASP, Mena and EVL enhance filament elongation to similar extends. | 39 |
| 2.5.2.2. Replacement of the GAB and FAB motifs of hVASP with those from DdVASP reveal the molecular requirement for fast filament elongation. | 41 |
| 2.5.2.3. The GAB motifs from hVASP and DdVASP display drastically different affinities to G-actin..... | 44 |
| 2.5.2.4. Replacement of the GAB of hVASP by high-affinity actin-binding WH2-motifs reveals the general mechanism of VASP mediated actin assembly. | 46 |
| 2.5.2.5. Nucleation properties of VASP and VASP-chimeras..... | 49 |
| 2.5.3. Discussion | 52 |
| 2.5.4. Material and methods..... | 59 |
| 2.6. Contributions | 62 |
| 3. Discussion..... | 63 |
| 3.1. <i>In vitro</i> TIRF microscopy as a tool for the biochemical characterization of actin filament dynamics | 63 |
| 3.2. Advantages and limitations of <i>in vitro</i> TIRF microscopy on single actin filaments | 64 |
| 3.3. Analysis of VASP-mediated actin assembly – a history of controversies..... | 67 |
| 3.3.1. Nucleation activity of Ena/VASP proteins..... | 68 |
| 3.3.2. Elongation activity of Ena/VASP proteins..... | 70 |
| 3.3.3. Anti-capping activity of Ena/VASP proteins..... | 72 |
| 3.4. Conclusions and outlook | 73 |
| 4. References..... | 77 |
| Curriculum vitae | 87 |
| Publications and presentations | 88 |

1. Introduction

1.1 The cytoskeleton

The cytoskeleton is a main feature of eukaryotic cells. It consists of an extensive network of filamentous proteins which organize intracellular structure and cell shape and are implicated in many important cellular processes. The fast remodeling of cytoskeletal polymers is required for directed movement of the cell and its interaction with the environment. The major components of the cytoskeleton are microtubules, intermediate filaments and actin filaments (Figure 1). Actin filaments are thin filaments with a diameter of 7 nm that undergo rapid polymerization and depolymerization (Figure 1A). They are responsible for the overall cell shape and mediate a multitude of cellular processes such as cytokinesis, cell migration as well as endo- and exocytosis, and constitute tracks for myosin motor proteins. Actin binds and hydrolyses ATP, which regulates the lifetime of actin filaments. Microtubules (MT) consist of α - and β -tubulin dimers that polymerize into stiff, hollow cylindrical filaments with a diameter of 25 nm (Figure 1B). They arise from the so called microtubule organizing center (MTOC) and are implicated in mitosis, vesicle transport and cytokinesis, and constitute tracks for kinesin and dynein motor proteins. Tubulin binds and hydrolyses GTP, which regulates microtubule lifetime. Intermediate filaments are heterogeneous protein fibers that consist of different classes of proteins like keratins, desmins and lamins, which are responsible for the tensile strength and overall shape of the cell (Figure 1C). In contrast to microtubules and actin filaments, intermediate filaments do not bind nucleotides and also lack polarity; hence no motor proteins for this filament class are known. Moreover, the turnover and assembly of intermediate filaments is much slower, which makes them the most static component of the cytoskeleton.

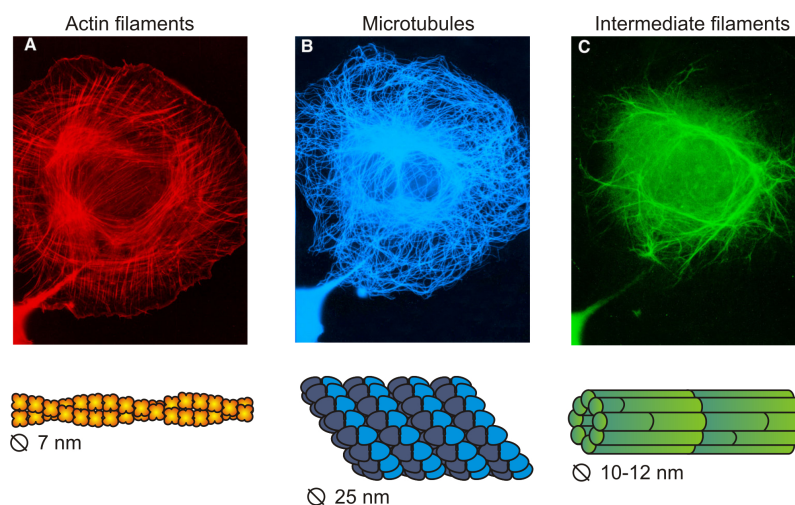


Figure 1: Components of the eukaryotic cytoskeleton. The eukaryotic cytoskeleton consists of actin filaments (A), microtubules (B) and intermediate filaments (C), which localize to different sides of the cell and contribute differently to cellular architecture and function. Images were taken from <http://cellix.imba.oeaw.ac.at>.

1.1.1 Actin

Actin is a disk-shaped 43 kDa protein, and is the most abundant protein among all eukaryotes, representing roughly 10% of total protein in the cell, and about 30-40% in muscle cells. It is highly conserved in different species, differing by not more than 20% in its amino-acid composition even in evolutionary distant organisms. Despite its ubiquitous presence in all eukaryotic cells, it was discovered rather late in the 1940s in muscle tissue and found to be the major component of the cytoskeleton in non-muscle cells even twenty years later (Hatano and Oosawa, 1966; Ishikawa et al., 1969). While lower eukaryotes like *Saccharomyces cerevisiae* and *Schizosaccharomyces pombe* have only one actin gene, different actin isoforms that are encoded by different genes are present in higher eukaryotes: α -actin isoforms are found in muscle, whereas β - and γ -isoforms coexist in other cell types and are implicated in the formation of different cytoskeletal structures. β -actin is the major actin isoform in protrusive structures like lamellipodia and filopodia, whereas γ -actin is enriched in stress fibers (Hooek et al., 1991; Tondeleir et al., 2009). There are 6 actin genes in man, 10 in *Arabidopsis thaliana*, 35 in mouse and 33 in *Dictyostelium discoideum* (Vandekerckhove et al., 1978; Joseph et al., 2008; Schleicher et al., 2008).

1.1.2. Actin structure

The actin monomer consists of four subdomains (1-4) with a nucleotide-binding cleft in-between subdomain 2 and 4 at the so-called minus- or “pointed” end. Actin binds ATP or ADP complexed with a divalent cation, mostly Mg^{2+} or Ca^{2+} (Figure 2). Subdomains 1 and 3 mark the so called plus- or “barbed” end of the protein.

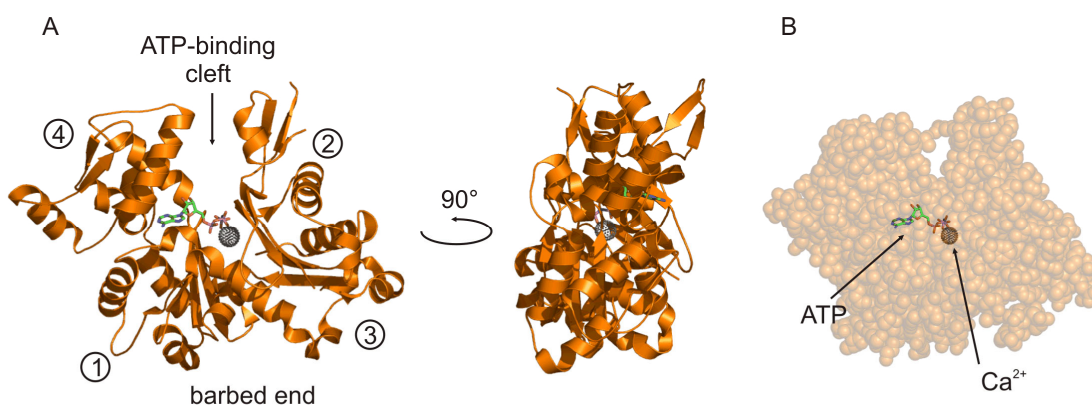


Figure 2: Structure of Ca-ATP-G-actin. (A) Molecular model of G-actin. The disk shaped actin monomer consists of four subdomains, with subdomain 1 and 3 forming the barbed- and 2 and 4 the pointed end. The ATP-binding cleft is located in-between subdomains 2 and 4 at the pointed end. (B) Actin binds ATP and a bivalent cation, in this case Ca^{2+} , in its ATP-binding cleft. PDB code: 1NWK.

The most remarkable property of actin is its ability to polymerize into double-helical, semi-flexible filaments (filamentous or F-actin) with a diameter of approximately 7 nm and a relatively large persistence length of 10 to 20 μm (Holmes et al., 1990; De La Cruz et al., 2000; Ismabert et al., 1995). 13 actins subunits form one turn, corresponding to a length of 35.7 nm. Due to the polarity of the monomer, the actin filament ends differ in their polymerization kinetics (see below). EM-analysis of isolated actin filaments decorated with the actin-binding heads of Myosin II revealed that both ends elongate with different rates (Pollard and Mooseker, 1981). These experiments were also eponymous for the ends of the actin filament, which were named the (fast growing) barbed end and the (slow growing) pointed end (see below) due to the arrowhead-like appearance of the Myosin II decorated actin filament.

Although the first structures of monomeric actin (globular or G-actin) in complex with the actin sequestering protein DNaseI were derived 1990 by Mannherz and colleagues, a detailed model for F-actin with atomic resolution was unavailable for a long time. The most popular model was the frequently refined “Holmes model” of F-actin, which combined data from fiber-diffraction and EM experiments as well as the atomic model of G-actin (Holmes et al., 1990; Lorenz et al., 1993; Lorenz et al., 1995). Recently, a more detailed structure with a 3Å resolution of the actin filament was derived by fiber-diffraction, showing that the actin monomer undergoes a considerable conformational change upon polymerization, resulting in a 20° tilt of subdomain 4 that leads to a much flatter appearance of the filament than initially proposed (Oda et al., 2009, Figure 3).

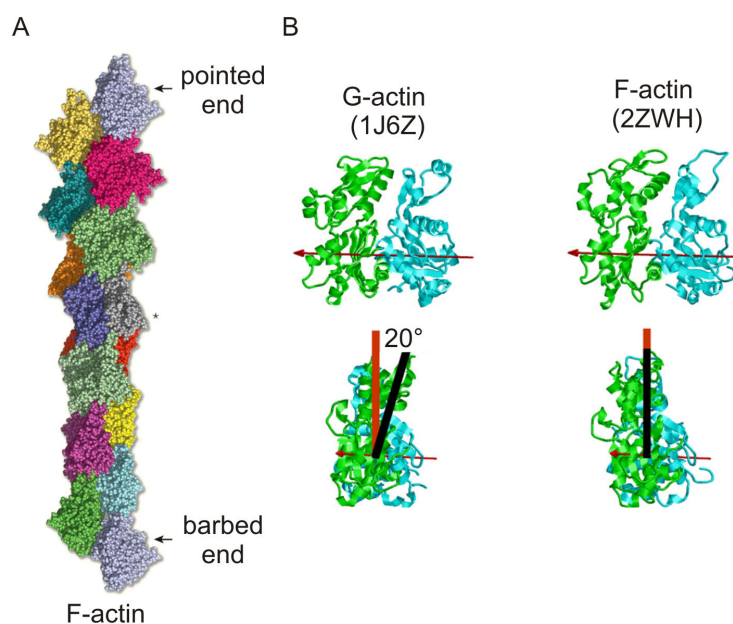


Figure 3: Structure of F-actin. (A) Molecular model of F-actin, showing one entire turn in the actin-helix. (B) Comparison of the molecular models of G- and F-actin. Note that subdomains 2 and 4 are tilted towards the filament axis in F-actin, resulting in a flattened structure of the actin subunit within the filament. (From Oda et al., 2009). PDB codes are indicated in the figure.

1.1.3. Biochemical properties of actin

Actin polymerizes spontaneously in the presence of mM amounts of monovalent and divalent cations. Since actin is a highly negatively charged protein (charge = -11.1 at pH 7), it is possible to obtain G-actin *in vitro* by using buffers with very low ionic strengths lacking Na⁺ or K⁺ ions at a slightly basic pH. Addition of mM amounts of K⁺-salts or, rarely used, lowering of the pH, results in compensation of the negative charges of the actin monomers and triggers spontaneous polymerization into filaments. The formation of actin filament nuclei is, however, energetically disadvantageous, since actin dimers and trimers easily disassemble into monomers. After a fourth actin subunit is added to an existing trimer, the elongation reaction proceeds until equilibrium is reached (Figure 4).

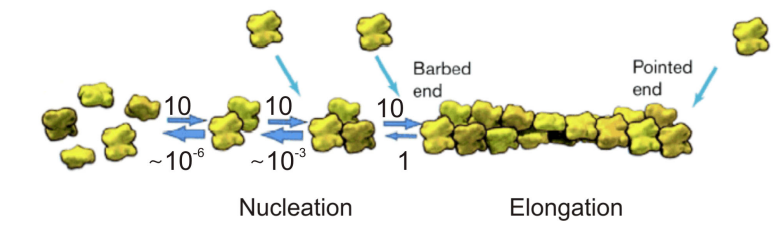


Figure 4: Actin filament nucleation. Actin dimers and trimers easily disassemble into monomers. The formation of an actin seed consisting of 4 subunits favors elongation. Estimated rate constants have units of $\mu\text{M}^{-1}\text{s}^{-1}$ for association and s^{-1} for dissociation reactions (from Pollard and Earnshaw, 2008).

The barbed and the pointed ends of the actin filament grow with different rates, since both ends have very different association and dissociation rates for ATP- and ADP actin (Figure 5). Thus, the critical concentrations ($C_c = k_-/k_+$) for polymerization of ATP-actin at the barbed and pointed end are different, with C_c (barbed) = 0.12 μM and C_c (pointed) = 0.62 μM (Pollard, 1983). For this reason actin monomers are continuously “treadmilling” in equilibrium, with actin monomers being added to the barbed end and released from the pointed end. If only ADP-actin is present, no treadmilling is observed since the critical concentrations for both ends are virtually identical.

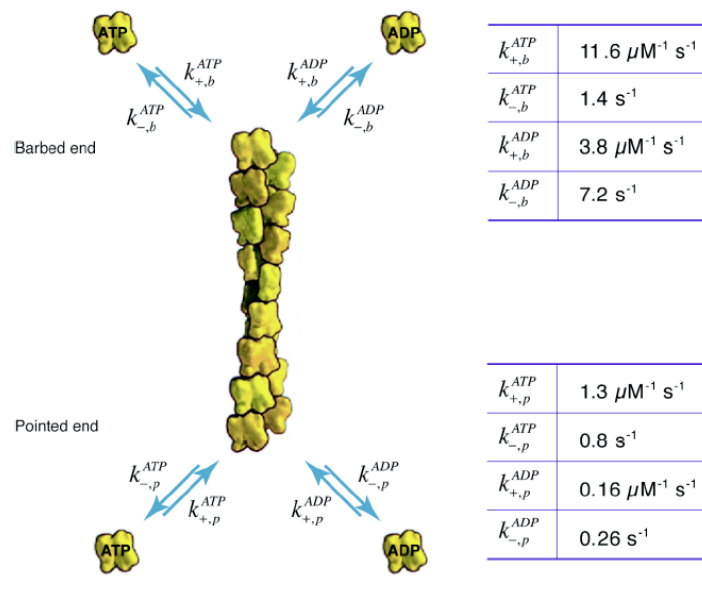


Figure 5: Actin filament elongation kinetics. Rate constants of ATP- and ADP actin association and dissociation to and from the filament ends (from Pollard 1986). Ratios of the rate constants yield the critical concentrations.

When ATP-actin is incorporated into the growing barbed end of the filament, ATP is rapidly hydrolyzed to ADP+P_i in an irreversible process. The lifetime of this ADP+P_i intermediate is quite long, with phosphate-release rates in the range of minutes (Figure 6, Carlier and Pantaloni, 1986). Finally, the γ -phosphate is released from the filament in a reversible reaction. This process discriminates newly polymerized and old filaments *in vivo* and is an important marker for proteins that selectively disassemble filaments, e.g. ADF/cofilin (see below).

| | |
|---------------------|------------------------|
| k (hydrolyse ATP) | 0.35s^{-1} |
| k (dissociation Pi) | 0.0019s^{-1} |

Figure 6: Actin ATPase activity. Comparison of the rates for ATP hydrolysis and γ -phosphate release (from Blanchoin and Pollard, 2002 and Carlier and Pantaloni, 1986)

1.1.4. Cellular actin structures

Actin filaments can be organized into very different cellular structures, each of them contributing to specific functions like membrane protrusion, substrate attachment, contraction or environment sensing.

The leading edge of a migrating cell consists of the lamellipodium, a flat, sheet like structure with a length of a few μm composed of a dense meshwork of actin filaments which point with their barbed ends towards the membrane (Abercrombie et al., 1970a; Small 1988). Lamellipodium sheets that detach from substrata show a distinct, rough appearance and are

referred to as membrane ruffles (Ingram, 1969; Abercrombie *et al.*, 1970b; Harris, 1973). The insertional assembly of actin subunits at the barbed ends of lamellipodial actin filaments and the simultaneous depolymerization at their pointed ends results in protrusion of the plasma membrane (Borisy and Pollard, 2003). However, there is still considerable controversy concerning the overall arrangement of the lamellipodial actin filaments and the mechanism that eventually leads to membrane protrusion (see chapter 1.1.10.; Small *et al.*, 2008; Koestler *et al.*, 2008; Chhabra and Higgs, 2007). Embedded in the lamellipodium, actin filaments are occasionally organized into dense, parallel bundles – so called filopodia - that protrude from the leading edge and form spiky, finger-like extensions of several μm in length (Figure 7, left). Filopodia consist of up to 50 actin filaments and are 100 – 300 nm in diameter (Small *et al.*, 2002; Faix and Rottner, 2006; Matilla and Lappalainen, 2007). Some cell types contain similar structures that are almost entirely embedded in the lamellipodium, which are referred to as microspikes. Filopodia are implicated in many cellular processes: They mediate substrate attachment via integrins to form initial adhesion sites, they are used as pathogen-sensing organelles by macrophages and dendritic cells and they form precursor structures for dendrite development. Additionally, they are important for nerve growth-cone guidance and are last but not least required for the zippering of epithelial sheets and many phagocytic processes (Matilla and Lappalainen, 2008; Faix *et al.*, 2009).

Besides the parallel filopodial actin bundles, many antiparallel bundles are embedded in a zone behind the protruding lamellipodium – the lamellum –, as well as in the rear of the cell and in the cytokinetic cleavage furrow (Figure 7, right). These structures are referred to as actin arcs, stress fibers (if attached to focal adhesions) and the cytokinetic (contractile) ring, respectively. All of them can mediate contraction by virtue of incorporated myosin motors which produce forces big enough to deform membranes (Naumanen *et al.*, 2008). These contractions are employed to retract the trailing edge of the cell during cell migration and to withstand shear forces in tissues and dividing cells during mitosis.

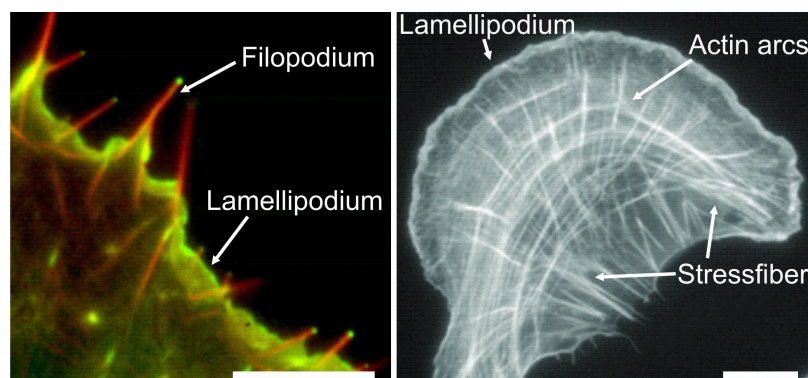


Figure 7: Intracellular actin structures. (left) A fish fibroblast expressing GFP-VASP and mCherry actin shows numerous filopodia emerging from the leading edge. Scale, 2 μm . Courtesy of Vic Small. (right) A TRITC-phalloidin stained U2OS cell shows a network of stress fibers and actin arcs. Scale, 10 μm . Adapted from Naumanen *et al.* (2008).

1.1.5. Actin-binding proteins in the leading edge of the cell

The eukaryotic cell is able to rapidly remodel the actin cytoskeleton upon external and internal signals. Assembly and disassembly of actin filaments at the leading edge of the cell is strictly regulated *in vivo* by a vast number of proteins that interact directly with monomeric and filamentous actin. These proteins can be separated into different classes, depending on their activity and interactions with monomeric or filamentous actin:

- **G-actin sequestering proteins**

Cells have to provide a large amount of unpolymerized, monomeric actin to quickly trigger site-specific polymerization upon external or internal signals (Pollard and Borisy, 2003; Pollard et al., 2000; Pantaloni et al., 2001). Since monomeric actin polymerizes spontaneously at physiological salt concentrations to form F-actin, specialized proteins are necessary to keep actin in its monomeric state (Pollard and Borisy, 2003). The major G-actin sequestering proteins are the small peptide Thymosin β 4 (T β 4) and the ADP-ATP exchange factor profilin (Dominguez, 2007; Jokusch et al., 2007). Profilin is a globular 15 kDa protein that binds the barbed end of actin monomers in a 1:1 complex with μ M affinity, therefore inhibiting the formation of multimeric nucleation seeds and hence polymerization. Besides this function, it also facilitates the exchange of ADP to ATP within the actin monomer to refill the ATP-actin pool of the cell. Profilin is recruited by many proteins containing stretches of poly-proline to sites of active actin assembly (see chapter 1.1.7. and 1.1.9). Thymosin β 4 and its actin-binding mechanism are described in more detail in chapter 1.1.8.

- **Actin nucleation factors**

The initiation of actin polymerization requires the presence of specialized proteins or protein complexes to overcome the kinetic barrier of actin polymerization as well as the inhibitory effect of G-actin sequestering proteins mentioned above. The first identified of these factors referred to as actin nucleators was the Arp2/3 complex (Welch et al., 1997a; Welch et al., 1997b; Machesky et al., 1997). This extraordinary multiprotein complex consists of seven proteins, two of which, ARP2 and ARP3 (*Actin Related Proteins*), closely resemble the structure of actin (Robinson et al., 2001, Schleicher et al., 2008). In a series of stimulating publications, the basic mechanism of Arp2/3 mediated actin nucleation was rapidly revealed: After its activation by so called nucleation promoting factors (NPFs) such as Scar/WAVE (*Suppressor of cyclic AMP receptor mutation and WASP and Verprolin homologous protein*) and WASP proteins (*Wiskott-Aldrich Syndrome Protein*), the Arp2/3 complex binds either a filament barbed end at the tip or the side of a filament and nucleates a new “daughter” filament that starts to grow

from the two actin-related proteins towards the membrane in an Y-shaped angle of approximately 70° (Mullins et al., 1997; Mullins et al., 1998; Welch et al., 1998; Svitkina et al., 1999; Machesky et al., 1999). These findings, in combination with the localization of the Arp2/3 complex at the lamellipodium tip, led to the formulation of the dendritic nucleation model explaining actin-based protrusion (see chapter 1.1.10).

An entirely different nucleating mechanism is accomplished by a relatively new protein family, the formins. These proteins are thought to stabilize the transient dimeric and trimeric actin nucleation seed intermediates by virtue of their dimerized FH2 (*Formin Homology 2*) domain which wraps around the filament barbed end (Pring et al., 2003; Xu et al., 2004; Otomo et al., 2005). Different formin isoforms can be found in a variety of cellular localizations, from the tips of filopodia to the cytokinetic ring (Faix and Grosse, 2006). The mechanism of formin-mediated actin assembly will be described in more detail in chapter 1.1.7.

The most diverse class of filament nucleators is composed of the so called WH2-containing proteins. WH2 motifs (*WASP Homology domain 2*) were first identified in the NPF WASP and are short, T β 4-related peptide sequences of about 20 to 25 amino acid residues that bind actin monomers and filaments (Paunola et al., 2002). Over the last years, many different WH2-containing proteins were identified, and some of them were shown to be very potent actin-filament nucleators (Qualmann and Kessels, 2009). The WH2 motif and the WH2-containing protein VASP will be described in detail in chapters 1.1.8. and 1.1.9.

- **Actin elongation factors**

Over a long period of time, models explaining actin-based protrusion did not consider the possibility that actin filaments might be actively elongated by specialized proteins. The discovery of formins and their subsequent biochemical characterization revealed that these dimeric proteins did not only nucleate new filaments, but also processively “stair stepped” at the tip of the growing barbed end and accelerated filament elongation by delivery of profilin-actin complexes (Goode and Eck, 2007; Chesarone and Goode, 2009). Since this work focuses on the mechanisms of filament elongation factors, formins will be introduced in detail in chapter 1.1.7.

Other proteins that were supposed to accelerate filament elongation are Ena/VASP proteins. These tetrameric proteins harbor G- and F-actin-binding sites, which led to the postulation of an elongation mechanism comparable to the one of formins (Dickinson and Purich, 2002; Ferron et al., 2007). However, most studies only considered theoretical models, and concrete experimental evidence for an active role of Ena/VASP proteins in actin filament elongation was missing (Dickinson and Purich, 2002; Ferron et al., 2007;

Dickinson, 2008). The dissection of the molecular mechanism by which Ena/VASP proteins affect actin filament assembly and the characterization of their biochemical properties constitute an essential part of this work. Ena/VASP proteins will be introduced in detail in chapter 1.1.9.

- **Capping proteins**

Once a new actin filament has been nucleated, it continues to grow until the G-actin concentration drops below the critical concentration of the barbed end. Cells use specific proteins, referred to as capping proteins (CP), to bind actin-filament barbed ends, therefore arresting filament elongation and preventing polymerization of the entire G-actin pool. *In vitro*, this effect results in an increase of the critical concentration of actin and in inhibition of filament depolymerization from barbed ends (Caldwell et al., 1989). CPs can be subgrouped into different protein families. Macrophage capping protein CapG, gelsolin, fragmin and severin are a diverse group of monomeric capping proteins. A second group of CPs consists of heterodimeric proteins with a molecular mass in the range of 30 kDa per subunit that bind actin-filament barbed ends with high nM affinity (Cooper and Sept, 2008). Their activity is supposed to be regulated by PIP₂ and the uncapping-protein carmil (Haus et al., 1991; Schafer et al., 1996; Uruno et al., 2006).

- **Actin depolymerization factors**

It is obvious that actin, once polymerized, must be somehow depolymerized and recycled to refill the cellular G-actin pool. This task is accomplished by specialized depolymerization factors such as ADF/cofilin (*Actin Depolymerizing Factor*), which binds to ADP-actin filaments with high affinity and untwists the actin filament, resulting in severing and subsequent depolymerization. Cofilin activity is strictly regulated by phosphorylation by LIM-kinase and slingshot phosphatase, which in turn are regulated by small GTPases from the Rho family (Van Troys et al., 2008). ADF/Cofilin is described in chapter 1.1.6. in more detail.

- **Bundling and cross-linking proteins**

Within a typical cell, actin filament bundles can be arranged in different orientations and structures. Actin filaments in filopodia or microvilli for instance are compacted into dense parallel bundles by proteins like fascin, villin or fimbrin to generate stiff structures that protrude from the cell periphery (Faix and Rottner, 2006; Matilla and Lappalainen, 2007). The parallel orientation of the filaments ensures exclusive elongation at the front of the bundle to generate forces high enough to push the membrane outward. Ena/VASP tetramers were also supposed to contribute to filament bundling at the tips of filopodial

actin filaments (Schirenbeck et al., 2006; Matilla and Lappalainen, 2007; Chhabra and Higgs, 2007). Stress fibers which are important for cell adhesion are instead composed of antiparallel actin filaments with periodic accumulations of the bundling protein α -actinin (Naumanen et al., 2007).

1.1.6. ADF/Cofilin

ADF/cofilins (*Actin Depolymerization Factor*) are small (15-19 kDa), ubiquitous proteins, that are composed of a single ADF-H domain (*Actin Depolymerizing Factor-Homology*). These domains can also be found in the G-actin-binding protein twinfilin and in the F-actin-binding protein Abp1. Cofilin binds to both, F- and G-actin, with preferences for ADP-actin monomers and filaments. The 3D structure of many cofilin isoforms from yeast, *Acanthamoeba*, *Arabidopsis* and mammals have been determined by x-ray crystallography or NMR, showing that all isoforms have the same overall-structure of 5 β -sheets surrounded by three or four α -helices (Figure 8A; Hatanaka et al., 1996; Fedorov et al., 1997; Leonard et al., 1997; Bowman et al., 2000; Pope et al., 2004). The ADF/cofilin family in mammals consists of the three paralogues cofilin-1, cofilin-2 and ADF (van Troys et al., 2008).

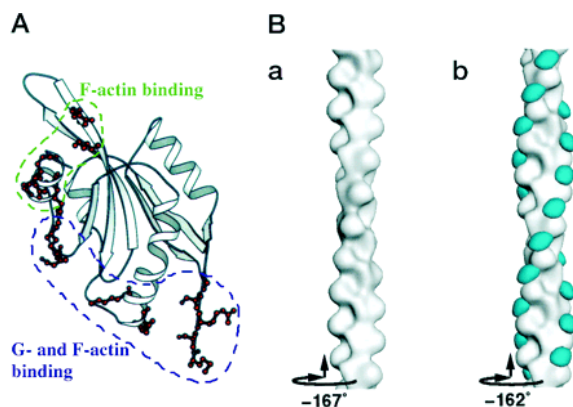


Figure 8: Structure and F-actin-binding of ADF/cofilin (from Carrier et al., 1999): (A) Ribbon structure of *S. cerevisiae* cofilin depicting regions for F- and G-actin-binding. (B) Surface model of the “Holmes-model” of F-actin (a) and a cofilin-decorated filament (b). Binding of cofilin unwinds the filament and disrupts the interactions of subdomains 1 and 2 along the helix.

1.1.6.1. Biochemical properties of ADF/cofilin

ADF/cofilin is an important regulatory protein that accelerates actin-filament turnover (Carrier et al., 1997). It binds ADP-actin filaments in a cooperative fashion and modulates the mechanical properties of the filament: The persistence length of the actin filament is lowered by a factor of 5, the subunit tilt is altered and the interactions of subdomains 1 and 2 along the long pitch helix are disrupted (see Figure 8B; McGough et al., 1997; McGough and Chiu, 1999; McCulloch et al., 2008; Galkin et al., 2003). Cofilin also accelerates the γ -phosphate release from ADP- P_i filaments (Blanchoin and Pollard, 1999). As a consequence, cofilin-decorated filaments tend to break much more easily to produce short fragments that can either depolymerize rapidly or serve as new nucleation seeds. Recent studies showed that cofilin acts synergistically with the F-actin-binding proteins coronin and Aip1 to rapidly

depolymerize F-actin (Kueh et al., 2008) and preferably disassemble Arp2/3-formed actin-filament branches (Chan et al., 2009). Interestingly, it was shown that the F-actin-binding protein coronin also protects newly polymerized ATP-actin filaments from cofilin, making coronin both a negative as well as positive regulator of cofilin activity (Gandhi et al., 2009). *In vitro*, the presence of cofilin selects for complex filament structures like bundles, since single filaments are severed much faster than bundled filaments (Michelot et al., 2007). A controversially discussed study by the Pollard laboratory has found several different effects of cofilin on actin assembly and disassembly: At low nM concentrations, cofilin is proposed to sever filaments, whereas it stabilizes filaments at higher/equimolar concentrations, and at very high concentrations, cofilin even seems to promote the nucleation of new actin filaments (Andrianantoandro et al., 2006).

1.1.6.2. Function and regulation of ADF/cofilin *in vivo*

The disassembly of actin filaments is a critical step in cell motility and necessary to refill the cellular pool of G-actin, which in turn is needed for constant actin polymerization e.g. at the leading edge of a migrating the cell. Consistently, cells expressing low levels of ADF/cofilin showed defects in both, polymerization and depolymerization of actin (Mouneimne et al, 2004; Hotulainen et al., 2005). The local activation of cofilin by the slingshot phosphatase (see below) in cells in turn stimulates actin polymerization, most likely due to enhanced filament turnover (Ghosh et al., 2004). Cofilin localizes to sites of active actin assembly and is found within the entire lamellipodium (Lai et al., 2008).

The activity of cofilin is regulated either directly by phosphorylation and dephosphorylation or indirectly by F-actin-binding proteins that compete with cofilin for filament binding. Phosphorylation of cofilin by LIM- or TES-kinases leads to inactivation of the proteins, whereas dephosphorylation by the slingshot-phosphatase (*SSH*) reactivates cofilin (Huang et al., 2006; Scott and Olson, 2007). The activities of these kinases and the phosphatase are in turn regulated by small-GTPases like Cdc42, Rho and Rac that link intracellular signaling to a great number of cytoskeleton-associated proteins (see Figure 9; van Troys et al., see 2008).

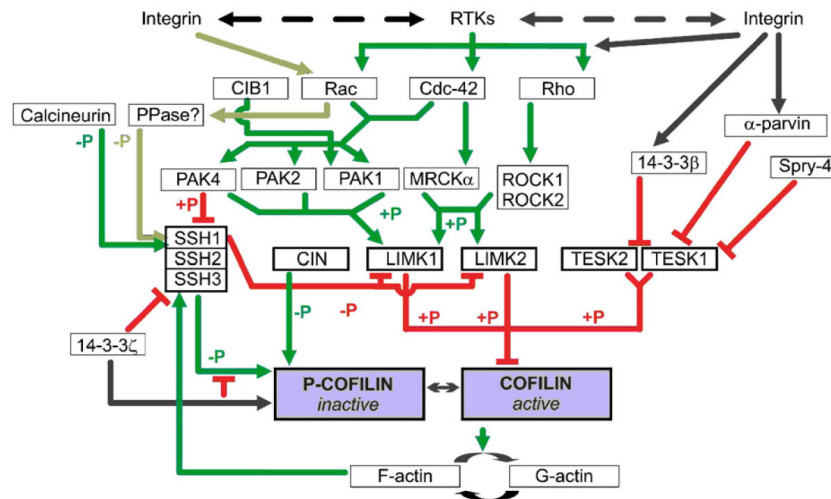


Figure 9: Regulation of cofilin (from van Troys et al., 2008). The activity of cofilin is directly regulated by phosphorylation, which in turn is regulated by small Rho-family GTPases. Abbreviations: CIB, calcium- and integrin binding protein; MRCK myotonic dystrophy kinase-related Cdc42-binding kinase; PPase: Phosphatase; CIN: chronophin phosphatase; PAK: p21 activated kinase; Spry-4: Sprouty-4.

Another important aspect of cofilin regulation is the finding that most actin filaments are associated with F-actin-binding proteins *in vivo*. Proteins like Aip1 and coronin were shown to synergize the effects of cofilin in filament disassembly (Rodal et al., 1999; Kueh et al., 2008; Gandhi et al., 2009). On the other hand, tropomyosin-decorated actin filaments are resistant to cofilin-mediated filament severing, therefore stabilizing actin filaments in the lamellum and explaining the absence of cofilin in this region (DesMarais et al., 2002; Iwasa and Mullins, 2007). The effects of other F-actin-binding proteins like fascin or α -actinin on cofilin-mediated filament severing were not yet analyzed.

1.1.7. Formins

Non-muscle cells contain a large pool of monomeric actin, mainly complexed with profilin or T β 4, which is assembled into filaments upon external or internal signals. Two of the so far best studied actin nucleators are the Arp2/3 complex (see chapter 1.1.5. and 1.1.10.) and formins. Over the last decade, formins became recognized as potent nucleators of linear actin filaments that control a large variety of important cellular and morphogenetic functions (Faix and Grosse, 2006; Goode and Eck, 2007). They are ubiquitous multidomain proteins that are implicated in the regulation of many cytoskeleton-dependent processes such as cytokinesis, cell adhesion, cell motility, filopodia formation and morphogenesis. Many of them can interact with both, microtubules and actin filaments (Bartolini et al., 2008; Basu and Chang, 2007). Since the focus of this work is on the active assembly of actin filaments, the interactions of formins and actin will be described in more detail.

1.1.7.1. Biochemical and structural properties of formins

Proteins of the formin family form homodimers and harbor several characteristic domains. They are defined by their dimeric, doughnut shaped FH2 domain and an adjacent proline-rich FH1 domain (Figure 10A and B). The FH2 core domain was shown to be sufficient to nucleate new actin filaments *in vitro* (Kovar et al., 2003; Pruyne et al., 2002). In contrast to the Arp2/3 complex, formins nucleate linear actin filaments and subsequently elongate these filaments in a processive fashion by tracking their barbed end with their FH2 domain and concomitant recruitment of profilin-actin complexes with their adjacent FH1 domains (Figure 10C). This unique property was first observed by Kovar and colleagues using *in vitro* TIRF microscopy with purified proteins (see chapter 1.1.11.3; Kovar et al., 2003, Kovar et al., 2004, Kovar et al., 2006).

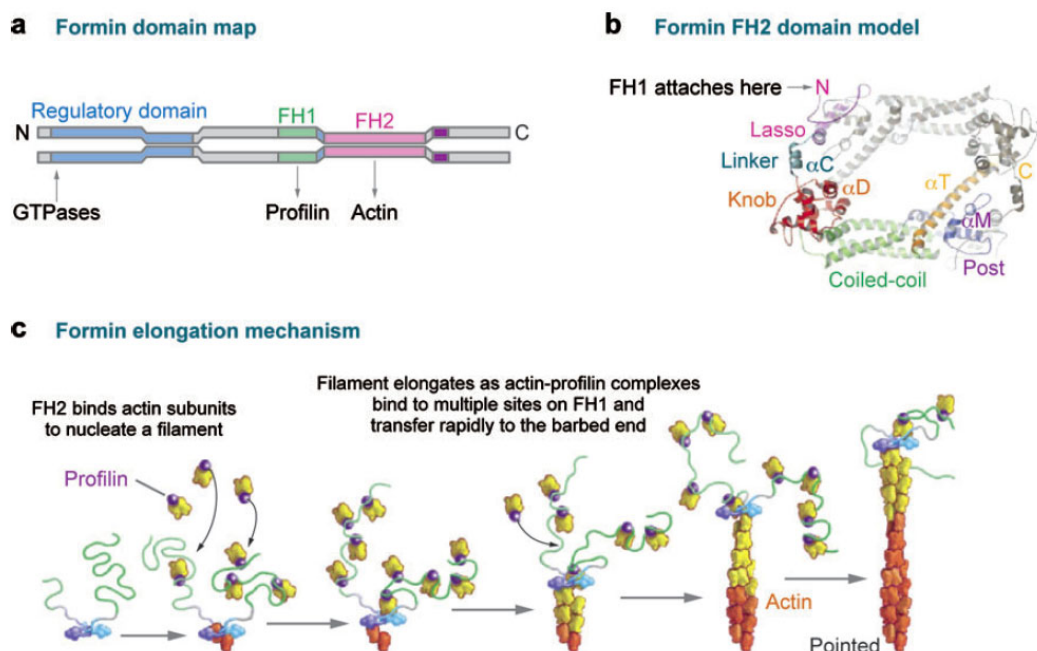


Figure 10: Overview of formin structure and function (from Pollard, 2007). (A) Formins consist of an N-terminal regulatory domain, a central proline-rich FH1 domain and the C-terminal FH2 domain. Dimerization and F-actin interaction is mediated by the FH2 and GBD domain (*GTPase Binding Domain*). (B) Crystal structure of the FH2 dimer from yeast formin Bni1p. (C) Simplified scheme of formin-mediated actin filament elongation. The FH1 domain recruits profilin-actin complexes that are inserted into the growing filament-barbed end by the FH2 domain. The FH2 domain processively translocates at the barbed end as the filament elongates.

How formins modulate actin assembly at the molecular level is still not fully understood, but in most cases their properties are changed considerably by the small G-actin-binding protein profilin. The FH1 domain, composed of consecutive stretches of polyproline residues, binds profilin-actin complexes with μM affinity and is therefore able to recruit and deliver new ATP-G-actin subunits to the FH2 domain for incorporation into growing filaments barbed ends (Evangelista et al., 1997; Watanabe et al., 1997; Chang et al., 1997; Sagot et al., 2002).

Moreover, it was shown for the yeast formin Bni1p that the rate of barbed-end elongation increases with the number of polyproline tracks within the FH1 domain, suggesting that the establishment of a locally increased actin concentration at the barbed end is responsible for the enhanced elongation rates (Paul and Pollard, 2008). Although binding of profilin to isolated FH1-FH2 fragments increases the elongation rates of formin-bound filaments, the effect of profilin on formin-mediated actin polymerization differs greatly between various formin isoforms (Kovar and Pollard, 2004; Romero et al., 2004; Kovar et al., 2006). The conserved FH2 domain nucleates new actin filaments, most likely by stabilizing an actin dimer (Pring et al., 2003), and remains bound to the barbed ends of the filaments with low nM affinity (Pruyne et al., 2002; Moseley et al., 2004). In addition, the FH2 domains of the formins Bni1p, mDia1, dDia2, Cdc12 and FLR efficiently block the inhibitory activities of capping protein and gelsolin, which also interact with low nM affinities with actin filament barbed ends (Zigmond et al., 2003; Harris and Higgs, 2004; Schirenbeck et al., 2005; Neidt et al., 2009).

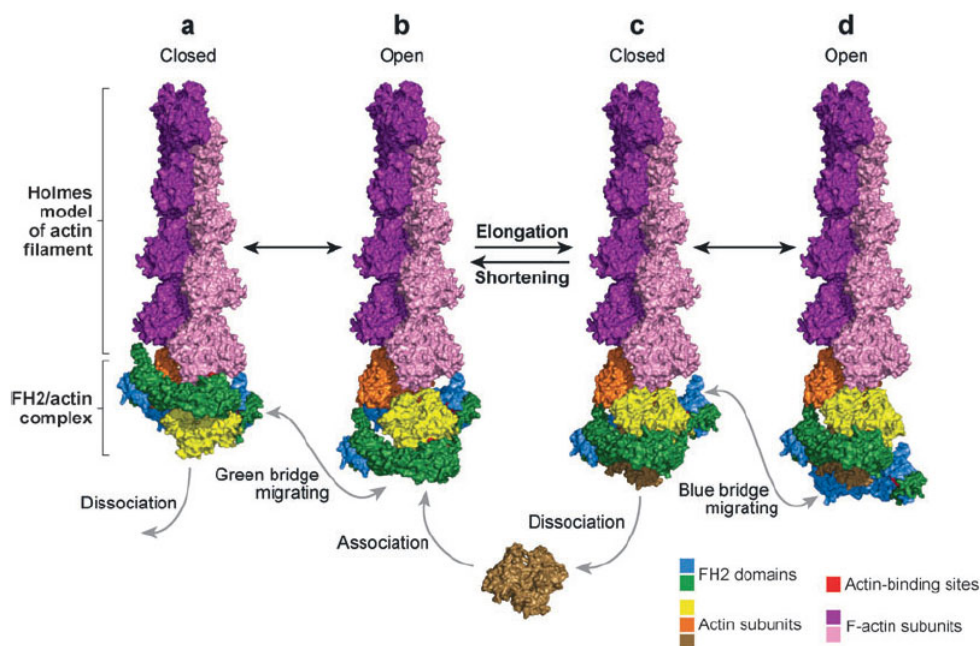


Figure 11: Structural basis of processive, formin-mediated actin assembly (from Goode and Eck, 2007). The FH2 dimer (colored green and blue) binds the barbed end of the actin filament. Processivity is achieved by a dynamic equilibrium of the FH2 dimer between a closed and an open state. (A) In the closed state, both FH2 domains are bound tightly to the barbed end, preventing monomer association or dissociation and are therefore “capping” the barbed end. (B) Free migration of one of the two FH2 domains (green) leads to binding in the “open” state, which allows incorporation of a new monomer. (C) This binding again triggers the closed state. (D) After dissociation of the previously bound FH2 domain (blue), the formin again converts into the open state. Repetition of these events results in processive association of the formin with the growing barbed end.

Crystallographic studies combined with sophisticated *in vitro* assays and theoretical calculations have led to a model of formin-mediated actin assembly, in which the FH2 dimer

translocates stepwise at the growing filament end, alternately allowing new actin subunits to incorporate onto the barbed end (Figure 11; Otomo et al., 2005; Kovar et al., 2006; Paul and Pollard, 2009). This working model implicates that formins exist in two distinct binding modes during processive barbed end elongation. In the “closed” binding mode, both FH2 domains have contact with the barbed end and the addition of new actin monomers is inhibited. During migration of one of the two FH2 domains, the formin binds in the “open” mode, allowing new monomers to incorporate into the barbed end, which in turn leads to the “closed” confirmation. Subsequently, the previously bound FH2 domain migrates freely, again allowing a monomer to incorporate into the filament. This model explains both, the ability of formins to processively assemble actin filaments and the diversity in elongation rates between formin isoforms. One can distinguish different types of formins: Those that spend a long time in the “closed” confirmation, therefore greatly inhibiting filament elongation in the absence of profilin, like Cdc12 or mDia2, and those that spend a long time in the “open” confirmation, only weakly inhibiting monomer addition to the barbed end, like mDia1 or the nematode formin CYK1 (Kovar et al., 2006; Neidt et al., 2008, Neidt et al., 2009). This property is described by the “gating factor”, which represents the time a formin spends in the open state (Vavylonis et al., 2006; Pollard and Paul, 2009). This parameter can be easily determined by measuring the filaments elongation rates using *in vitro* TIRF microscopy. However, the nature of the different gating factors is still elusive. It was initially assumed that the gating factor is largely determined by the length of the linker region connecting the two FH2 domains within the FH2 dimer, thereby determining its flexibility (Figure 10B), as the linker length apparently correlated directly with the elongation rates of various formins (Higgs 2005). However, a recent study using Bni1p-chimeras with different linker regions from other formins could not corroborate this hypothesis (Paul and Pollard, 2009).

1.1.7.2. Cellular localization and regulation of formins

Formins contribute to a large variety of actin-based processes in the cell. They localize to the tips of filopodia in *Dictyostelium* and mammalian cells, to the cytokinetic ring of *S. pombe*, *Drosophila* and *C. elegans* and to the bud neck and cell poles of *S. cerevisiae* (Chang et al., 1997; Imamura et al., 1997; Swan et al., 1998; Tominaga et al., 2000; Tolliday et al., 2002; Peng et al., 2003; Ingouff et al., 2005; Schirenbeck et al., 2005, Block et al., 2008).

A large subgroup of formins, the so-called Diaphanous-related formins (DRFs), is regulated by small GTPases which are important regulators of the actin cytoskeleton. DRFs have a conserved domain organization, with an N-terminal GTPase-binding domain (GBD) followed by a diaphanous inhibitory domain (DID) and a C-terminal diaphanous autoregulatory domain (DAD) (Figure 12; Higgs, 2005; Faix and Grosse, 2006). In the inactive state, the DRF is autoinhibited by interaction of the DID with the DAD, cannot bind or nucleate actin filaments and usually does not localize to sites of actin assembly (Alberts et al., 2001; Li and Higgs,

2003). This autoinhibition is released by high-affinity binding of an activated Rho-GTPase to the GBD which disrupts the DID-DAD interaction and allows appropriate subcellular localization (Figure 12B; Watanabe et al., 1999; Lammers et al., 2005; Lammers et al., 2008, Block et al., 2008; Yang et al., 2008). The GBDs of different formins have very different affinities to Rho-GTPases, which results in a high specificity of a given GTPase-formin interaction and therefore to a very strict regulation of formin isoforms by different signaling pathways (Figure 12C; Rose et al., 2005; Lammers et al., 2008).

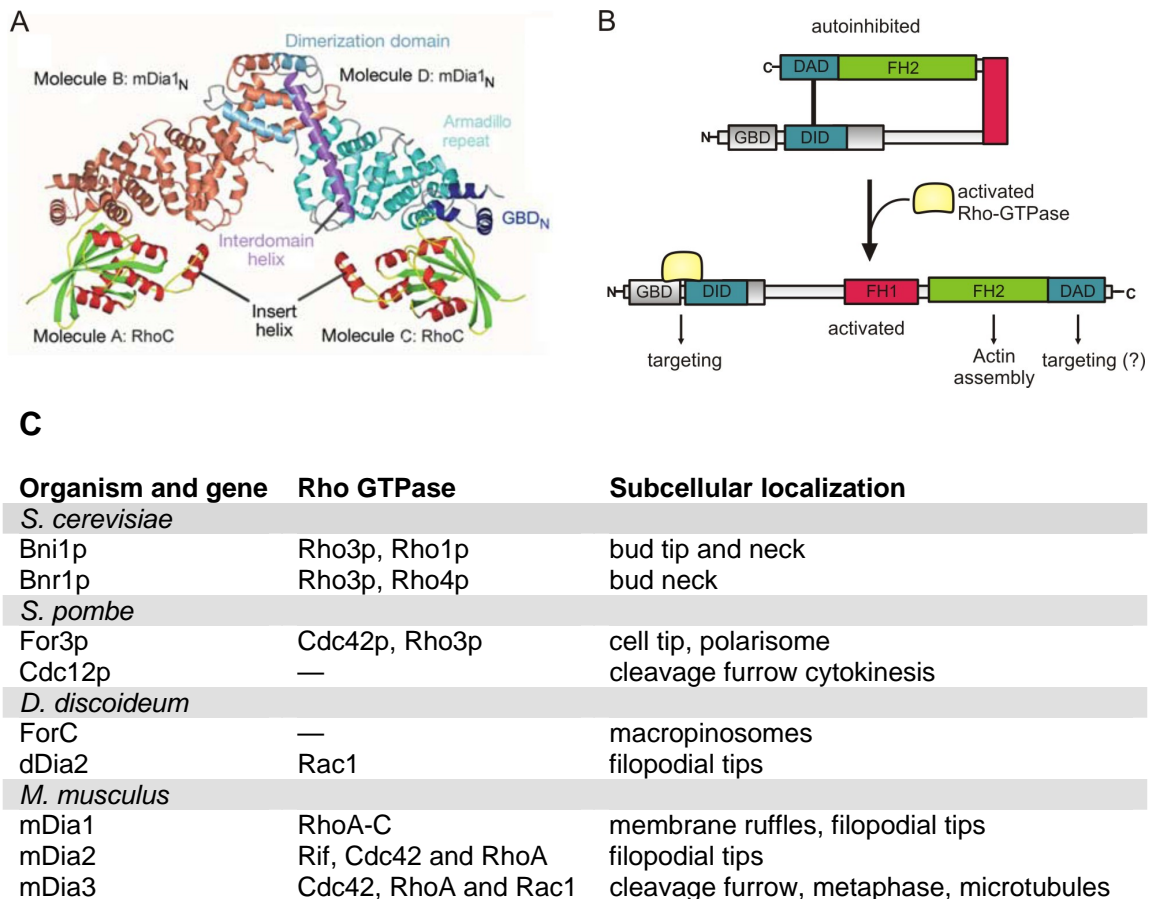


Figure 12: Interactions of GTPases and formins: (A) Crystal structure of the RhoC-mDia1 complex (from Rose et al., 2005). (B) Scheme of the activation of DRFs by activated small GTPases from the Rho subfamily. Binding of the GTPase to the GBD disrupts the DID-DAD interaction, which leads to the opening of the molecule. The active formin can interact with actin and other accessory proteins at specific subcellular compartments. (C) Overview of a selection of formins, their corresponding Rho-GTPases and their subcellular localization (adapted from Faix and Grosse, 2006).

1.1.8. The Thymosin β 4/WH2 motif

Thymosin β 4 is a small 5 kDa peptide and can be found in concentrations of up to 0.4 mM in mammalian cells (Huff et al., 2001). It consists of a C-terminal α -helix which binds the pointed end of G-actin to prevent filament nucleation and an N-terminal region which binds to

a hydrophobic pocket between subdomains 1 and 3 at the barbed end of the actin monomer (Figure 13; Irobi et al., 2004).

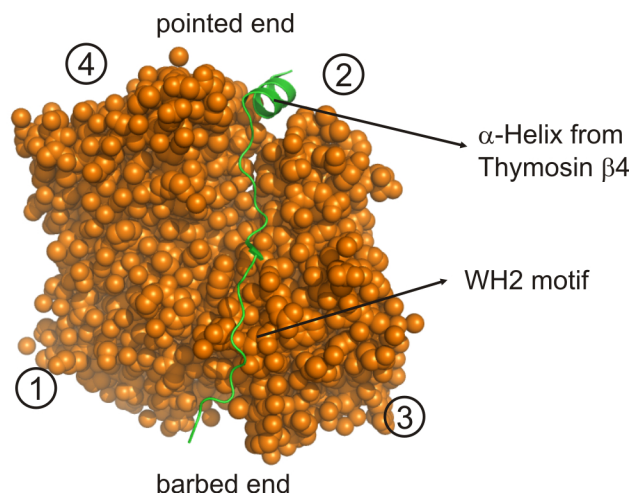


Figure 13: Structure of the T β 4-actin complex. The T β 4 peptide binds to the hydrophobic cleft between subdomains 1 and 3 and inhibits nucleation due to the interaction of the C-terminal α -helix with the pointed end of the filament. The structure was obtained with a gelsolin G1-T β 4 N-terminal fusion protein (from Irobi et al, 2004). PDB code: 2FF6.

Many cytoskeleton associated proteins harbor short-amino acid sequences consisting of 17-29 residues homologous to the N-terminal region of T β 4. This region is referred to as the WH2 motif (*WASP Homology domain 2*) because it was first recognized as an essential element for the regulation of Arp2/3-mediated filament nucleation mediated by the mammalian Wiskott-Aldrich syndrome protein (WASP) family (Paunola et al., 2002). However, a considerable diversity between T β 4 and other WH2 motifs has sparked a controversial debate in the field whether or not those actin-binding regions belong to a common family of actin-interacting domains (Edwards 2004). Numerous studies on the structure and biochemical properties of these small actin adaptors over the past years strengthened the hypothesis that all WH2-like actin-binding motifs interact with actin monomers at the same binding side (Figure 14A, Hertzog et al., 2004; Cherau et al., 2005; Aguda et al., 2006; Dominguez, 2007, Rebowski et al., 2008).

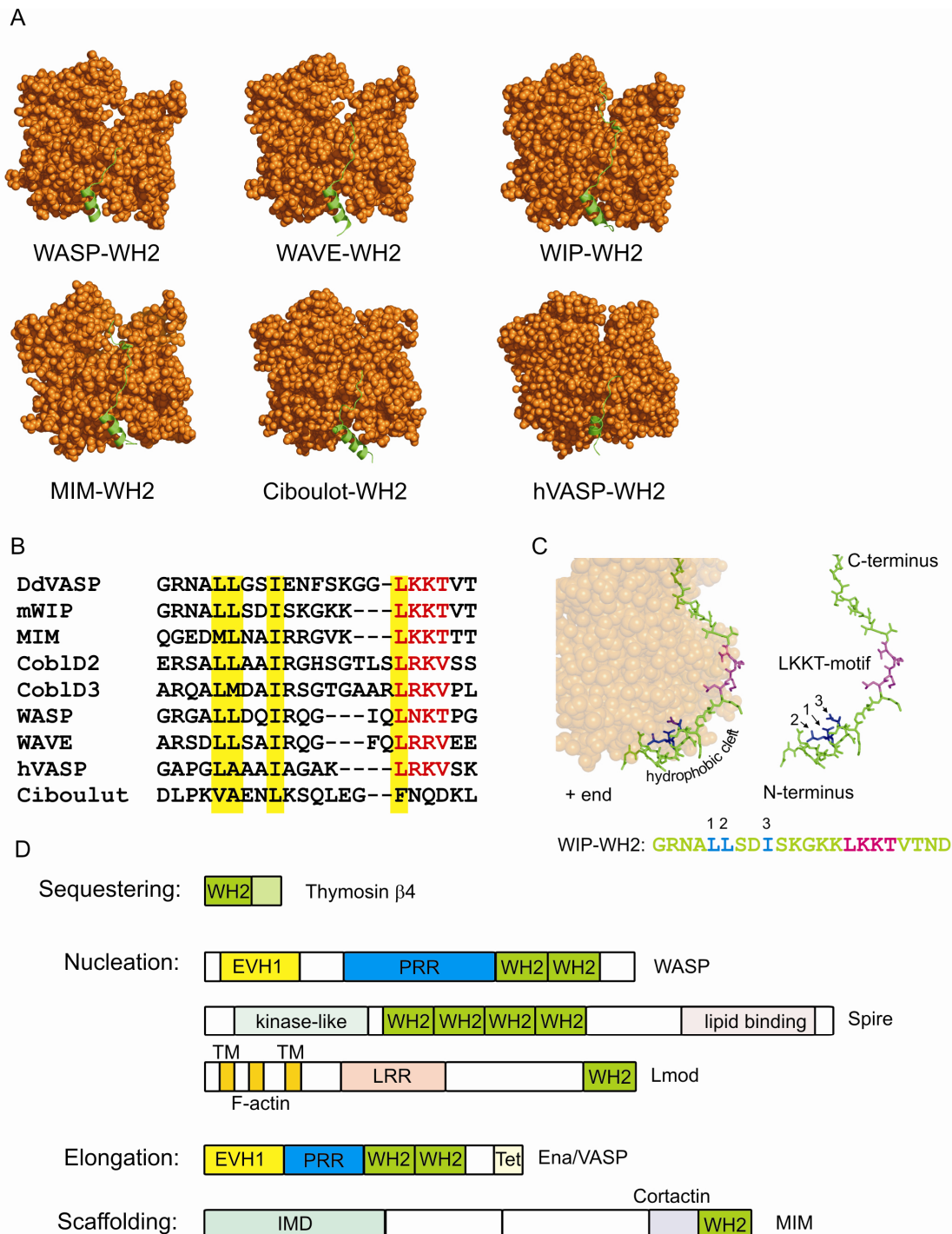


Figure 14: Diversity of WH2 motifs. (A) Crystallization of different WH2-actin complexes revealed that all WH2 motifs bind actin monomers in the same orientation and at the same binding site. The slight displacement of the WH2 of human hVASP (lower right) results from additional binding of profilin, which is not shown in the figure. (B) Sequence alignment of a selection of different WH2 motifs illustrates the conserved hydrophobic amino acids (yellow) and the conserved LxxT/V motif (red letters). (C) Binding of the long WH2 motif from WIP to actin. The three hydrophobic amino acids highlighted in blue bind to the barbed end, whereas the LKKT motif (magenta) binds to the side of the monomer. (D) WH2-containing proteins exert diverse functions. Besides the sequestering protein T β 4, WH2 motifs are also found in actin nucleators, elongators and scaffolding proteins (adapted from Dominguez, 2007). PDB codes: WASP-WH2: 2A3Z; WIP-WH2: 2A41; MIM-WH2: 2D1K; WAVE-WH2: 2A4O; Ciboulot-WH2: 1SQK; hVASP-WH2: 2PBD. Abbreviations: DdVASP, *Dictyostelium* VASP; mWIP: murine WASP-interacting protein; hVASP: human VASP.

The binding of WH2 motifs to actin is mainly mediated by 2-3 conserved hydrophobic amino acids that extend into the hydrophobic cleft between actin subdomains 1 and 3 at the barbed end, and by interactions of the widespread LxxV/T motif (x = basic amino acid; mostly LKKT) with the side of the actin monomer (Figure 14B and C, Huff et al., 2004; Cherau et al., 2005, Aguda et al., 2006; Ferron et al., 2007). The absence of the C-terminal helix of T β 4 in most WH2 motifs results in the loss of the actin sequestering activity and enables WH2 motifs to bind monomeric actin in order to nucleate and/or elongate actin filaments in a profilin-like fashion (Hertzog et al., 2004).

Up to now, more than 60 WH2-containing modular proteins were discovered. Astonishingly, these proteins differ greatly in the number and the arrangement of their WH2 motifs and are implicated in very different actin-related processes (Figure 14D). Biochemically, one can distinguish between actin sequestering proteins (T β 4), actin nucleators like Spire and Cobl, nucleation promoting factors that deliver monomeric actin like WASP, JMY (*Junction-mediating and -regulatory protein*), Lmod and WHAMM (*WASP homolog-associated protein with actin, membranes and microtubules*), scaffolding proteins like MIM (*Missing in metastasis*) and IRSp53 (*insulin receptor tyrosine kinase substrate p53*) and filament elongators like Ena/VASP (Mattilla et al., 2003; Quinlan et al., 2005; Ahuja et al., 2007, Lee et al., 2007; Co et al., 2007, Cherau et al., 2008, Ferron et al., 2007; Zuchero et al., 2009). Many of them are thought to be key components of the actin-assembly machinery in the leading edge of migrating cells, promoting nucleation, elongation, bundling and resistance against capping protein in order to drive cell protrusion (Cherau et al., 2005; Ferron et al., 2007; Chesarone and Goode, 2009; Qualmann and Kessels, 2009). Interestingly, three WH2-containing proteins have been found in bacterial pathogens that “hijack” the cytoskeleton of the host cell to trigger their internalization: The *Vibrio outer proteins* VopF and VopL as well as the *Chlamydia translocated actin-recruiting phosphoprotein* TARP. These proteins are secreted into the host cell and nucleate actin assembly in the absence of additional activating factors, corroborating the hypothesis that WH2-mediated actin nucleation is a general, independent molecular mechanism (Liverman et al., 2007; Tam et al., 2007).

An emerging question at the moment is: what determines the different biochemical functions of WH2 containing proteins? Recent structural and biochemical studies on the WH2-containing nucleators Spire and Cobl suggest that it is rather their overall arrangement into aligned WH2 repeats with different linker length, instead of an intrinsic biochemical property of the WH2 motif itself, which renders them potent F-actin nucleators (Figure 15; Quinlan et al., 2005; Ahuja et al., 2007; Rebowski et al., 2008).

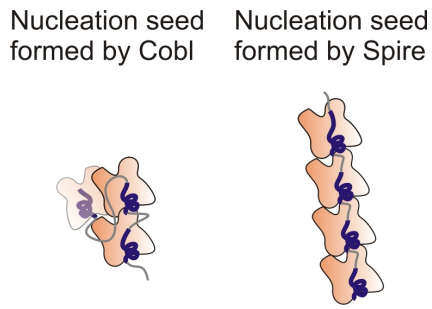


Figure 15: Schematic illustration of potential structures of nucleation seeds formed by Cobl and Spire. The WH2 motifs of Cobl are separated by linkers with different lengths, which allow the peptide to wrap around and stabilize an actin trimer. Spire possesses four WH2 repeats separated by short, identical linkers, leading to the formation of an unusual linear actin minifilament. WH2 motifs are colored blue. (Adapted from Ahuja et al., 2007).

In the case of Spire, the spatial arrangement of the four WH2 motifs in close proximity to each other leads to the formation of an unusual linear actin tetramer. Since the KIND domain (*kinase non-catalytic C-lobe domain*) of Spire can bind the FH2 domain of the formin Cappuccino with high affinity, it was hypothesized that two of these linear actin tetramers are fused to form an actin filament upon binding of two Spire molecules to the FH2 dimer (Quinlan et al., 2007; Quinlan et al., 2008). In contrast to Spire, the WH2 domains of Cobl are separated by linker regions with very different lengths, allowing it to wrap around and stabilize a natural actin trimer which is also formed during spontaneous nucleation. Deletion of the extended linker of Cobl indeed abolished its nucleating activity, supporting this structural model (Ahuja et al., 2007). Nevertheless, all WH2 motifs of actin nucleators have a relatively high actin monomer affinity in common, ranging from K_d s of 1 μ M for the WH2 motif in WASP to 39 nM for WH2 motifs in Cobl (Cherau et al., 2005; Co et al., 2007; Ahuja et al., 2007). The WH2 motifs of scaffolding proteins like MIM and IRSp53 show comparable G-actin-binding properties with K_d s in the same range, but are additionally able to bind F-actin with μ M affinity (Cherau et al., 2005; Millard et al., 2007). However, the precise effects of most of the WH2-domain containing proteins on filament nucleation, elongation and bundling still need to be determined on the single filament level.

The only WH2-containing filament elongators known so far are Ena/VASP proteins and – potentially – N-WASP (Dickinson and Purich, 2006; Co et al., 2007; Ferron et al., 2007; Dickinson 2008). Both proteins have a unique WH2 arrangement in common, in which a G-actin-binding WH2 motif is followed by a modified WH2 motif that allows for F-actin binding (Figure 14D). Ena/VASP proteins will be discussed in more detail in the next chapters.

1.1.9. Ena/VASP proteins

The protein VASP (*Vasodilator stimulated phosphoprotein*) was first described as a PKA substrate in platelets (Halbrugge et al., 1989; 1990). VASP, EVL (*Ena/VASP-like*) and Ena (*Enabled*) are grouped together in the conserved family of Enabled/vasodilator-stimulated phosphoprotein (Ena/VASP) proteins, which are found in vertebrates, invertebrates and *Dictyostelium* cells. All members of the family share a conserved domain architecture: an N-terminal *Ena/VASP homology 1* (EVH1) domain required for subcellular localization followed

by a central proline-rich domain (PRD), and finally a C-terminal EVH2 domain encompassing two WH2-like actin-binding motifs, referred to as the G-actin-binding site (GAB) and the F-actin-binding site (FAB) as well as a tetramerization domain at the C-terminus (Figure 16). All members of this protein family localize to sites of active actin assembly, including the tips of lamellipodia and filopodia and focal adhesions (Sechi and Wehland, 2004).

1.1.9.1. Biochemical and structural properties of Ena/VASP proteins

Ena/VASP proteins contain long stretches of intrinsically disordered amino-acid sequences. The only structured domains are the N-terminal EVH1 domain and the tetramerization domain at the C-terminus of the protein. The PRD as well as the GAB and FAB motifs appear to be largely unstructured.

Typical ligands for the N-terminal EVH1 domain of Ena/VASP to target the protein to specific sites are either FP₄ motifs or LIM domains (named after the proteins *Lin11*, *Isl-1* and *Mec-3*). The crystal structures of the EVH1 domain from EVL in complex with a FP₄ motif of the bacterial surface protein ActA and the EVH1 domain of Mena (*mouse Ena*) in complex with Tes were solved by Prehoda et al., 1999 and Boeda et al., 2008 (Figure 16). Homologous EVH1 domains can also be found in WASP, Spred and Sprouty (Bundschuh et al., 2006). A recent study showing that Tes binds specifically to the EVH1 of Mena and thereby replaces bound FP₄-Ligands (like zyxin and vinculin, Figure 16) gives rise to a great number of possible new regulatory interactions for Ena/VASP localization (Boeda et al., 2007).

The proline-rich domain is the most divergent region of the mammalian Ena/VASP proteins and binds to numerous adaptor proteins, some of them bearing SH3 domains or WW motifs (Krause et al., 2003; Sechi and Wehland, 2004), but presumably mainly recruits profilin-actin complexes for filament assembly (Reinhard et al., 1995; Kang et al., 1997). Recently, the crystal structure of the PRD of VASP in complex with profilin and the structure of a PRD-GAB peptide in complex with profilin-actin were solved, showing that profilin is recruited by the PRD and that PRD and GAB can bind simultaneously to profilin-actin complexes (Figure 16; Kursula et al., 2008; Ferron et al., 2007). The binding of profilin-actin to the polyproline region of hVASP was reported to be 5-fold stronger than the binding of profilin alone (Cherau et al., 2006). Although it was previously proposed that profilin-actin recruitment by VASP could be used to speed up actin filament elongation as in formins, actually only minor effects of profilin-actin on VASP mediated actin assembly were experimentally detected (Barzik et al., 2005; Ferron et al., 2007; Dickinson, 2008; Pasic et al., 2008).

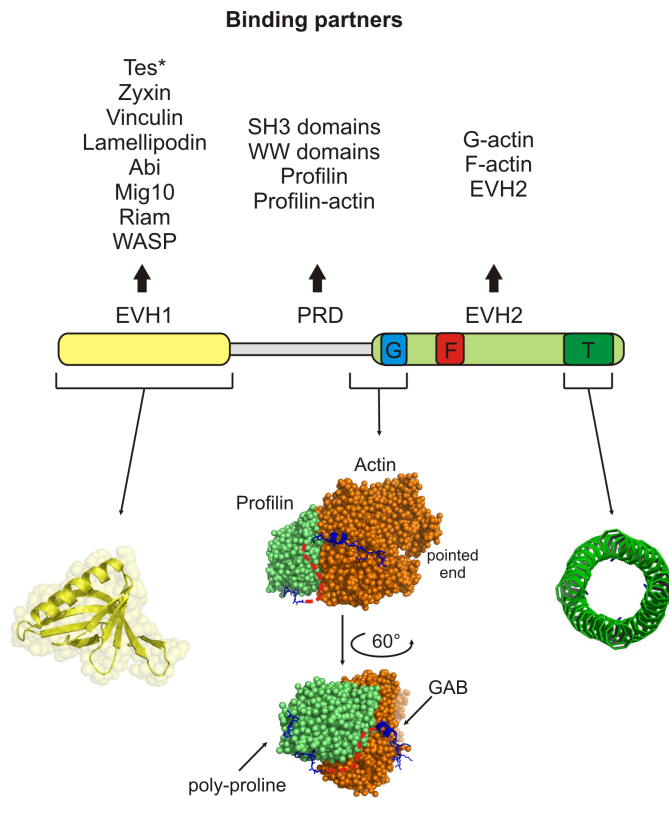


Figure 16: Domain organization and binding partners of Ena/VASP.

All Ena/VASP family members consist of an N-terminal EVH1 domain, a central proline-rich domain (PRD) and a C-terminal EVH2 domain. Mena additionally harbors a LER-rich region N-terminal of the PRD. The globular EVH1 domain binds to proteins with FP₄- and, newly identified, LIM-motifs as found in Tes (*). The central PRD binds SH3- and WW containing proteins as well as profilin and profilin-actin complexes. The EVH2 domain mediates binding of G- and F-actin and tetramerization of Ena/VASP proteins. The crystal-structure of a PRD-GAB peptide revealed that profilin-actin can bind the PRD and GAB simultaneously (Ferron et al., 2007). PDB codes: EVH1: 1EVH; PRD-GAB profilin-actin: 2PBD; Tetramerization domain: 1USD.

In the early years after the discovery of Ena/VASP proteins, several studies investigated the effects of the EVH2 domain on actin assembly *in vitro*. It soon became evident that VASP forms stable tetramers by virtue of its C-terminus, that it binds to both, G- and F-actin, that it promotes actin assembly and prominently bundles actin filaments (Bachmann et al., 1999; Huettelmaier et al., 1999; Bearer et al., 2002; Walders-Harbeck et al., 2002). Despite these findings, its precise mode of action remained controversial, as VASP function *in vitro* was strongly dependent on the salt concentration and the experimental conditions used (Trichet et al., 2008; Gertler and Bear, 2009).

One frequently used tool to quantify actin polymerization is the pyrenyl-actin (“pyrene actin”) polymerization assay (see chapter 1.1.11.1.). Although much information can be extracted from these assays, the versatility of VASP-actin interactions caused many ambiguous results. While it was reported for instance that VASP enhances filament nucleation under low salt conditions (Huettelmaier et al., 1999, Laurent et al., 1999), others found no indication for a nucleating activity of VASP at higher salt conditions (Barzik et al., 2005). Ena/VASP proteins artificially targeted to the mitochondrial surface also did not lead to a detectable actin accumulation, apparently supporting the latter finding (Bear et al., 2000). However, a similar experimental setup using zyxin fused to a mitochondrial tag resulted in VASP recruitment and actin accumulation - an effect that was also recently observed after targeting of *Dictyostelium* VASP (DdVASP) to late endosomes (Fradelizi et al., 2001; Schmauch et al., 2009). An even bigger controversy arose concerning the potential ability of VASP to enhance

actin filament elongation and its ability to compete with capping protein for barbed end binding. Again, some laboratories detected enhanced barbed end elongation by VASP, using spectrin actin seeds in pyrene assays and VASP-coated beads (Skoble et al., 2001; Plastino et al., 2004; Barzik et al., 2005), whereas others failed (Bear et al., 2002; Samarin et al., 2003). The crystallization of profilin-actin in complex with a PRD-GAB peptide from hVASP confirmed the assumption that both peptides can bind profilin and actin simultaneously, suggesting that VASP may be a processive filament elongator like the formins (Figure 17; Ferron et al., 2007; Dickinson et al., 2008). However, a recent study employing *in vitro* TIRF microscopy on single actin filaments found no indications for any processive interaction of VASP with the filament barbed end or for enhanced filament elongation (Pasic et al., 2008). Early investigations in cells with reduced Ena/VASP levels at the leading edge lead to the suggestion that VASP may prevent CP from binding to barbed ends (Bear et al., 2002). This working hypothesis was apparently substantiated by pyrene assays with spectrin-actin seeds and by *in vitro* TIRF microscopy (Bear et al., 2002; Barzik et al., 2005; Pasic et al., 2008). However, again other studies found no evidence for a specific anti-capping activity by Ena/VASP proteins (Boujemaa-Paterski et al., 2001; Samarin et al., 2003; Schirenbeck et al., 2006). Possible explanations for these controversial findings will be discussed in detail (see Discussion).

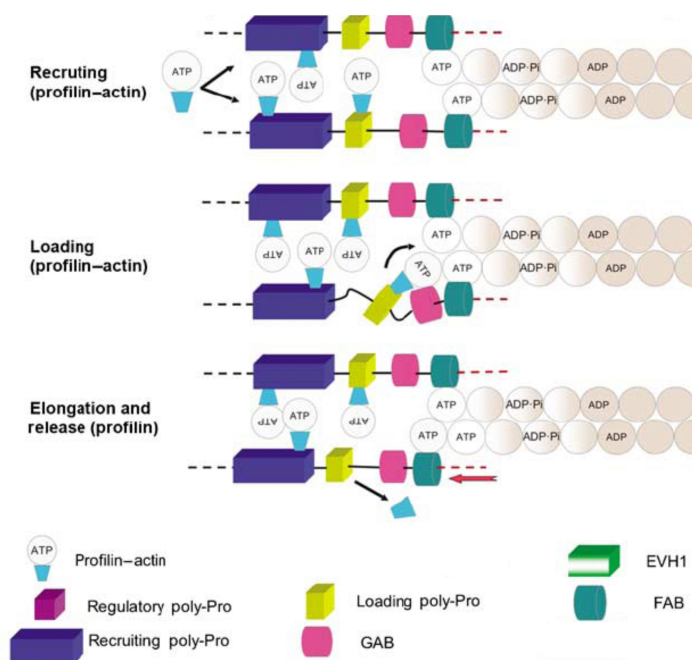


Figure 17: Model of VASP-mediated filament elongation (from Ferron et al., 2007). Schematic representation of the assumed mechanism of VASP-mediated actin assembly, based on the co-crystallization of a PRD-GAB peptide with profilin and actin (see Figure 16). The PRD of VASP recruits profilin-actin complexes. The “loading site”, which is the polyproline motif closest to the GAB, transfers the profilin-actin complex to the GAB, which results in profilin dissociation. The remaining actin monomer is subsequently transferred to the filament barbed end, which is tethered by the FAB. Eventually, the FAB releases the filament and binds the newly assembled barbed end, which allows the process to start again.

1.1.9.2. Cellular localization and function of Ena/VASP proteins

VASP and its mammalian isoforms Ena and EVL localize to the leading edge of the protruding lamellipodium, to filopodium tips, to focal adhesions and puncta along stress fibers

as well as to the immunological synapse and the surface of certain pathogens like *Listeria monocytogenes* (Figure 18A and B; Sechi and Wehland, 2004, Krause et al., 2004, Bear and Gertler, 2009). The single isoform in *Dictyostelium* (DdVASP) also localizes to sites of active actin assembly like filopodium and lamellipodium tips (Schirenbeck et al., 2006). The localization of Ena/VASP proteins to different actin-rich structures is mediated by its EVH1 domain, by interactions of actin filaments with the EVH2 domain as well as by binding of SH3 or WW-Motif containing proteins to the PRD. The activity of Ena/VASP proteins seems also to be regulated by phosphorylation by the kinases PKA, PKG and PKC (Butt et al., 1994, Lambrechts et al., 2000; Drees and Gertler, 2008).

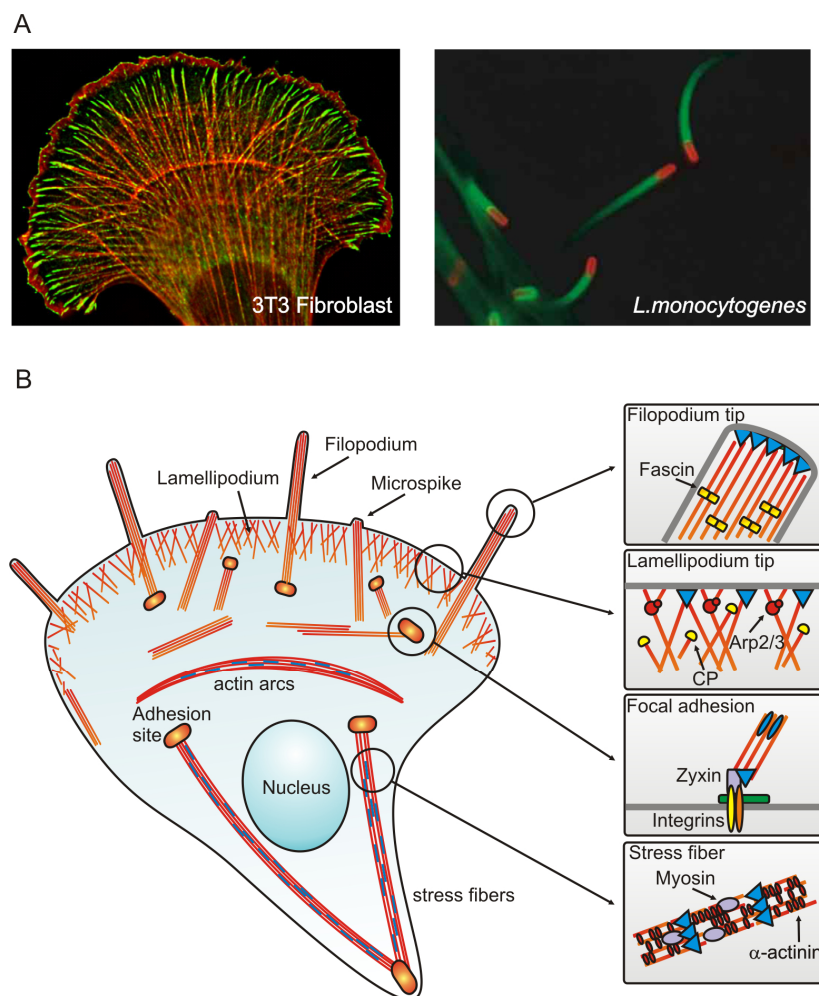


Figure 18. Localization of VASP. (A) VASP (green) localizes to the tips of lamellipodia and filopodia and to focal adhesions (from Gertler et al., 2009). It is also recruited to the surface of *L. monocytogenes* (red) to enhance actin-based propulsion. (B) Scheme of VASP localization to different actin structures. In filopodia, VASP is part of the filopodium tip complex alongside IRSP53, Myosin X, formins and others (Faix et al., 2009). It is also a major component of the lamellipodium tip. It is recruited to focal adhesions by Zyxin and it is also found in defined areas within stress fibers, which precise formation mechanism is still elusive. VASP is shown as blue triangles.

After the identification of Ena/VASP proteins in platelets, *in vivo* studies soon revealed that they have numerous effects on actin-based processes. Ena/VASP proteins localize

prominently to focal adhesions which mediate substrate attachment via integrins (Gertler et al., 1995, Vasioukhin et al., 2000). Their attachment and detachment are key events in cell motility, anchoring the moving cell to substrata and forming fixed spots for stress fiber-dependent contraction (Lauffenburger and Horwitz, 1996). Ena/VASP proteins are recruited exclusively by interactions of their EVH1 domain with zyxin and vinculin during early stages of focal adhesion formation (Brindl et al., 1996; Drees et al., 2000; Zaidel-Bar et al., 2003). As recently reported, the isoform Mena is specifically recruited by Tes, which additionally excludes binding of FP₄-containing proteins (Boeda et al., 2007). Morphogenetic studies on triple-knockout mice lacking all three Ena/VASP isoforms have also revealed that VASP proteins play important roles in establishing endothelial barriers and cadherin/ β -catenin cell-cell junctions (Furman et al., 2007). However, the contribution of Ena/VASP proteins in focal-adhesion and cell-cell junction formation is still elusive.

In addition to its enrichment at adhesion sites, it has also been shown that VASP density at the leading edge of migrating fibroblasts and keratocytes directly correlates with the protrusion rate of the lamellipodium (Rottner et al., 1999, Bear et al., 2002; Lacayo et al., 2007, Koestler et al., 2008). Targeting of VASP to the leading edge of the cell is mediated by EVH1-receptors such as lamellipodin, PREL1/RIAM, Abi and possibly by direct interactions with the PRD of WASP (Castellano et al., 2001; Tani et al., 2002; Krause et al., 2004; Lafuente et al., 2004; Jenzora et al., 2005). Additionally, proper F-actin interaction via the EVH2 domain is required for localization to the leading edge, suggesting that both, EVH1 interaction and F-actin binding by the EVH2 domain are necessary to target the protein to protrusive actin structures (Loureiro et al., 2002; Bear et al., 2002, Applewhite et al., 2007). VASP was shown to have a global negative effect on fibroblast motility, since mislocation of VASP to mitochondria resulted in enhanced cell motility (Bear et al., 2000, Bear et al., 2002). However, others again reported opposite effects (Moeller et al., 2004). There is nevertheless general agreement that the presence of VASP in the lamellipodium results in a much more dynamic protrusion of the leading edge. Additionally, displacement of VASP from the lamellipodial tip changes lamellipodium architecture, resulting in shorter, more densely branched filaments, whereas enhanced targeting to the membrane produces longer, less branched filaments, suggesting that VASP alters Arp2/3-complex activity (Bear et al., 2002). However, an effect of VASP on Arp2/3-mediated filament branching could not be corroborated *in vitro* (Boujemaa-Paterski et al., 2001). These observations, together with *in vitro* data, led to the hypothesis of a specific anti-capping activity of VASP proteins to protect growing actin filament barbed ends from capping proteins and therefore indirectly promoting the growth of actin filaments towards the plasma membrane (Sutherland et al., 2002, Bear et al., 2002; Barzik et al., 2005;). Although early cell biological observations and biochemical studies also proposed a possible direct involvement of VASP in filament elongation (Fradelizi

et al. 2001; Jonckheere et al., 1999), this issue was initially neglected and it was widely accepted that VASP was primarily an anti-capping protein. Ena/VASP proteins were also shown to enhance *Listeria* motility in cells and cell extracts after binding to the surface protein ActA (Laurent et al., 1999; Geese et al., 2002; Samarin et al., 2003). However, this effect was initially explained by CP resistance and/or altered Arp2/3-branching kinetics rather than by a direct involvement of VASP in filament elongation.

In addition to its role in lamellipodial actin assembly, all three mammalian isoforms as well as the orthologue from *Dictyostelium* were shown to localize prominently to filopodium tips and contribute to filopodium formation in *Dictyostelium*, fibroblasts and neurons (Han et al., 2002; Schirenbeck et al., 2006; Kwiatkowski et al., 2007, Dent et al., 2007, Applewhite et al., 2007). Deletion of the FAB in the *Dictyostelium* orthologue greatly abolished filopodia and also resulted in a loss of filament-bundling activity of VASP *in vitro*, suggesting that VASP's function in filopodium formation might be bundling and crosslinking of filament barbed ends in the filopodium tip complex (Schirenbeck et al., 2006). Neurons from Ena/VASP deficient mice lacking Mena, VASP and EVL (mmvvee-mice) failed to form functional filopodia (Dent et al., 2007). Studies with MV^{D7} mouse fibroblasts, which do not express Mena and VASP, have shown that the FAB, GAB and the Tet domain all contribute to filopodium formation (Applewhite et al., 2007). Many studies suggested that Ena/VASP proteins promote filopodium formation by protecting branched lamellipodial actin filaments from capping proteins, therefore allowing them to grow and converge into compact actin bundles which may then protrude to form filopodia. This model is also known as the "convergent elongation model" of filopodia formation and will be described in more detail below (Svitkina et al., 2003; Meijllano et al., 2004; Yang et al., 2007).

1.1.10. Models of actin-based protrusion

The directed assembly of actin filaments is essential to drive protrusion of cellular structures like lamellipodia and filopodia as well as propulsion of a number of intracellular pathogens like *L. monocytogenes* (Pollard and Borisy, 2003; Carlier and Pantaloni, 2007; Insall and Machesky, 2009). The identification of a growing number of actin interacting proteins at sites of active actin assembly led to different models of actin-based protrusion.

The foundation for our current understanding of lamellipodial actin assembly was laid by the discovery of the actin nucleating Arp2/3 complex in the lamellipodium (Welsh et al., 1997; Machesky et al., 1997). Besides its localization to lamellipodia, the Arp2/3 complex is also recruited and activated by *L. monocytogenes* and promotes actin nucleation at its surface to form - in combination with Ena/VASP proteins – actin comet tails that propel the bacterium through the cytosol (Welsh et al., 1997; Welsh et al., 1999; Laurent et al., 1999). *In vitro* studies showed that Arp2/3 complex promotes nucleation of new barbed ends by forming filament branches (Blanchoin et al., 2000; Amann and Pollard, 2001). On the basis of this

nucleation mechanism, the dendritic nucleation model of lamellipodial actin filaments was postulated (Figure 19; Svitkina and Borisy, 1999; Pollard and Borisy 2003; Pollard 2007): Lamellipodium protrusion is initiated by activating the Rho GTPase Rac which in turn activates WASP/Scar proteins (Aspenström et al., 1996). After binding to and activation of the Arp2/3 complex by WASP, it binds the side or tip of the filament and nucleates a daughter filament that grows towards the membrane in a 70° angle. After incorporation of a limited number of actin subunits, filament elongation is inhibited by binding of heterodimeric capping proteins to the barbed end. In this scenario, a dense meshwork of short, capped actin filaments is formed that can push the membrane forward (Pollard and Borisy 2003). The aging filaments are subsequently severed by ADF/Cofilin, which binds specifically to ADP-actin filaments in a cooperative manner and facilitates filament breakage and disassembly (Prochniewicz et al., 2005; Cao et al., 2006; Pavlov et al., 2007; McCullough et al., 2008). Disassembled ADP-actin monomers are finally charged with ATP by the small G-actin-binding protein profilin to refill the ATP-G-actin pool required for polymerization at the leading edge (Didry et al., 1998; Blanchoin et al., 2000).

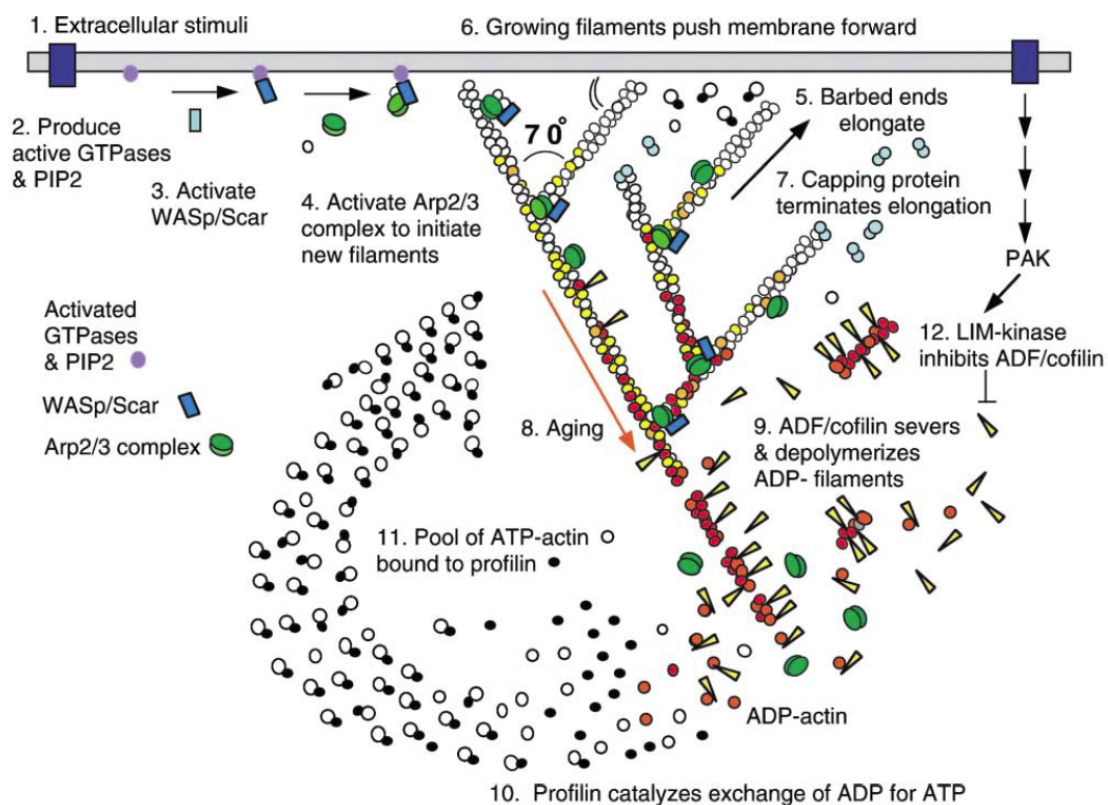


Figure 19: Dendritic nucleation model of lamellipodium protrusion (from Pollard and Borisy, 2003): 1-4 Extracellular signals activate GTPases that activate WASP-family proteins, which in turn bind to and activate Arp2/3 complex. 5-7 Newly nucleated filaments grow towards the membrane and push it forward. Capping proteins soon inhibit barbed end elongation. 8+9 ADF/Cofilin severs aging filaments. 10+11 Profilin recovers ATP-actin from ADP-actin. 12 Cofilin activity is regulated by LIM phosphorylation (and Slingshot dephosphorylation).

Although this model is supported by reconstituted motility systems using beads coated with the Arp2/3 activating VCA domain (Verprolin Central Acidic) of WASP and the above mentioned purified proteins (Wiesner et al., 2003), its *in vivo* relevance has been questioned in the recent past. Novel electron microscopic studies of the lamellipodium architecture in combination with improved fixation procedures have revealed that Arp2/3 complex-induced actin filament branches are absent in many different cell types. Instead, a great number of long, unbranched filaments were observed (Small et al., 2008; Koestler et al., 2008). Furthermore, it could previously be shown that the fixation method used by Svitkina and colleagues (1999) produces actin branches even with purified F-actin, suggesting that the observed branches might be artifacts (Resch et al., 2002). Taking these findings into account, it seems more likely that actin branches only exist transiently, and that protrusion of the lamellipodium is driven by the elongation of a defined number of appropriately oriented filaments that are protected from capping protein rather than by the pushing-force of many short and branched filaments.

Based on the dendritic nucleation model, Svitkina and colleagues also proposed an attractive model for filopodium formation coined the convergent elongation model (Figure 20; Svitkina et al., 2003; Mejillano et al., 2004). This model predicts the elongation and convergence of a selected number of lamellipodial actin filaments into filopodial actin bundles by protection of their barbed ends from the inhibitory effect of CP by VASP. The protected and continuously growing filaments eventually merge into compact actin filament bundles crosslinked by the actin-bundling protein fascin. Actin polymerization at the tips of these bundles can produce sufficient force to push the membrane outward in order to form nascent filopodia.

However, a number of independent studies recently provided solid evidence clearly arguing against the convergent elongation model of filopodium formation. It could be shown for instance, that filopodia form normally in cells where lamellipodia formation was suppressed (Steffen et al., 2006; Gomez et al., 2007; Sarmiento et al., 2008; Nicholson-Dykstra and Higgs, 2008). These data imply that filopodial actin filaments may exclusively be formed through nucleators other than the Arp2/3-complex. In line with this finding, in *Dictyostelium* cells, the Diaphanous-related formin dDia2 was shown to be critical for filopodium formation (Schirenbeck et al., 2005). In mammalian cells, the formins mDia1 and mDia2 have been implicated in the assembly of filopodial actin filaments, supporting a “de novo nucleation” model of filopodium formation (Faix and Grosse, 2006; Block et al., 2008; Yang et al., 2008), in which filopodial actin filaments are exclusively nucleated by proteins of the formin family. This model implicates the formation on a “filopodium tip complex”, composed of actin nucleators, elongators and potentially membrane-deforming proteins, to trigger the formation of filopodia solely by nucleation and subsequent elongation of newly formed filaments (Faix and Rottner, 2006).

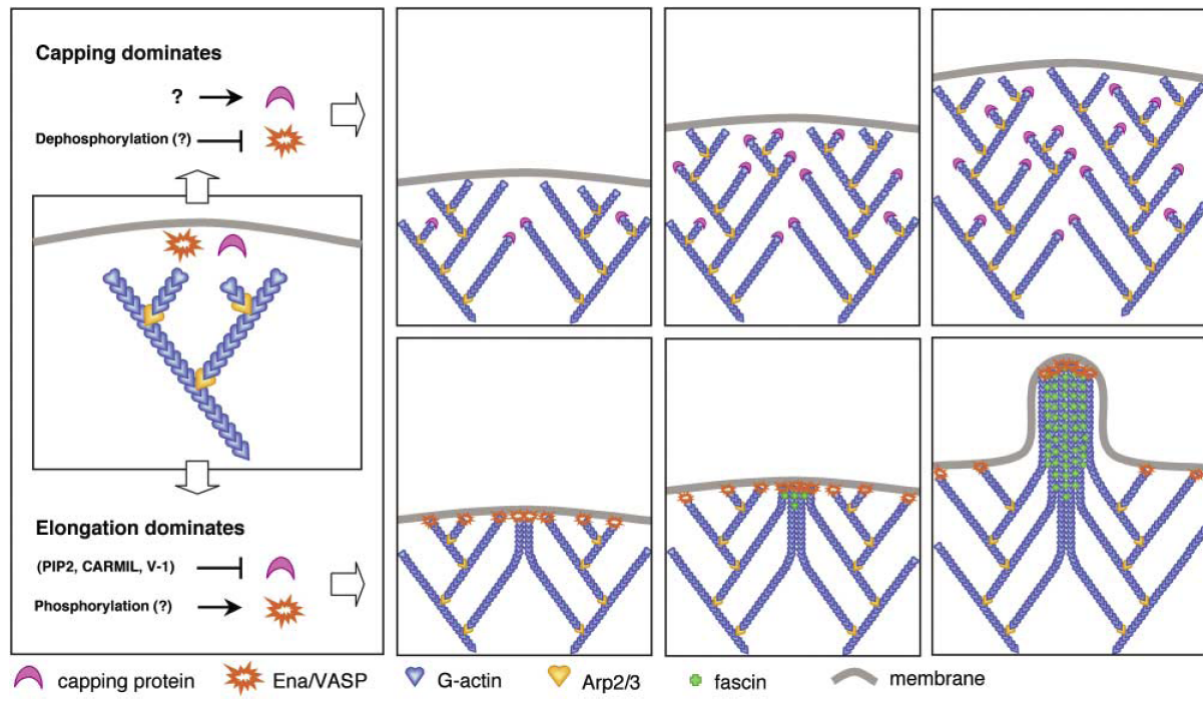


Figure 20: Schematic representation of the convergent elongation model (from Mejillano et al., 2004): Upper row: During lamellipodium protrusion, a dense meshwork of branched and subsequently capped actin filaments is formed to push the membrane forward. Lower row: Activation of anti-capping proteins (VASP) protects lamellipodial actin filaments from CP which results in continuous elongation and eventually the convergence into filopodial actin bundles crosslinked by fascin. Note that nucleation of new filaments is only mediated by Arp2/3 complex in this model.

1.1.11. Biochemical approaches to study actin dynamics *in vitro*

Over the past decades, many methods were established to quantify actin polymerization processes *in vitro*. Besides classical biochemical approaches like spindown-, densitometric- and light-scattering experiments, fluorimetric and microscopic assays soon became essential tools in analyzing the transition from G- to F-actin.

1.1.11.1. Pyrenyl-actin assays

One of the first fluorimetric assays to quantify the kinetics of actin polymerization was the pyrenyl-actin polymerization assay (“pyrene assay”) (Cooper et al., 1983). For this assay, actin monomers are covalently labeled at their reactive Cys-374 residue with the fluorescence dye Pyrenyl-iodoacetamide and subsequently mixed with unlabeled actin monomers to a final fraction of 3-30 % labeled actin, depending on the approach and the detector sensitivity of the fluorimeter. Polymerization of actin is initiated by transferring labeled actin monomers into polymerization buffer. The pyrene-fluorescence increases about 20-fold when incorporated into an actin filament, allowing the time-resolved quantification of F-actin by fluorescence spectroscopy (Figure 21). This approach is used to determine many different parameters of actin assembly and disassembly, e.g. the on-rates of barbed end and pointed end assembly (in combination with proteins that cap either barbed ends (capping proteins) or pointed ends (spectrin)), the critical concentration of actin and its

depolymerization-rate after dilution of F-actin below the critical concentration as well as nucleation rates. Typical pyrene assays are shown in figure 21.

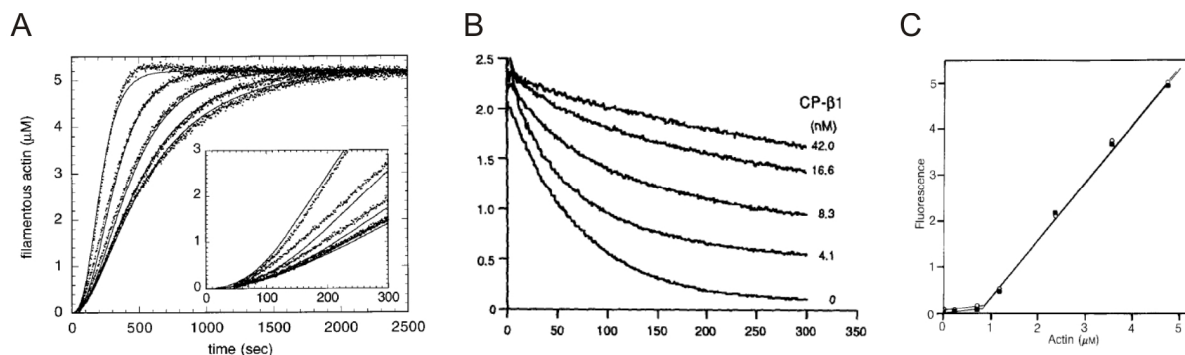


Figure 21. Examples for different pyrene actin assembly and disassembly assays. (A) Monitoring of spontaneous actin assembly after transfer of pyrene-labeled actin monomers into polymerization buffer. The curves represent actin polymerization at different concentrations of the Arp2/3 complex (Mullins et al., 1998). (B) Spontaneous depolymerization of pyrenyl-F-actin after dilution below the critical concentration of actin. The curves show the inhibition of barbed-end depolymerization by different amounts of the capping protein CP-β1 (Schafer et al., 1996). (C) Determination of the critical concentration using different concentrations of pyrenyl-F-actin. Since actin polymerizes only at concentrations above the critical concentration, a kink appears in a plot of actin concentration against pyrenyl-actin fluorescence (Carlier et al., 1986).

Although a great number of information can be extracted from pyrene assays, these bulk experiments do not provide information on the kinetics of single actin filaments, nor do they allow visualizing changes of filament architecture, e.g. filament branching by the Arp2/3 complex or filament bundling by fascin etc. Furthermore, the biochemical properties of proteins that concomitantly alter nucleation and elongation cannot be precisely quantified, and single molecule effects on actin filament assembly are evened out using these bulk assays.

1.1.11.2. Biomimetic motility assays

Marie-France Carlier and co-workers developed a microscopic assay to reconstitute actin-based motility, using small beads coated with proteins that activate the Arp2/3 complex (Wiesner et al., 2003). Addition of a mixture of actin, profilin, CP, ADF/cofilin and the Arp2/3 complex in polymerization buffer resulted in massive nucleation of actin at the bead surface that eventually led to the propulsion of the bead and the formation of an actin tail, which was assembled at the bead surface and disassembled at the rear (Figure 22).

The propulsion rates of the microspheres strictly depend on numerous parameters like coating density, viscosity of the solution, bead size and last but not least the protein composition of the motility medium. This assay allows observing global effects of accessory proteins on propulsion speed and actin-tail formation, and was an important assay supporting

the dendritic nucleation model of lamellipodium protrusion. However, this method does not allow evaluating the precise effect of a given accessory protein on actin filament dynamics.

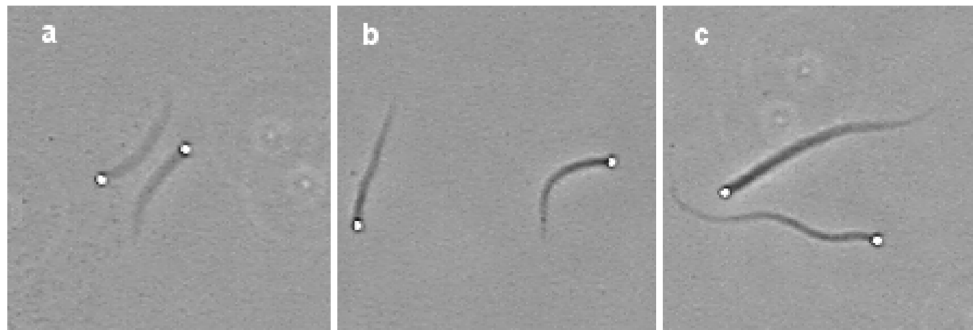


Figure 22. Biomimetic motility of functionalized beads. Beads coated with the Arp2/3 activating VCA domain of WASP trigger the nucleation and elongation of actin filaments at the bead surface to push the beads through the medium. The used motility medium contains actin, Arp2/3 complex, gelsolin, ADF/cofilin and profilin. Figures a-c show an altered actin tail length and density depending on the viscosity of the medium (Wiesner 2003).

1.1.11.3. *In vitro* TIRF microscopy

It is of great interest to observe the polymerization and depolymerization of single actin filaments directly, since this is the only way to verify interactions of binding proteins with the filament in real time. Single actin filaments can be visualized by fluorescence microscopy using the actin-binding peptide phalloidin conjugated to a fluorescent dye (mostly TRITC-phalloidin). However, phalloidin changes the binding behavior of many accessory proteins, e.g. the Arp2/3 complex, and it nucleates new actin filaments, prevents depolymerization and enhances filament stiffness (Blanchoin et al., 2000; Mahaffy et al., 2008).

This obstacle was overcome by the *in vitro* TIRF microscopy (*Total internal reflection fluorescence*) of actin filaments. TIRF microscopy is a special technique which greatly reduces background fluorescence by generating an evanescent wave at the coverslip surface that migrates only a few hundred nanometers into the specimen. In the actin-polymerization TIRF-assay, fluorescently labeled actin monomers in a viscous polymerization buffer are applied to a specially treated flow cell which is coated with NEM-inactivated myosin heads. Nucleated filaments are captured by the myosin at the surface of the coverslip and continue to grow freely. Using TIRF-microscopy, the captured filaments can be excited and visualized at the coverslip surface while the fluorescently labeled monomers in solution are not excited, resulting in an optimal signal-to-noise ratio. This technique is described in appendix 1 in more detail.

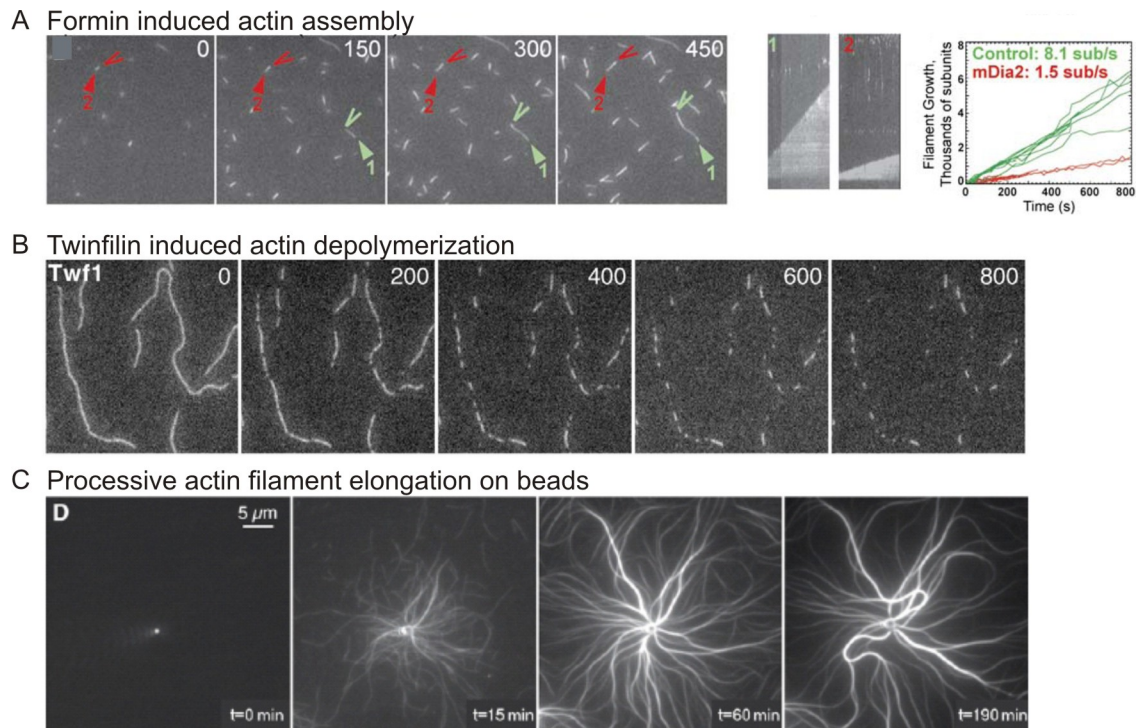


Figure 23. *In vitro* TIRF microscopy on single actin filaments. (A) Time-lapse micrographs of single actin filaments growing from a pool of 1 μM G-actin (30 % Oregon Green labeled) in the presence of nM amounts of the formin mDia2. The different elongation rates of formin-associated and freely-growing barbed ends are clearly distinguishable (Kovar et al., 2006). (B) Time-lapse micrographs of the depolymerization of single actin filaments after addition of twinfilin (Kovar et al., 2005). (C) Time-lapse micrographs of actin bundles formed on the surface of 2 μm polystyrene beads coated with the formin mDia1. The filaments growing at the bead surface are processively elongated by mDia1 which results in buckling of the bundles (at $t=190$ min) (Michelot et al., 2007).

This method is perfectly suited to evaluate the effects of accessory proteins on the single filament level. It allows measuring the on- and off-rates of actin polymerization and depolymerization directly (Kuhn and Pollard, 2005). Furthermore, it is possible to quantify mechanical properties of single filaments as well as the mechanism of the formation of complex actin structures (Amann and Pollard, 2001; Popp et al., 2006; McCullogh et al., 2008).

2. Results

2.1. Manuscript 1: Analysis of Actin Assembly by *In vitro* TIRF Microscopy

Breitsprecher D, Kieseewetter AK, Linkner J, Faix J (2009) *Methods Mol Biol.* 571:401-415.

(see appendix)

Abstract:

Since directed movement towards an extracellular chemoattractant requires rapid and continuous reorganization of the actin cytoskeleton to form complex structures such as a protruding lamellipodium, it is of great interest to analyze and understand the individual contribution of proteins specifically involved in this process. Over the last decade, enormous progress has been made towards understanding the versatile molecular mechanisms underlying actin-based cell motility and the regulation of site-specific F-actin assembly and disassembly. In spite of this wealth of knowledge and due to the constant discovery of novel regulatory factors, many questions remain to be answered. In this chapter, we describe a powerful method that allows studying the effects of actin-binding proteins on the assembly of single filaments by *in vitro* total internal reflection fluorescence (TIRF) microscopy using purified proteins and fluorescently labeled actin.

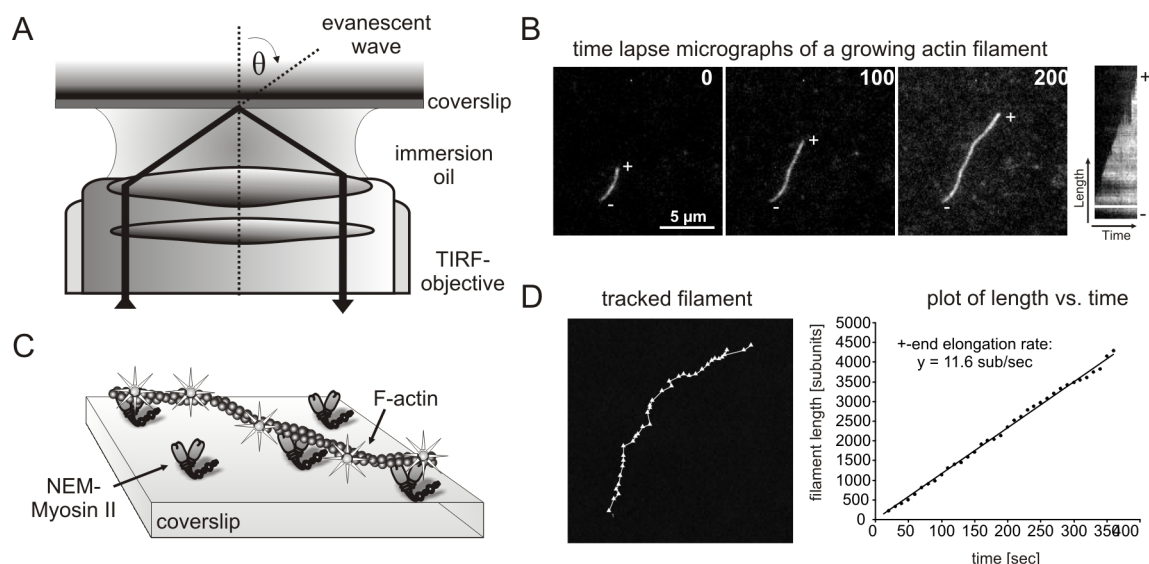


Figure 24: *in vitro* TIRF microscopy of actin assembly. (A) Principle of objective-based TIRF microscopy. (B) Time lapse micrographs of spontaneous filament assembly using 1.3 μM G-actin (30% labeled with Alexa-488-C₅ maleimide) in TIRF buffer on a NEM-myosin II coated coverslip. (C) Scheme of the visualization of single actin filaments using TIRF-microscopy. (D) Determination of elongation rates of single filaments. The elongation rate in subunits per second can be calculated from the slope of a plot of filament length vs time.

2.2. Manuscript 2: Arp2/3 complex interactions and actin network turnover in lamellipodia

Lai FP, Szczodrak M, Block J, Faix J, *Breitsprecher D*, Mannherz HG, Stradal TE, Dunn GA, Small JV, Rottner K (2008) *EMBO J* 27:982-992. (see appendix)

Abstract:

Cell migration is initiated by lamellipodia-membrane-enclosed sheets of cytoplasm containing densely packed actin filament networks. Although the molecular details of network turnover remain obscure, recent work points towards key roles in filament nucleation for Arp2/3 complex and its activator WAVE complex. Here, we combine fluorescence recovery after photobleaching (FRAP) of different lamellipodial components with a new method of data analysis to shed light on the dynamics of actin assembly/disassembly. We show that Arp2/3 complex is incorporated into the network exclusively at the lamellipodium tip, like actin, at sites coincident with WAVE complex accumulation. Capping protein likewise showed a turnover similar to actin and Arp2/3 complex, but was confined to the tip. In contrast, cortactin-another prominent Arp2/3 complex regulator-and ADF/cofilin-previously implicated in driving both filament nucleation and disassembly-were rapidly exchanged throughout the lamellipodium. These results suggest that Arp2/3- and WAVE complex-driven actin filament nucleation at the lamellipodium tip is uncoupled from the activities of both cortactin and cofilin. Network turnover is additionally regulated by the spatially segregated activities of capping protein at the tip and cofilin throughout the mesh.

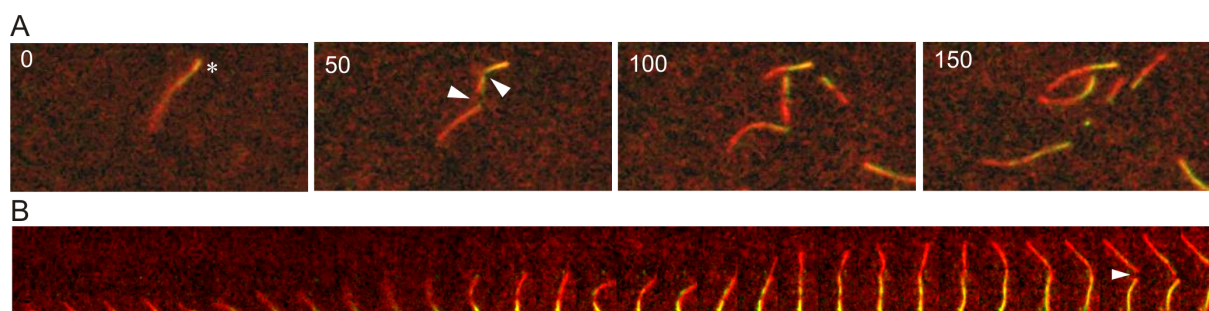


Figure 25: Filament severing by GFP-cofilin. (A) Time lapse micrographs of the polymerization of 1.3 μ M actin (30% Alexa 633-labelled, red) in presence of 400 nM GFP-cofilin (green). GFP-cofilin preferably binds and severs the aged filament containing ADP-F-actin. (B) Kymograph of GFP-cofilin mediated actin filament severing.

2.3. Manuscript 3: Clustering of VASP actively drives processive, WH2 domain-mediated actin assembly

Breitsprecher D, Kieseewetter AK, Linkner J, Urbanke C, Resch GP, Small JV, Faix J (2008) *EMBO J* 27:2943-2954. (see appendix)

Abstract:

Vasodilator-stimulated phosphoprotein (VASP) is a key regulator of dynamic actin structures like filopodia and lamellipodia, but its precise function in their formation is controversial. Using *in vitro* TIRF microscopy, we show for the first time that both human and Dictyostelium VASP are directly involved in accelerating filament elongation by delivering monomeric actin to the growing barbed end. In solution, DdVASP markedly accelerated actin filament elongation in a concentration-dependent manner but was inhibited by low concentrations of capping protein (CP). In striking contrast, VASP clustered on functionalized beads switched to processive filament elongation that became insensitive even to very high concentrations of CP. Supplemented with the *in vivo* analysis of VASP mutants and an EM structure of the protein, we propose a mechanism by which membrane-associated VASP oligomers use their WH2 domains to effect both the tethering of actin filaments and their processive elongation in sites of active actin assembly.

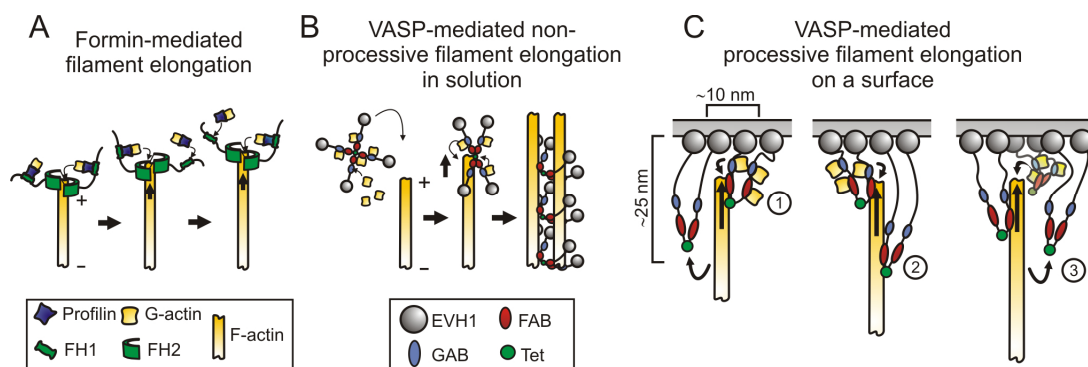


Figure 26: Models of VASP-mediated actin assembly. (A) Processive filament elongation by formins is shown for comparison. (B) Proposed mechanism for non-processive filament elongation by VASP in solution. VASP tetramers loaded with actin monomers hit a free barbed end, transiently bind and deliver bound actin subunits to it, resulting in non-processive filament elongation. Subsequent side binding of VASP results in decoration of the filament and mediates bundle formation. (C) Proposed mechanism for processive filament elongation on a surface: 1) VASP tetramers tethered to the surface bind actin filaments and deliver monomers via their WH2 domains to the barbed end. 2) After delivery, VASP remains bound to the side of the filament as the barbed end elongates in response to the delivery of actin monomers by other VASP molecules. 3) VASP molecules eventually detach from the filament due to continuous elongation of the barbed end and are subsequently available for a new cycle of actin addition. During the detachment period, the growing filament is constantly tethered to the surface by other VASP molecules.

2.4. Manuscript 4: Filopodia: Complex models for simple rods

Faix J, Breitsprecher D, Stradal TE, Rottner K (2009) *Int J Biochem Cell Biol* 41:1656-1664.

(see appendix)

Abstract:

Filopodia are prominent cell surface projections filled with bundles of linear actin filaments that drive their protrusion. These structures are considered important sensory organelles, for instance in neuronal growth cones or during the fusion of sheets of epithelial tissues. In addition, they can serve a precursor function in adhesion site or stress fibre formation. Actin filament assembly is essential for filopodia formation and turnover, yet the precise molecular mechanisms of filament nucleation and/or elongation are controversial. Indeed, conflicting reports on the molecular requirements of filopodia initiation have prompted researchers to propose different types and/or alternative or redundant mechanisms mediating this process. However, recent data shed new light on these questions, and they indicate that the balance of a limited set of biochemical activities can determine the structural outcome of a given filopodium. Here we focus on discussing our current view of the relevance of these activities, and attempt to propose a molecular mechanism of filopodia assembly based on a single core machinery.

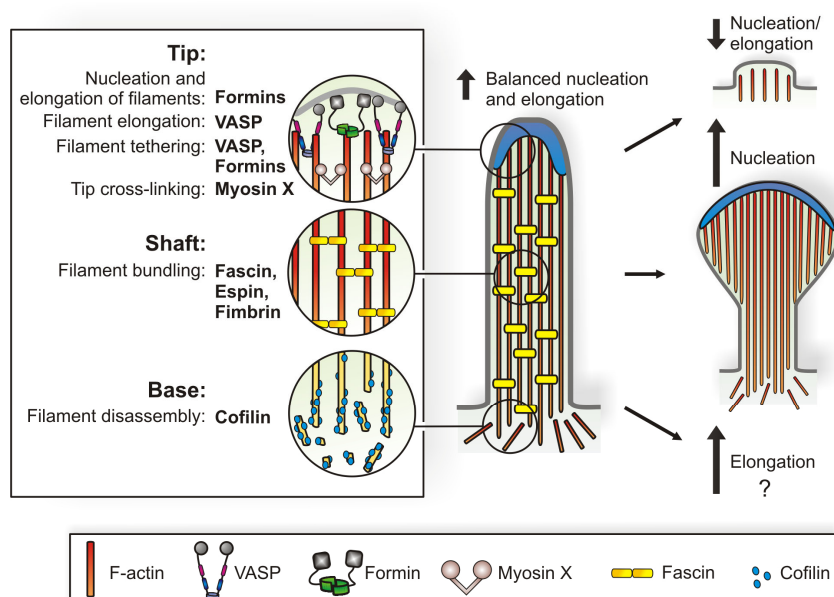


Figure 27: Filopodium formation requires a balance of biochemical activities. These activities include nucleation of actin filaments, as induced for instance by formins, their elongation and concomitant tethering to membranes, potentially mediated by various factors such as formins or VASP, bundling or cross-linking, represented by fascin and perhaps myosin X at filopodia tips, and their disassembly. We propose the ultrastructure of filopodia to be modulated by these core biochemical activities, which are all operating simultaneously, and in a balanced fashion during continuous protrusion of filopodia.

2.5. Manuscript 5: Affinity-based mechanism of fast Ena/VASP-mediated actin filament elongation

Breitsprecher D, Kieseewetter AK, Curth U and Faix J (2009) (manuscript in preparation)

Abstract:

Ena/VASP proteins are ubiquitous actin regulators that are implicated in a variety of fundamental cellular processes including cell migration, axon guidance and endothelial zippering. They are clustered at the tips of lamellipodia and filopodia where they processively assemble actin filaments in the presence of capping proteins to drive their protrusion. However, the molecular details underlying the mechanism employed by Ena/VASP proteins are still elusive, as VASP proteins from distinct species display drastic differences in their ability to accelerate filament elongation *in vitro*. Employing a domain-swapping approach generating chimeras from fast and slow elongating VASP proteins, we show here that filament elongation directly correlates with the saturation of the G-actin recruiting WH2 domains *in vitro*. Based on these results and under consideration of the physiological concentrations of the respective reaction partners, we propose a general affinity-based mechanism predicting rapid Ena/VASP-mediated actin filament elongation *in vivo*.

2.5.1. Introduction

The precise control of actin filament elongation is a key event in eukaryotic cells to establish coordinated cell movement driven by the formation of protrusive structures like filopodia and lamellipodia, to assemble the contractile ring at the cleavage furrow during cell division and to coordinate endocytosis and phagocytosis (Faix et al., 2009; Chesarone and Goode, 2009; Insall and Machesky 2009; Chhabra and Higgs 2007). The only proteins known so far that directly enhance filament elongation by interaction with the growing barbed end and recruitment of monomeric actin for polymerization are formins and Ena/VASP proteins. Proteins of the Ena/VASP family were previously shown to regulate the protrusion rate of lamellipodia (Rottner et al., 1999; Koestler et al., 2008) as well as the length of actin filaments and their branching density within lamellipodia (Bear et al., 2002) and *Listeria* comet tails (Plastino et al., 2004). Ena/VASP proteins are implicated in the formation of filopodia in mammals and *Dictyostelium* (Schirenbeck et al., 2006; Dent et al., 2007; Applewhite et al., 2007) and were also shown to enhance the actin-driven propulsion of *Listeria monocytogenes* (Loisel et al., 1999; Laurent et al., 1999; Geese et al., 2002) as well as of beads coated with ActA (Samarin et al., 2003). Additionally, they are required for neuritogenesis and cortex development (Kwiatkowski et al., 2007; Kwiatkowski et al., 2009)

and are implicated in tumor development and progression (Hu et al., 2008; Phillipar et al., 2009).

Ena/VASP proteins display a conserved tripartite architecture encompassing a N-terminal EVH1 domain required for subcellular targeting followed by a central proline-rich domain (PRD) implicated in recruitment of profilin-actin complexes (Jonkheere et al., 1999; Ferron et al., 2007), and a C-terminal EVH2 domain mediating tetramerization and interaction with monomeric and filamentous actin (Huettelmaier et al., 1999; Bachmann et al., 1999; Breitsprecher et al., 2008). The two actin-binding motifs within the EVH2 domain, referred to as the G-actin binding site (GAB) and the F-actin binding site (FAB), display sequence homology to WH2 motifs which are present in many actin regulators (Paunola et al., 2002; Dominguez 2007, Dominguez 2009).

Recently, it was shown that VASP accelerates actin filament barbed-end elongation *in vitro*, making it the second known actin filament elongator besides formins (Breitsprecher et al., 2008). However, the mechanisms employed by these two protein classes to enhance filament elongation are entirely different: formins remain processively associated with the growing filament barbed end by virtue of their dimeric FH2 domain which in turn also protects the filament from heterodimeric capping proteins (CP) (Zigmond et al., 2003; Harris and Higgs, 2004; Schirenbeck et al., 2005). Moreover, formin-mediated enhanced filament elongation depends on the recruitment of profilin-actin complexes by the adjacent proline-rich FH1 domain (Chang et al., 1997; Sagot et al., 2002, Kovar et al., 2006). By contrast, although VASP captures growing barbed ends (Pasic et al., 2008), it is not processively associated with the barbed end in solution, it does therefore not prevent CP from barbed end binding, and additionally profilin appears not to be mandatory to speed up filament elongation *in vitro* (Samarin et al., 2003; Schirenbeck et al., 2006; Breitsprecher et al., 2008). Most notably, mimicking localization of VASP to membranes by clustering the protein on a surface changes its mode of action and triggers processive filament elongation even in the presence of very high concentrations of CP. Collectively, this suggests that a multitude of VASP tetramers cooperate in tethering and elongating actin filaments to surfaces, which is likely to take place at sites of actin assembly at the cell periphery as well as at the surface of *L. monocytogenes* (Breitsprecher et al., 2008, Laurent et al., 1999; Footer et al., 2008, Faix et al., 2009). Although the filament elongation activity of VASP could be addressed to its GAB and FAB motifs, the underlying general mechanisms of VASP-mediated actin assembly remained obscure, as VASP from human (hVASP) showed a drastically reduced elongating activity when compared to the orthologue from the highly motile soil amoeba *Dictyostelium discoideum* (DdVASP) in *in vitro* assays (Breitsprecher et al., 2008).

Here we chose a domain shuffling approach by replacing the GAB, FAB and their connecting linker region of hVASP by those of the fast-elongating DdVASP to gain insights into the

molecular mechanism of Ena/VASP-mediated filament elongation. We found that the DdGAB has the most profound effect on filament elongation when transplanted into the backbone of hVASP. Biochemical analysis of the actin/GAB interaction revealed that the actin affinity of the GAB from the fast elongating *Dictyostelium* orthologue is more than three orders of magnitude higher than that of the slow elongating mammalian counterparts, suggesting that the actin affinity of the GAB might determine the VASP-mediated elongation rate *in vitro*. Consistent with this hypothesis, replacement of the GAB motif of hVASP by related WH2 domains from other proteins with different actin affinities in fact showed a direct correlation between the affinity to G-actin and the measured filament elongation rates. Our results allow us to formulate a general mechanism for affinity-based, WH2 domain-mediated actin assembly performed by Ena/VASP proteins, showing that the filament elongation rate is directly correlated to the saturation of the GAB with actin. Our results strongly suggest that the differences in the activities of Ena/VASP orthologues result from low actin concentrations used *in vitro*, and that therefore all Ena/VASP isoforms rapidly elongate actin filaments at high G-actin concentrations *in vivo* to drive actin-based protrusion.

2.5.2. Results

2.5.2.1. VASP, Mena and EVL enhance filament elongation to similar extends.

It was previously shown that hVASP only weakly accelerates actin elongation *in vitro*, whereas the *Dictyostelium* orthologue DdVASP strongly enhanced the growth of single filaments by a factor of 7 (Breitsprecher et al, 2008). Mammalian cells express two additional Ena/VASP proteins, referred to as Ena (Enabled) and EVL (Ena/VASP-like), the latter of which is abundantly expressed in the fast migrating neutrophils, suggesting that this particular paralogue might mediate faster filament elongation. In a search for the underlying reason causing differences in filament elongation, we compared DdVASP and the three mammalian Ena/VASP proteins and found that the WH2-like GAB motif sequences and the lengths of the linkers separating the GAB and FAB motifs differ greatly. Recently it was shown that the lengths of the linkers separating the three WH2 motifs in the protein Cobl are essential for its nucleation activity (Ahuja et al., 2007). Since models of VASP-mediated actin assembly propose that a GAB-bound actin monomer is handed over directly to the barbed end of the FAB bound filament (Dickinson 2008; Breitsprecher et al., 2008; Ferron et al., 2007), we assumed that the short 18 residues linker of hVASP might impair this transfer and hence cause the lower elongation activity of hVASP when compared to DdVASP. Notably, the linkers of VASP, EVL and Mena differ considerably in their length, encompassing 18, 27 and 35 residues, respectively (Figure 28 B). This notwithstanding, the sequences of their

GAB and FAB motifs are almost identical, suggesting that they display comparable actin-binding properties, which in turn makes them well suited candidates to investigate the effects of the linker lengths on filament elongation. We therefore employed TIRF microscopy to visualize the effect of recombinant Ena/VASP isoforms on single filament elongation *in vitro*. However, similar to hVASP, the EVH2 domain from Mena and full length EVL only slightly increased the elongation rate of actin filaments approximately 1.5 fold, both non-processive in solution and processively in the presence of CP when clustered on beads (Figure 28C and D). Thus, all three mammalian Ena/VASP isoforms possess virtually the same actin filament elongation properties and mediate considerably slower elongation rates when compared to DdVASP (Figure 28E).

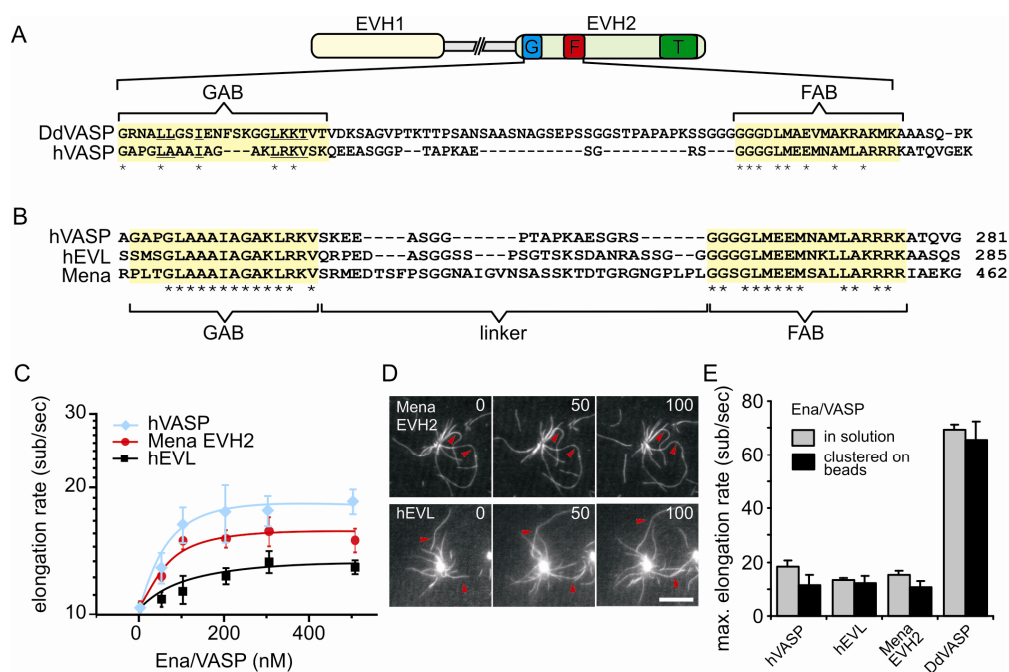


Figure 28: Effects of hVASP, Mena and hEVL on actin filament elongation. (A) General domain organization of Ena/VASP proteins and sequence alignment of the corresponding GAB-linker-FAB region within the EVH2 domains of DdVASP and hVASP. (B) Sequence alignment of the GAB-linker-FAB region of hVASP, hEVL and Mena. The linker length differs in all three proteins. Conserved amino acids are marked with an asterisk. (C) Elongation rates of 1.3 μ M OG-actin (30 % labeled) in presence of different concentrations of hVASP, Mena EVH2 and hEVL determined by single-filament TIRFM in TIRF buffer. (D) Mena EVH2 and hEVL both processively elongate actin filaments in the presence of 200 nM heterodimeric CP on saturated beads. Arrows indicate growing filaments. (E) Comparison of the maximal elongation rates of the three mammalian Ena/VASP isoforms and DdVASP on beads and in solution.

Analysis of the actin polymerization properties of the three Ena/VASP isoforms using pyrene assays revealed that Mena, EVL and hVASP also slightly increase the spontaneous nucleation of actin filaments, raising the concentration of barbed ends from about 0.5 nM for spontaneous actin assembly to 1.5-2.5 nM at 3 μ M G-actin (Figure 29A and B). Quantification of the bundling properties of the three constructs using low speed

sedimentation showed that hVASP and EVL had identical effects on bundle formation and triggered massive filament bundling already at low Ena/VASP:actin ratios, whereas the EVH2 domain of Mena had a much weaker bundling activity (Figure 29C). However, this effect might result from the usage of the EVH2 domain of Mena, since it was shown before that the EVH2 domain of VASP alone also has a reduced bundling activity when compared to the full-length protein, most likely due to a increased negative charge that impairs actin filament binding (Laurent et al., 1999; Huettelmaier 1999).

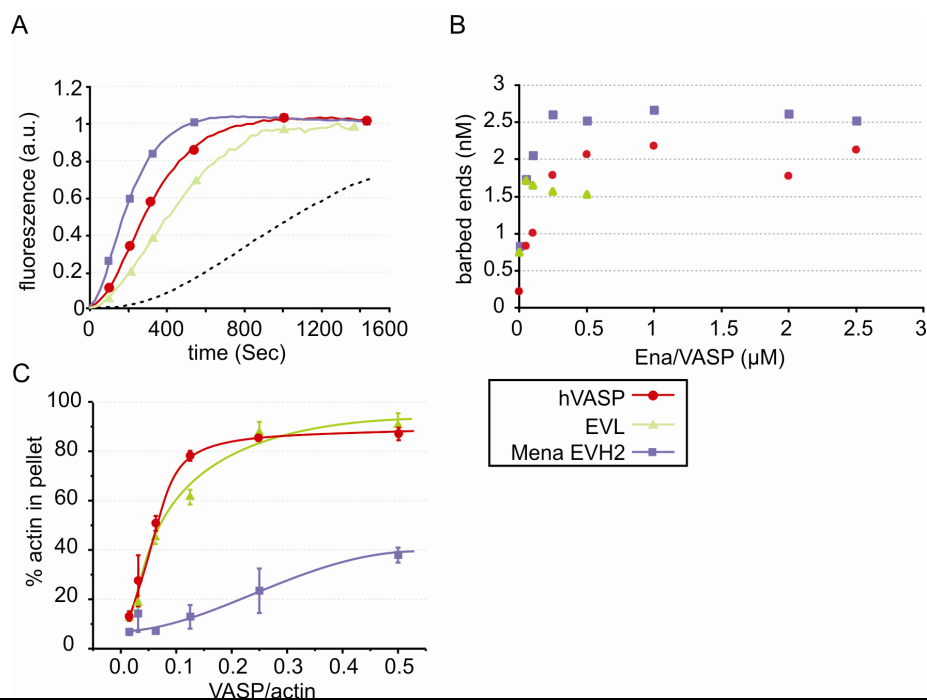


Figure 29: Effects of hVASP, Mena and hEVL on actin filament nucleation and bundling.

(A) Representative pyrene-assays of the polymerization of 3 μM G-actin (10 % pyrene labeled) in presence of 500 nM of the Ena/VASP proteins indicated. (B) Number of barbed ends formed in the presence of Ena/VASP proteins obtained from the slopes measured by pyrene assays and the elongation rates obtained by TIRF-microscopy for different Ena/VASP concentrations. (C) Bundling properties of hVASP, EVL and Mena EVH2. 5 μM actin were polymerized in presence of different amounts of Ena/VASP constructs indicated. The bundling activity was quantified by low-speed sedimentation assays and SDS-PAGE analysis of pellets and supernatants. Each experiment was repeated three times. Error bars represent s.d.

2.5.2.2. Replacement of the GAB and FAB motifs of hVASP with those from DdVASP reveal the molecular requirement for fast filament elongation.

Next, we tested whether the differences of both WH2-like actin binding motifs GAB and FAB from DdVASP and hVASP determine the elongation rate of VASP-mediated filament elongation. For this we constructed chimeric proteins in which the GAB and FAB of hVASP were replaced either alone or in combination with the corresponding motifs of DdVASP (Figure 30A). Chimera hVASP DdGABFAB, harboring both WH2 motifs from the

Dictyostelium protein, mediated virtually the same elongation rates as DdVASP, both in solution and clustered on beads (Figure 30B-D, Table 1).

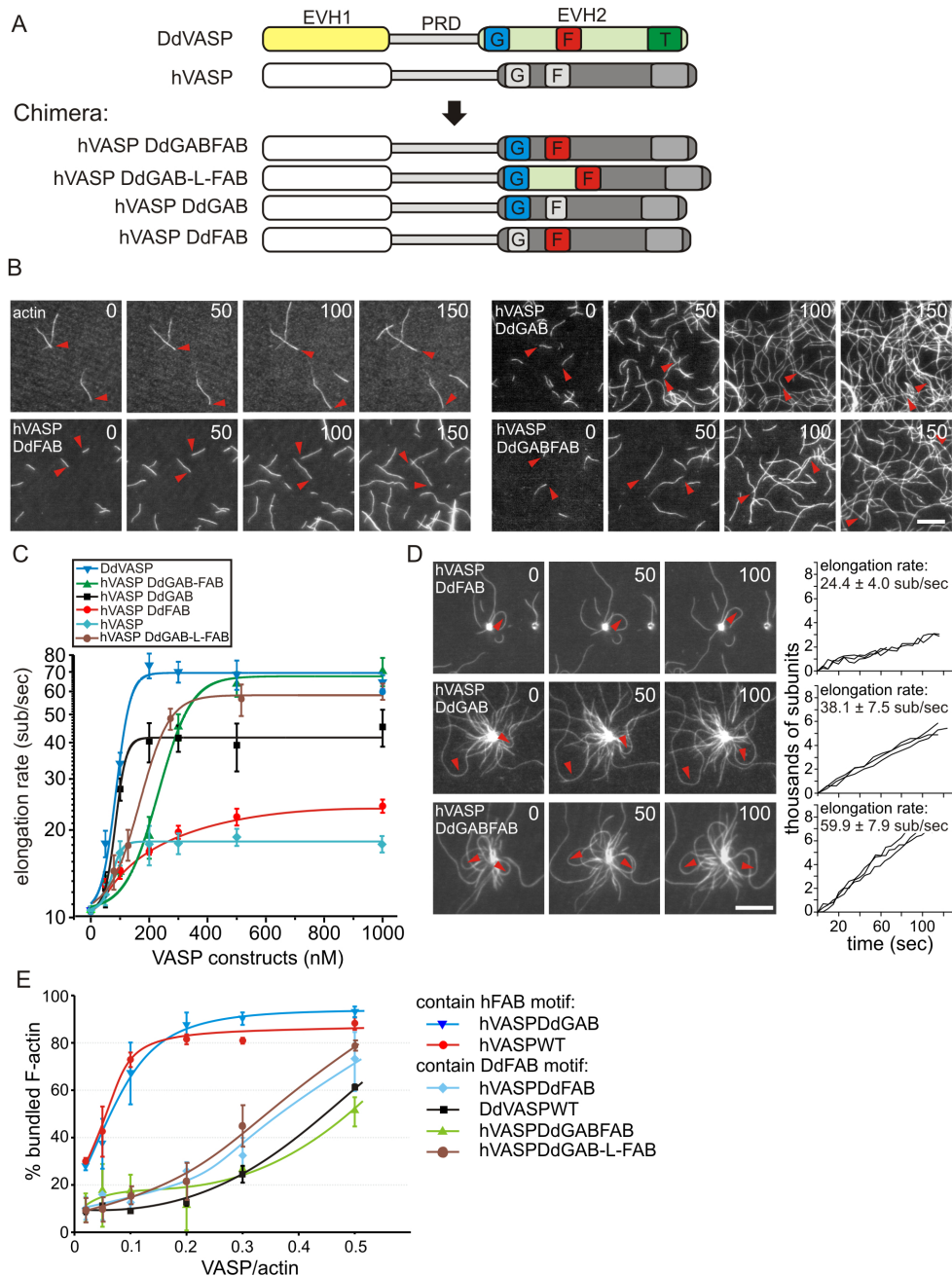


Figure 30: Replacement of the GAB and FAB in hVASP with the corresponding DdVASP motifs accelerates actin filament elongation. (A) Scheme of hVASP chimeras bearing different domains of DdVASP. DdVASP components are colored, hVASP components are shown in grayscale. (B) TIRFM micrographs of the assembly of 1.3 μ M OG actin (30 % labeled) in TIRF buffer containing 500 nM of the chimeras indicated. (C) Elongation rates of the chimeras in solution in a concentration range from 25 nM to 1 μ M. (D) TIRFM micrographs of the assembly of 1.3 μ M OG actin (30 % labeled) in TIRF buffer in presence of 200 nM CP and beads saturated with the hVASP chimeras indicated (left). Scale = 10 μ m. Time is indicated in seconds. Plots of the length of individual filaments versus time yield filament elongation rates (right). (E) Low-speed sedimentation analysis of the bundling activity of the different chimeras. Note that chimeras containing the hFAB motif bundle much more efficiently than those bearing the DdFAB motif. Error bars represent s.d.

Similar results were obtained with hVASP DdGAB-L-FAB, additionally containing the entire linker region of DdVASP, corroborating our previous findings which showed that the linker region does not strongly affect filament elongation (Figure 30C, Table 1).

| | maximal (non-processive) elongation rate in solution (sub/sec) | maximal (processive) elongation rate on beads (sub/sec) |
|-------------------|--|---|
| DdVASP | 69.3 ± 2.0 | 65.4 ± 6.9 |
| hVASP DdGABFAB | 67.3 ± 2.8 | 59.9 ± 7.9 |
| hVASP DdGAB | 40.6 ± 4.0 | 38.1 ± 7.5 |
| hVASP DdFAB | 23.2 ± 2.3 | 18.9 ± 4.0 |
| hVASP DdGAB-L-FAB | 58.7 ± 2.4 | 59.9 ± 7.9 |
| hVASP | 18.4 ± 2.3 | 11.5 ± 3.6 |
| EVL | 13.3 ± 0.8 | 11.3 ± 0.8 |
| Mena EVH2 | 15.4 ± 1.4 | 10.7 ± 2.4 |

Table 1: Elongation rates of VASP-mediated actin assembly in solution and on VASP-coated beads.

Low-speed sedimentation assays with different concentrations of the chimeras revealed that the bundling activity of constructs bearing the human FAB motif was indeed much higher than that of chimeras bearing the DdFAB motif (Figure 30E). Chimera hVASP DdFAB mediated only a moderate acceleration of filament elongation up to 23.2 sub/sec, suggesting that the contribution of the FAB motif to filament elongation is smaller than that of the GAB motif (Figure 30B-D, Table 1).

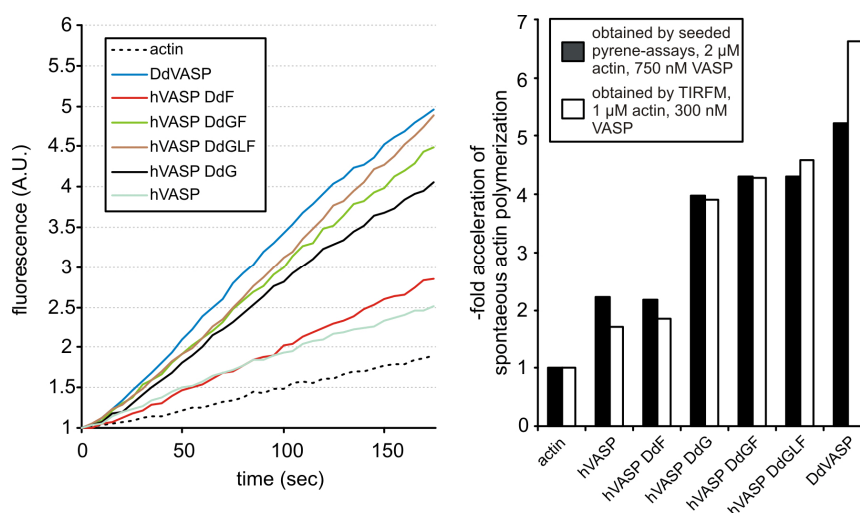


Figure 31: Differential acceleration of filament elongation by hVASP chimeras. (Left) Seeded pyrene assays of the spontaneous polymerization of 2 μM G-actin (10 % Pyrene labeled) and 50 nM F-actin seeds in polymerization buffer in the presence of 750 nM of the VASP constructs indicated. (Right) Comparison of filament-elongation rates obtained by seeded pyrene assays and TIRF-microscopy.

The differential enhancement of filament elongation by the VASP chimeras was confirmed by seeded pyrene actin polymerization assays, and the results obtained with this assay largely correspond to those obtained by TIRF microscopy (Figure 31).

2.5.2.3. The GAB motifs from hVASP and DdVASP display drastically different affinities to G-actin

Since the transplantation of the DdGAB motif into the hVASP backbone was already sufficient to enhance actin filament elongation 4-fold, we hypothesized that differences in the actin-binding properties of the GAB motifs from hVASP and DdVASP might be responsible for the different elongation rates. Therefore, we employed pyrene assays to analyze the effects of the WH2-like GABs of both proteins during actin assembly and in steady state at different concentrations of GAB peptides fused to MBP. Since many WH2-containing proteins have specific functions in actin assembly depending on the arrangement of their WH2 motifs, we simultaneously employed the same assays to analyze the effects of the entire EVH2 domains of hVASP and DdVASP, encompassing the GAB, FAB and Tet motif and which were shown to be already sufficient to maximally enhance filament elongation (Breitsprecher et al., 2008).

Excess amounts of MBP DdGAB did not sequester G-actin at equimolar concentrations and showed only a slight sequestering effect at a very high molar excess (Figure 32A). Additionally, excess amounts of MBP DdGAB decreased spontaneous actin nucleation as assessed by pyrene assays (data not shown). In contrast, the DdEVH2 domain, encompassing the GAB, FAB and tetramerization domain, strongly promoted actin assembly in pyrene actin polymerization assays at molar ratios lower than DdEVH2:actin 1:1, corroborating our previous finding that the EVH2 alone is sufficient to maximally enhance filament elongation (Figure 32B and C; Breitsprecher et al., 2008). Additionally, excess amounts of the DdEVH2 domain in polymerization and steady-state experiments lead to a massive sequestration of actin and a reduced polymerization rate already at molar ratios above DdEVH2:actin 1:1 (Figure 32A-C). Since pyrene actin polymerization assays monitor both, spontaneous nucleation and elongation of actin filaments, the decreased polymerization rate by excess amounts of DdEVH2 might result from decreased nucleation, elongation or both.

We reasoned that the DdEVH2 might bind monomeric actin with high affinity, resulting in a lower number of bound actin monomers per tetramer at excess amounts of DdEVH2, in turn leading to decreased filament elongation. Indeed, the elongation rate of single actin filaments dropped at excess amounts of DdEVH2 as assessed by TIRF microscopy (Figure 32D). Additionally, in agreement with the finding that WH2 domains exhibit profilin-like effects on actin assembly and inhibit spontaneous actin filament nucleation (Hertzog et al., 2004), the

total number of growing actin filaments in the TIRF assays decreased with increasing DdEVH2 concentrations (data not shown).

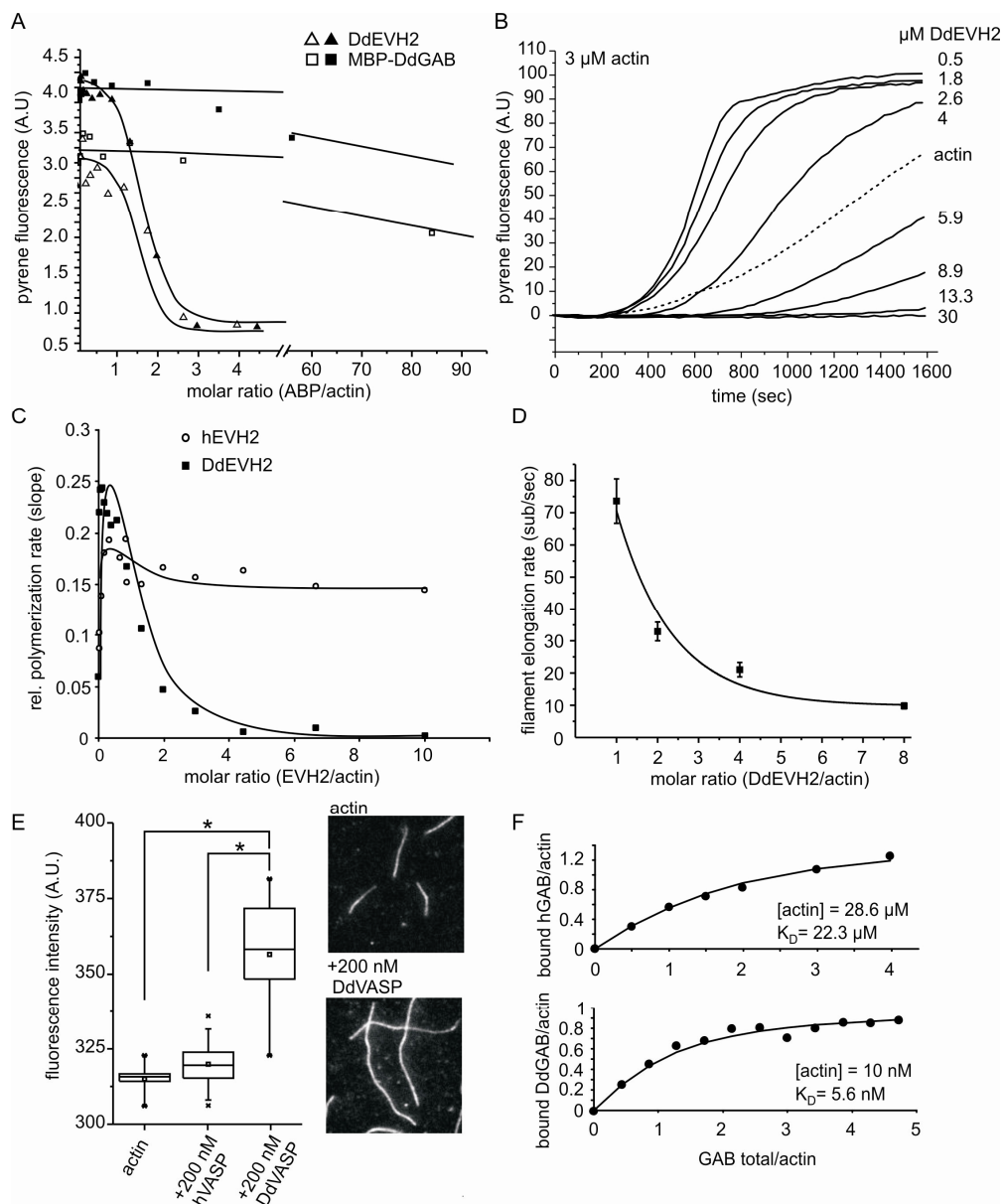


Figure 32: Analysis of G-actin-binding and sequestering activities of the EVH2 domains of hVASP and DdVASP. (A) Actin (4 μM , closed symbols; 3 μM , open symbols; 10% pyrene labeled) was polymerized in the presence of different concentrations of MBP-DdGAB or DdEVH2 over night. Pyrene fluorescence was measured to quantify F-actin. (B) Kinetics of the polymerization of 3 μM actin (10% Pyrene labeled) in presence of increasing amounts of DdEVH2. (C) Maximal polymerization rates determined from B decrease at molar ratios above DdEVH2:actin 1:1. Excess amounts of hEVH2 did not inhibit actin polymerization. (D) Filament elongation rates determined by TIRF microscopy at different excess amount of DdEVH2. (E) Enhanced fluorescence of single filaments polymerized by DdVASP. 1 μM G-actin (30% Alexa488-labeled) was polymerized in TIRF buffer in presence of 200 nM DdVASP or hVASP and visualized by TIRFM. The relative filament fluorescence was analyzed by profile-plotting using ImageJ. Representative micrographs are depicted. For each condition at least 50 filaments were analyzed. Boxes indicate 25th percentile, median and 75th percentile of all values; error bars indicate 10th and 90th percentile. * $p < 0.0001$. (F) Determination of the K_D s of the binding of GFP-DdGAB and GFP-hGAB to actin by analytical ultracentrifugation.

In contrast to the DdEVH2, excess amounts of the hVASP EVH2 domain (hEVH2) did neither markedly inhibit actin polymerization nor sequester actin monomers. The polymerization rate determined by pyrene assays rather dwelled at an intermediate level even at excess amounts of hEVH2 (Figure 32C). This in turn suggests that its G-actin-binding affinity is much lower when compared to DdEVH2.

To test whether filament-bound VASP is still able to recruit actin monomers, we analyzed the relative fluorescence intensity of single actin filaments polymerized in the presence and the absence of DdVASP and hVASP by TIRF microscopy. These experiments showed that the filaments which were formed in presence of DdVASP were significantly brighter than the control filaments, whereas filaments formed in presence of hVASP showed only a slight increase in their fluorescence intensity (Figure 32E). These results corroborate our proposed mechanism for VASP-mediated filament elongation in solution, in which VASP binds the actin filament barbed end, transfers its bound subunits and subsequently stays attached to the side of the filament (Breitsprecher et al., 2008), and further suggest that the differences in DdVASP- and hVASP-mediated actin assembly are primarily due to different affinities of their respective GABs to G-actin.

To test this hypothesis, we determined the G-actin affinities of the GAB motifs from hVASP and DdVASP. Common assays to quantify actin-WH2 interactions are fluorescence titrations with monomeric NBD-, pyrene- or acrylodan-labeled actin. However, the binding of MBP-hGAB and MBP-DdGAB constructs to actin did not cause a detectable change in the fluorescence signal of either of the labeled actin species mentioned above (data not shown). Therefore, we expressed GFP-GAB fusion proteins encompassing all residues in-between the last poly-proline stretch and the FAB of VASP and performed analytical ultracentrifugation, monitoring either GFP-fluorescence or absorption for quantification of G-actin-binding. Both GAB motifs bound to monomeric actin, albeit with markedly different affinities (Figure 32F). We determined the K_d for the DdGAB/actin interaction with single exponential fitting to 6 nM, whereas the K_d for the hGAB/actin interaction was in the range of 22 μ M, corroborating our previous assumption that the actin affinities of the human and *Dictyostelium* orthologues must differ greatly.

2.5.2.4. Replacement of the GAB of hVASP by high-affinity actin-binding WH2-motifs reveals the general mechanism of VASP mediated actin assembly.

Our finding that the binding affinity of the DdGAB to G-actin is about 3 orders of magnitude higher than that of the hGAB prompted us to speculate whether high-affinity G-actin binding is the key for fast WH2-mediated actin filament elongation *in vitro*. To analyze the effects of the G-actin affinity of the GAB in more detail, we replaced the GAB in hVASP with WH2 core motifs from other proteins that are *per se* not implicated in actin filament elongation, namely

the second WH2 motif from N-WASP, the WH2 motif from WIP, the WH2 motif from Thymosin β 4 (T β 4) and the second and third WH2 motif from the actin nucleator Cobl. The K_d s for these motifs have been previously determined at identical buffer conditions and span a range from 40 nM to 3.1 μ M (Figure 33A; Cherau et al., 2005; Ahuja et al., 2007, Co et al., 2007), suggesting that these chimeric VASP proteins will differentially accelerate actin assembly *in vitro*. All five WH2 motifs share the conserved amino acid residues typical for WH2 domains, including the LxxV/T motif and the N-terminal, hydrophobic residues that bind to the barbed end of actin (Figure 33A; Cherau et al., 2005).

All WH2 chimeras promoted actin assembly in an Ena/VASP-mediated fashion, enhancing actin elongation in solution and processively elongating actin filaments even in presence of CP when clustered on polystyrene beads (Figure 33B and C). As hypothesized, we found a direct correlation between the maximal filament elongation rate and the respective G-actin-binding affinities of the individual WH2 motifs. Namely, the elongation rates were faster with increasing actin affinities of the WH2 motifs both in solution and on VASP-saturated beads. This K_d -dependence was more pronounced with the proteins in solution, where the chimeras bearing the rather weakly binding WH2 motifs from Cobl (Cobl3; K_d = 432 nM) N-WASP (K_d = 900 nM) and T β 4 (K_d = 3.1 μ M) accelerated actin assembly only up to 24 and 20 sub/sec, respectively, whereas the chimera with the higher affinity WH2 motif from WIP (K_d = 160 nM) accelerated filament elongation already up to 32 sub/sec (Figure 33C). Surprisingly, construct hVASP Cobl2, which was expected to strongly accelerate filament elongation in solution up to 4-fold due to its high affinity to actin (K_d = 40 nM), enhanced filament elongation merely 2-fold up to 21 sub/sec in solution. Due to the previously reported strong sequestering activity of the Cobl-WH2 motifs (Ahuja et al., 2007), we employed pyrene-assays to elucidate whether chimera hVASP Cobl2 also has a sequestering activity, which in turn would explain the rather low elongation rate. hVASP Cobl2 strongly sequestered G-actin already at low concentrations as assessed by pyrene assays and steady state measurements of the F-actin fluorescence (Figure 34). Sequestering of actin in turn results in decreasing concentrations of free actin monomers in our TIRF assay with increasing amounts of hVASP Cobl2, therefore most likely limiting the maximal elongation rate of this chimera. However, the reason for the sequestering activity of this particular WH2 motif is currently unclear. Comparable effects were not observed for the other hVASP WH2 chimeras or hVASP DdGAB at concentrations used in TIRF assays (data not shown). Actin sequestering by hVASP Cobl2 was, however, negligible when it was coated to polystyrene beads due to the much lower overall-amount of hVASP Cobl2 in the reaction mixture. In this case, the elongation rate of processively growing filaments mediated by hVASP Cobl2 reached 35 sub/sec, a value in a range that was also initially expected for its activity in solution (Figure 33D). The chimeras hVASP WIP, hVASP N-WASP, hVASP T β 4 and hVASP

Cobl3 enhanced processive filament growth on beads to a slightly higher extend compared to the maximal elongation rate obtained in solution. To explain these differences, we calculated the saturation Θ of the WH2 motifs at 1.3 μM actin either for 1 μM of the respective chimeras in solution or for chimeras clustered on beads, showing that Θ indeed changes depending on the experimental setup due to different concentration ratios.

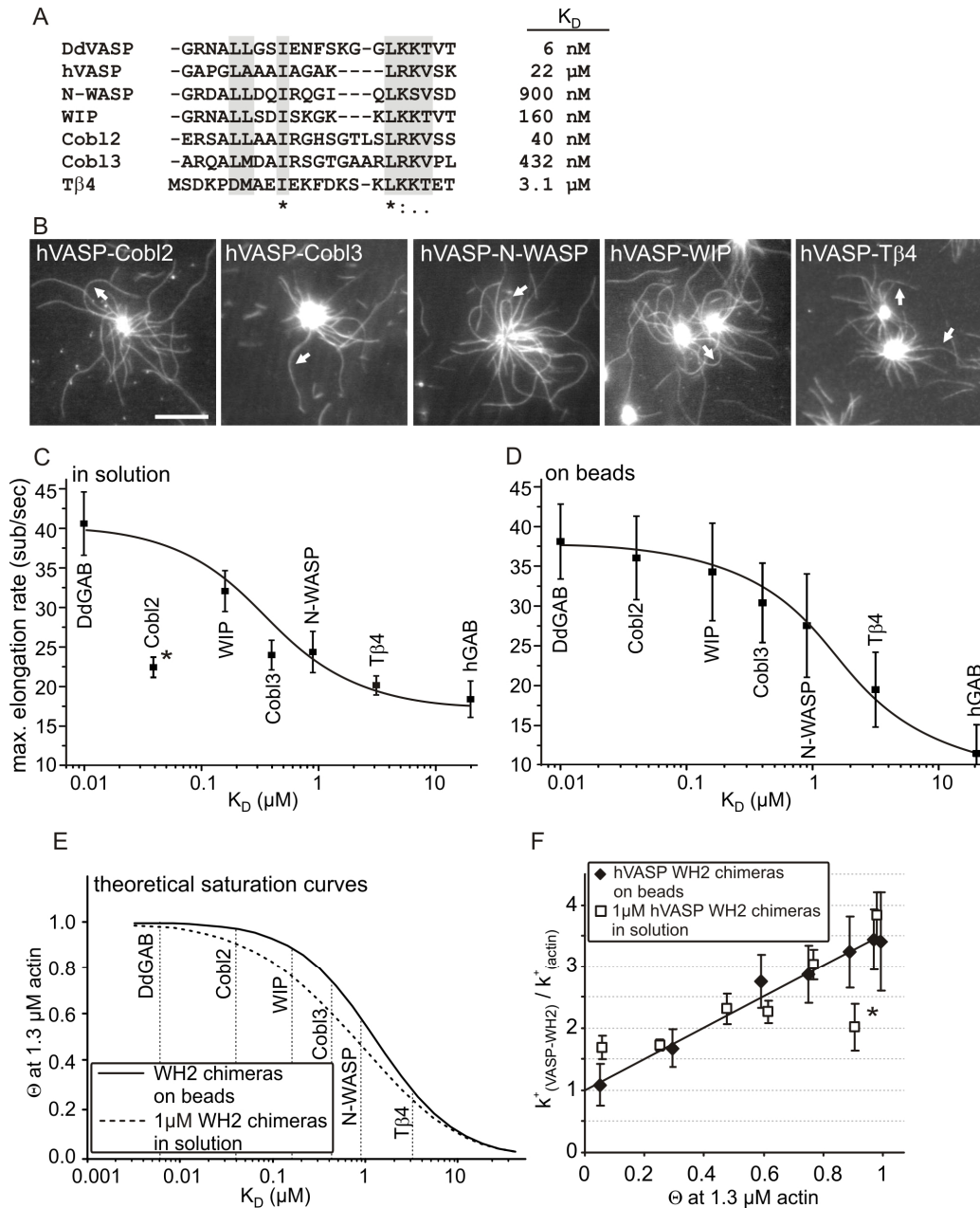


Figure 33: Exchange of the GAB with WH2 domains from other actin-binding proteins revealed the molecular basis of fast, VASP-mediated actin assembly. (A) The GAB of hVASP was exchanged for WH2 motifs indicated with previously determined K_D s (Ahuja et al., 2007; Cherau et al., 2005; Co et al., 2007). (B) All chimeras processively elongated actin filaments from 1.3 μM G-actin (30% OG labeled) in the presence of 50 nM CP when clustered on beads as assessed by TIRF-microscopy. (C) Maximal elongation rates of hVASP chimeras and WT in solution. *The Cobl2 chimera was excluded from fitting since it strongly sequestered G-actin already at low concentrations (see Figure 7). (D) Maximal elongation rates of hVASP chimeras and WT on beads. (E) Correlation between the theoretical saturation of the WH2 motifs with actin on beads and in solution. Note that the saturation of the WH2 motif is higher

when clustered on a bead surface (at an excess of actin). (F) Elongation rate enhancement of actin assembly of hVASP-WH2 mediated actin assembly in solution and on beads directly correlates with Θ (obtained from E). $n > 30$ for bead assays and $n > 50$ for assays in solution. Error bars represent standard deviations.

While the concentration of free actin was not altered by binding to WH2 motifs with hVASP chimeras clustered to the beads due to the low overall amount of WH2 motifs and therefore an excess of actin monomers in the reaction mixture, the concentration of free actin was changed when equimolar concentrations of the hVASP WH2 chimeras were present in solution, leading to slightly lower saturations of the WH2 motifs with actin, and hence resulted in slightly slower elongation rates (Figure 33E). Most notably, plotting of all calculated Θ values against the enhancement of filament elongation by the hVASP chimeras revealed a linear correlation, demonstrating that solely the saturation of the WH2 motif with actin is responsible for different elongation properties of the hVASP WH2 chimeras (Figure 33F).

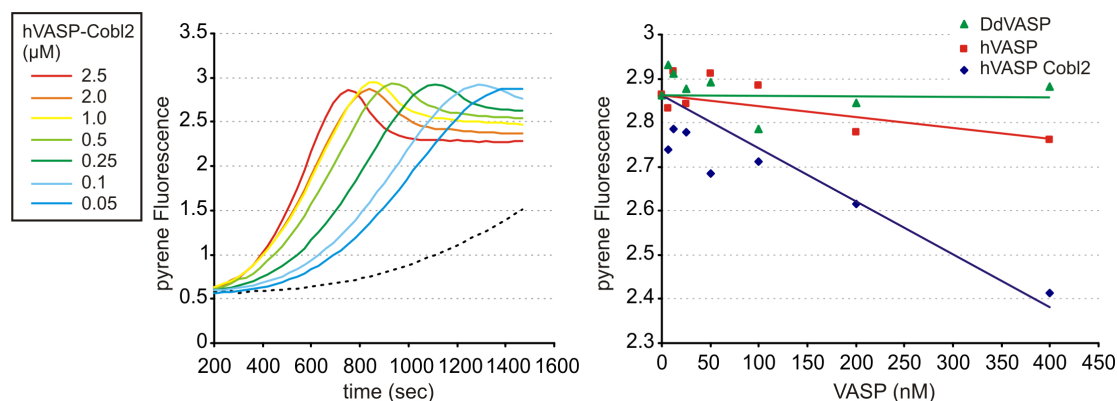


Figure 34: hVASP-Cobl2 sequesters G-actin. (left) Pyrene actin assembly assay of 3 μM G-actin (10 % pyrene-labeled) in presence of hVASP-Cobl2. (right) Plot of the F-actin fluorescence at steady state of 3 μM actin at different concentrations of DdVASP, hVASP and hVASP-Cobl2. Only hVASP-Cobl2 sequestered actin already at nM-concentrations.

2.5.2.5. Nucleation properties of VASP and VASP-chimeras

Recent studies showed that WH2-domain containing proteins like Spire, Lmod, Cobl or JMY are capable of nucleating filaments from G-actin employing different mechanisms (Quinlan et al., 2005; Ahuja et al., 2007; Cherau et al., 2008; Zuchero et al., 2009; Chesarone and Goode, 2009). It was previously reported that VASP has only a weak nucleation activity in pyrene assays (Huettelmaier et al., 1999; Walders-Harbeck et al., 2002; Laurent et al., 1999; Samarin et al., 2003). However, the finding that filaments grew even in the presence of high concentrations of CP on VASP coated beads indicated that this protein is also able to nucleate new filaments (Breitsprecher et al., 2008). Moreover, as the saturation of the mammalian Ena/VASP members with actin seems to be much higher at physiological actin

concentrations, it is worthwhile to address the question whether VASP may also be responsible for *de novo* actin nucleation *in vivo*.

The nucleation properties of chimera hVASP DdGAB were of particular interest, since this construct is already saturated with G-actin under our experimental conditions (Figure 33E), therefore most likely mimicking the state of hVASP WT at high actin concentrations *in vivo*. We used pyrene actin polymerization assays and TIRF microscopy to quantify the nucleation properties of the different VASP chimeras and wild type proteins. We found that all VASP constructs enhanced polymerization from G-actin, albeit with very different initial rates (Figure 35A and B). Calculation of the number of barbed ends formed in the presence of different VASP constructs within the first 200 seconds of polymerization showed that mutant hVASP DdGAB had the most pronounced effect on nucleation, raising the concentration of barbed ends up to 6 nM already at low nM concentrations (Figure 35C), which corresponds to a nucleation efficiency of 30% for the VASP tetramer (Figure 35D). Comparable nucleation efficiencies can be found for strong actin nucleators such as the Arp2/3 complex or formins (Marchand et al., 2001; Neidt et al., 2008). Constructs hVASP WT, hVASP DdGABFAB, and hVASP DdFAB had only minor effects on actin nucleation, raising the number of ends up to 2 nM only at considerable higher VASP concentrations, whereas DdVASP and hVASP DdGAB-L-FAB had virtually no effect on spontaneous actin nucleation (Figure 35C and D).

Differential nucleation by hVASP, hVASP DdGAB and hVASP DdGABFAB could also be observed on saturated beads (Figure 35E and F). The number of filaments formed by VASP in solution was directly proportional to the number of newly nucleated filaments on coated beads within 10 minutes, suggesting that clustering of VASP did not affect its nucleation properties (Figure 35G). Surprisingly, high affinity actin binding by the DdGAB alone was not sufficient to enhance spontaneous nucleation, since DdVASP WT, hVASP DdGABFAB and hVASP DdGAB-L-FAB did not maximally enhance nucleation. Instead, the highest nucleation activities were obtained for constructs bearing the hFAB motif (Figure 35G). Those constructs were also shown to bundle actin filaments more efficiently than those bearing the DdFAB motif, indicating a higher F-actin affinity of the hFAB motif (Figure 30E). The reason for the very high nucleation activity of the hVASP DdGAB chimera might therefore be the combination of the high-affinity G-actin-binding DdGAB motif and the strong F-actin-binding hFAB motif. While the DdGAB motifs recruit G-actin very effectively, therefore raising the local actin concentration, actin dimers and trimers might be stabilized by the hFAB. Consistently, hVASP WT, harboring the low-affinity G-actin-binding hGAB, showed a five times lower nucleation activity when compared to hVASP DdGAB but, however, due to the proposed stabilizing effect on nucleation seeds, it still enhanced nucleation activity when compared to the constructs bearing the DdFAB motifs (Figure 35C-G). Furthermore, hVASP

DdGABFAB nucleated new filaments about 2 times more efficient than DdVASP WT (Figure 35C and D).

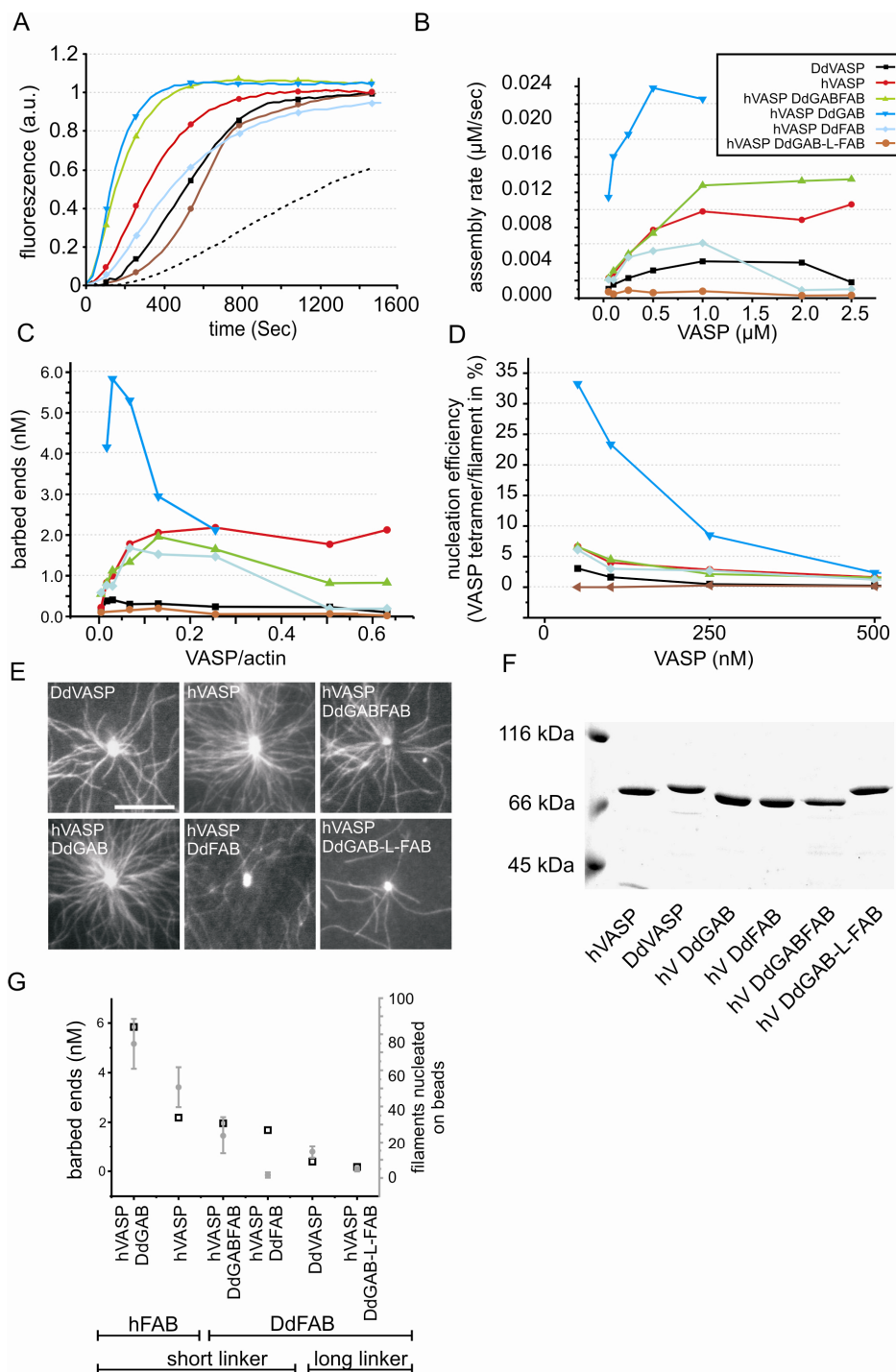


Figure 35: hVASP chimeras differentially nucleate actin filaments. (A) Kinetics of the polymerization of 4 μM G-actin (10 % pyrenyl-labeled) in the presence of 1 μM of VASP proteins indicated. (B) Plot of the dependence of the initial actin assembly rate on the concentration of VASP constructs. Assembly rates for hVASP DdGAB concentrations higher than 1 μM were not accessible due to light scattering caused by filament bundling. (C) Plot of the nucleation efficiency of the VASP chimeras indicated. Values were calculated from assembly rates from B and elongation rates determined by TIRFM (Figure 28C and 30C). (D) Nucleation efficiency of chimeric hVASP tetramers. (E) Micrographs of the assembly of 1.3 μM actin (30% OG labeled) on representative beads coated with VASP chimeras indicated. Pictures were taken after 10 minutes of

polymerization. Scale bar 10 μm . (F) SDS-PAGE of VASP-chimeras eluted from beads shown in D. (G) The number of filaments nucleated on VASP-coated beads was directly proportional to the number of barbed ends nucleated by VASP in solution. Error bars represent s.d.

This might be caused by the shorter linker between GAB and FAB in the chimeric protein. If the formation of filaments from GAB-bound actin monomers and FAB-bound nucleation seeds is a diffusion-dependent process, the nucleation efficiency is expected to drop with increasing linker lengths. However, this correlation was not observed for the three Ena/VASP isoforms VASP, Mena and EVL, where Mena was the best nucleator despite having the longest linker region and the weakest bundling/F-actin-binding activity (Figure 29).

2.5.3. Discussion

Cells utilize the power of actin polymerization to mediate their locomotion by the formation of actin rich protrusions like lamellipodia and filopodia. The spatial and temporal enhanced elongation of actin filaments by specialized proteins is a key event in the formation of these highly dynamic structures (Faix et al., 2009, Matilla and Lappalainen, 2007; Chhabra and Higgs, 2007, Insall and Machesky, 2009). Filament assembly driven by actin filament elongating proteins is required to prevent capping of barbed ends by CP and therefore allowing filament growth exclusively in specific sites. As yet, only two classes of proteins have been identified that directly accelerate the polymerization of actin filaments, namely formins and Ena/VASP proteins. Whereas the mechanism of formin-mediated actin filament elongation is already quite well understood (Paul and Pollard, 2009; Goode and Eck, 2007), the molecular mechanism underlying Ena/VASP-mediated actin assembly is still elusive.

In this work, we describe a general, affinity-based mechanism by which Ena/VASP proteins differentially enhance actin-filament elongation, both non-processively in solution and processively on functionalized surfaces. The comparison of hVASP chimeras encompassing WH2 motifs with different actin affinities revealed that enhanced filament elongation by Ena/VASP proteins results from direct binding and incorporation of actin monomers by their WH2-like actin-binding motifs, and moreover, that their G-actin affinity correlates directly with the filament elongation rate.

Previously, it was shown that hVASP and DdVASP both accelerated actin-filament elongation *in vitro*, albeit to markedly different extents: while DdVASP enhanced the growth of single filaments 7-fold, hVASP had rather small effects accelerating filament elongation not even two-fold (Breitsprecher et al., 2008). In this line, the two remaining mammalian Ena/VASP members EVL and Mena analyzed here showed comparable low filament-elongating activities as hVASP. To elucidate the molecular requirement for the massive enhancement of actin-filament elongation by DdVASP, the two WH2-like actin-binding motifs GAB and FAB from hVASP were replaced by those from DdVASP and analyzed by TIRF

microscopy *in vitro*. These analyses showed that both DdVASP motifs separately enhance filament elongation. The combination of both motifs in the hVASP backbone was already sufficient to elicit equally high elongation rates as those mediated by wild type DdVASP. The finding that the G-actin affinity of the DdGAB motif was more than three orders of magnitude higher than that of the hGAB motif prompted us to speculate that the elongation rate of VASP-mediated actin assembly might be directly correlated with the actin affinity – and therefore the saturation of the VASP tetramer with actin subunits. This hypothesis was substantiated by subsequent experiments using hVASP chimeras encompassing, instead of the GAB, WH2 motifs from other actin-binding proteins with varying actin affinities. These experiments moreover revealed a linear correlation between enhancement of filament growth and the calculated saturation of the VASP tetramer with actin.

A theoretical model describing the processive elongation of actin filaments by elongation factors is the so-called “actoclampin” model of clamped elongation (Dickinson and Purich, 2002; Dickinson 2008). The hypothetical actoclampin protein mediates filament elongation by two actin-binding modules, one processively tracking and tethering the growing filament end and the other binding and delivering monomeric actin for elongation. Rate limiting factors for filament elongation are therefore either the translocation speed of the filament binding module or the number of actin monomers recruited and delivered by the monomer binding module. This model can in principle be transferred to the action of both, formins and Ena/VASP proteins. However, due to the considerable structural and biochemical differences concerning their interaction with G- and F- actin, it is obvious that these two protein families employ different mechanisms to enhance filament elongation (Chesarone and Goode, 2009; Ferron et al., 2007; Breitsprecher et al., 2008; Kovar et al., 2006). Formins consist of a conserved, dimeric FH2 domain that tightly binds to and processively translocates at the growing end of the filament while actin monomers are recruited by the adjacent FH1 domains in form of profilin-actin complexes that are subsequently added to the growing barbed end to speed up filament assembly. Profilin is mandatory to enhance filament elongation by formins *in vitro*, since the FH2 domain alone has only a negligible affinity towards G-actin (Kovar et al., 2006; Pring et al., 2003). Therefore, in the absence of profilin, formin-assembled actin filaments grow slower than spontaneously assembled actin filaments, which would correspond to a rate-limiting effect on filament elongation of the translocating filament binding module in the actoclampin model (Kovar et al., 2004; Kovar et al., 2006, Dickinson 2008). This parameter is quantified by the “gating factor” of the FH2 domain, which describes the fraction of the time the formin spends in the open state, allowing actin monomer incorporation (Paul and Pollard, 2009).

In contrast to formins, we have recently shown that VASP does not processively translocate at the growing barbed end of the filament in solution – and does therefore not prevent CP

from capping barbed ends – but that it only transiently binds the barbed end and subsequently stays attached to the side of the filament when the protein is soluble (Breitsprecher et al., 2008). Most notably, clustering of VASP on a surface changes its mode of action and triggers processive filament elongation even in the presence of CP, a finding that might resemble its task *in vivo*, where it is clustered to the plasma membrane in sites of rapid membrane protrusion (Rottner et al., 1999, Koestler et al., 2008; Breitsprecher et al., 2008). Enhanced filament elongation by VASP relies on the small, WH2 like actin-binding motifs GAB and FAB within the C-terminus of the protein (Breitsprecher et al., 2008; Dominguez 2007, Ferron et al., 2007). Furthermore, we have shown that profilin is not mandatory to enhance VASP-mediated filament elongation *in vitro* despite the presence of several proline-rich regions comparable to those in the FH1 domain of formins.

In this work, we addressed the differences in filament elongation by hVASP and DdVASP to different actin-affinities of their WH2-like GABs. While the hGAB binds G-actin with a K_d of only 22 μM , the affinity of the DdGAB to monomeric actin was found to be very high (K_d of 6 nM). Since insertion of the DdGAB into the hVASP backbone was already sufficient to speed up filament elongation 4-fold, we hypothesized that the high-affinity actin binding and therefore the saturation of the protein with actin is key for rapid Ena/VASP-mediated filament elongation, and that each GAB within the tetramer delivers only one actin monomer. On the basis of this result and after analyzing chimeric proteins encompassing WH2 motifs from other actin-binding proteins with different actin affinities, we conclude that i) the function of the GAB in filament elongation can be mimicked by other WH2 motifs, corroborating a profilin-like function of WH2 motifs in barbed end elongation (Hertzog et al., 2004), ii) the general modular arrangement of a G-actin-binding WH2 motif and a F-actin-binding site are sufficient to promote processive actin filament elongation in the presence of CP after clustering on surfaces, and iii) that the elongation rate mediated by these filament elongators is directly proportional to the saturation of the WH2 motifs with actin.

Our hypothesis of an affinity-based elongation mechanism by Ena/VASP proteins also strongly suggests that the mammalian members EVL, Mena and hVASP are similarly active filament elongators as DdVASP *in vivo*. At the given high actin concentrations in the range of several hundred μM in cells, e.g. 300 μM in neutrophils, 160 μM in *Dictyostelium* and 220 μM in platelets (Pollard et al., 2000) and apparently similar concentrations of monomeric actin near the plasma membrane in the leading edge (Koestler et al., 2009) all mammalian Ena/VASP proteins are expected to be fully saturated with G-actin *in vivo* (Figure 36). Thus, under these conditions Ena/VASP proteins should allow for rapid assembly of actin filaments with elongation rates several times faster than spontaneous actin assembly – an effect which is observable for DdVASP *in vitro* due to its high actin-affinity. The calculation of the fraction of GAB-bound actin monomers to the DdGAB and hGAB revealed that the DdGAB is already

fully saturated with actin at low μM actin concentrations which are being used in TIRF assays, whereas the hGAB is only saturated to 10%. However, hVASP would reach saturation at physiological actin concentrations and therefore also maximally enhance filament elongation (Figure 36). Consistently, replacement of the hGAB of hVASP with the DdGAB did not result in a significant enhancement in the protrusion rates of lamellipodia and filopodia in MV^{D7} cells transfected with GFP-hVASP and GFP-hVASP DdGAB constructs (data not shown), most likely since both GABs are fully saturated with actin *in vivo*. Our results let us propose that the growth of a majority of lamellipodial and filopodial actin filaments is actively accelerated by the action of Ena/VASP proteins during rapid membrane protrusion in motile cells. Application of our model on findings from previous *in vivo* and *in vitro* studies are in line with our hypothesis: biomimetic motility assays performed with ActA-coated beads in the presence of 7 μM actin and profilin have shown an increase of propulsion speed by a factor of 2.5 when VASP was added, which is consistent with a direct involvement of Ena/VASP in enhancing filament elongation, as VASP is expected to be saturated with actin and profilin-actin to approximately 50% (Figure 36, Samarin et al., 2003). Reconstitution of *Listeria* motility using pure proteins at the same actin concentration even showed a ten-fold increase in protrusion rates after addition of VASP (Loisel et al., 1999). MV^{D7} cells infected with *Listeria* also showed an enhancement of bacterium protrusion by a factor of 7 upon expression of either Mena or VASP (Geese et al., 2002). Consistently, *in vivo* experiments in Rat2 fibroblasts showed a reduction of lamellipodium protrusion rates by a factor of 4 when VASP was mislocated to mitochondria, and several other studies showed that the protrusion rate of the lamellipodium directly correlates with VASP density at the leading edge (Rottner et al., 1999; Bear et al., 2002; Koestler et al., 2008). However, due to a lack of proof for a direct involvement of all Ena/VASP members in accelerating actin assembly in these studies, it was proposed that Ena/VASP enhances protrusion of lamellipodia and propulsion of ActA coated beads and *Listeria* in reconstituted motility assays indirectly by preventing capping of barbed ends by CP, by lowering the number of Arp2/3-dependent filament branches or by mediating rapid attachment-detachment cycles of actin filaments to allow both the binding of F-actin and insertion of monomers by brownian motion (Laurent et al., 1999; Bear et al., 2000; Bear et al., 2002; Samarin et al., 2003). In contrast, we propose that all of these results can be largely explained by enhanced actin-filament elongation by Ena/VASP proteins.

Future experiments to unambiguously test this hypothesis will require reconstituted bead-motility assays, using ActA coated beads, Arp2/3 complex, cofilin and CP as well as hVASP and hVASP DdGAB at low, intermediate and high actin concentrations between 3 and 15 μM . Since we hypothesize that hVASP DdGAB is already saturated under each of these conditions, we expect to detect no differences in the extent of bead motility acceleration after

addition of hVASP DdGAB when compared to the actin control. In contrast, we expect to detect a much stronger acceleration by hVASP WT at high actin concentrations than at low actin concentrations, as the saturation of VASP would be noticeably higher when more G-actin is present.

One important question remains to be addressed: what is the evolutionary need for a high-affinity DdVASP in *Dictyostelium* cells? One possible explanation might be that the most fundamental processes of *Dictyostelium* cells are fast migration and phagocytosis, and that actin monomers are primarily “funneled” into the actin polymerization machinery in the front of the cell.

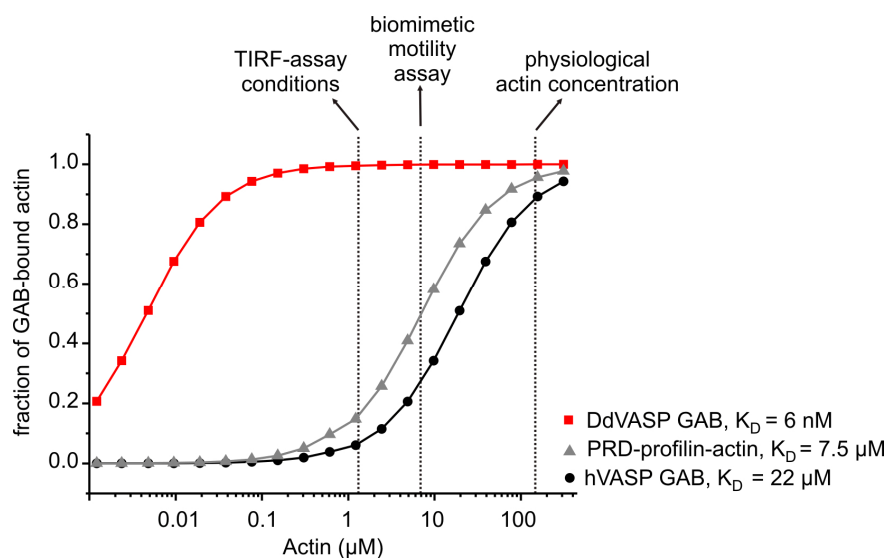


Figure 36: Model for saturation-based Ena/VASP-mediated actin filament elongation. The saturation of the GAB with G-actin and the PRD with profilin-G-actin (from Ferron et al., 2007) at different actin concentrations used in *in vitro* assays and under physiological conditions is shown. Curves were calculated for an excess of actin, using the equation $\Theta = [\text{actin}]/(K_D + [\text{actin}])$. Since the elongation rate of VASP directly correlates with its saturation with actin, it is likely that all Ena/VASP proteins similarly enhance actin polymerization at physiological G-actin concentrations above 100 μM.

Another controversially discussed issue is the ability of Ena/VASP proteins to nucleate actin filaments (Plastino et al., 2008). A common feature of many proteins encompassing a multitude of WH2 motifs is their ability to trigger *de novo* nucleation of actin filaments (Chesarone and Goode, 2009). Cobl and Spire, which harbor three and four adjacent WH2 motifs, respectively, were shown to efficiently compensate the kinetically unfavorable step of the spontaneous formation of dimeric and trimeric nucleation seeds by aligning actin monomers into polymerization competent seeds that subsequently elongate into filaments (Qualmann et al., 2005; Ahuja et al., 2007). However, despite the presence of 8 WH2-like actin-binding motifs in the VASP tetramer, early analyses have shown that hVASP only weakly nucleates actin filaments *in vitro* (Huettelmaier et al., 1999; Laurent et al., 1999; Samarín et al., 2003; Barzik et al., 2005). Therefore, this potential activity was neglected over

the last years. Interestingly, *in vivo* studies with Ena/VASP proteins lead to conflicting results: studies with VASP mislocated to mitochondria or with *Listeria* impaired for Arp2/3-complex recruitment reported no evidence for a significant nucleation activity of VASP (Bear et al., 2000; Skoble et al., 2000), whereas other studies using VASP targeted to mitochondria or late endosomes reported intermediated to massive actin accumulations at these structures (Fradelizi et al., 2001; Schmauch et al., 2009).

Analysis of hVASP WT and chimeric proteins bearing the GAB and FAB motifs from DdVASP by pyrene actin-polymerization assays revealed that most constructs indeed only slightly increased *de novo* filament nucleation *in vitro* with nucleation efficiencies in the range of maximally 5%. However, chimera hVASP DdGAB, encompassing the high-affinity actin-binding GAB as well as the high-affinity hFAB, triggered a remarkable increase in the number of barbed ends with a nucleation efficiency of 30%, which renders this construct a potent filament nucleator. Comparable nucleation efficiencies were previously obtained for strong-nucleating formins like Cdc12 or for the Arp2/3 complex (Marchand et al., 2001; Neidt et al., 2009). This finding is of particular interest, as we hypothesize that hVASP DdGAB is already saturated with G-actin under our *in vitro* conditions, therefore most likely reflecting the saturation of hVASP at physiological actin concentrations. In this regard, it seems likely that Ena/VASP proteins are also involved in the *de novo* nucleation of actin filaments *in vivo*.

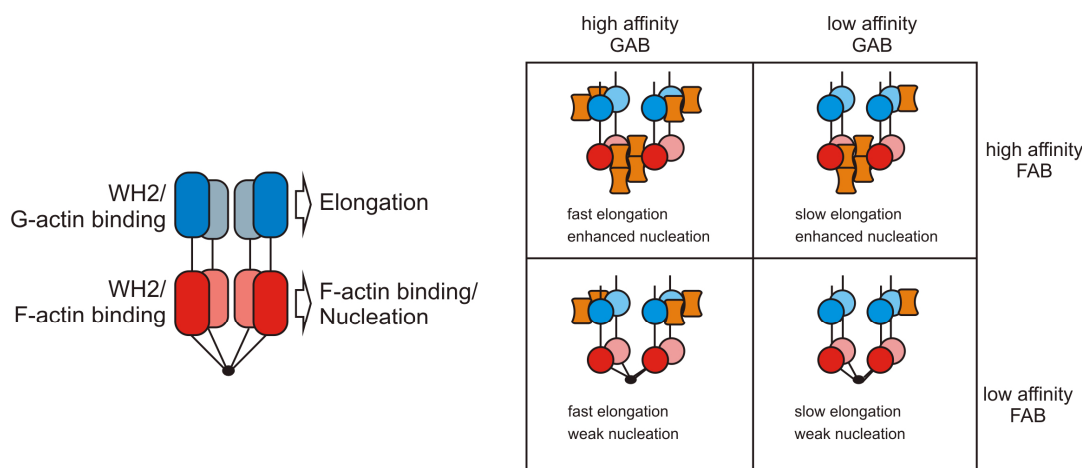


Figure 37: Dissection of affinity-based nucleation and elongation activities of Ena/VASP proteins. The Ena/VASP tetramer consists of the GAB (blue), which primarily recruits actin monomers for filament elongation, and the FAB (red), which mediates F-actin binding and presumably nucleation by stabilization of actin seeds. Depending on the affinity of the GAB for G-actin and the FAB for F-actin, different VASP constructs promote mainly elongation, nucleation, or both.

The mechanism of actin nucleation employed by VASP seems to be different to those of already characterized nucleators, which either recruit and align actin monomers (like Cobl and Spire), mimic nucleation seeds (like the Arp2/3 complex) or stabilize actin dimers or trimers (like formins) (Chesarone and Goode, 2009). Since the presence of the high affinity

DdGAB alone was not sufficient to trigger efficient nucleation, we propose that maximal nucleation effectiveness of VASP relies on both, stabilization of nucleation intermediates like actin dimers by virtue of the FAB, and recruitment of actin monomers for subsequent elongation by the GAB. Hence, chimera hVASP DdGAB, in which GAB and FAB have the highest G- and F-actin affinities, respectively, shows the highest nucleation efficiency of all constructs tested, while those proteins harboring only one of the two high affinity actin-binding sites have only moderate effects on actin nucleation (Figure 37). Thus, based on these results a potential nucleation activity of Ena/VASP proteins *in vivo* should be reexamined.

2.5.4. Material and methods

In vitro TIRF microscopy

Time-lapse evanescent wave fluorescence microscopy was essentially performed as described (Breitsprecher et al., 2008). Images from an Olympus IX-81 inverted microscope were captured every 5 s with exposures of 100 ms with a Hamamatsu Orca-R2 CCD camera (Hamamatsu Corp., Bridgewater, NJ). The pixel size corresponded to 0.11 μm .

The recorded data were analyzed with ImageJ software using the plugin MtrackJ. Every experiment was repeated at least 3 times. For each measurement, at least 30 barbed ends of individual filaments were manually tracked. In case of filaments growing on beads, the total length of the filament was measured for at least 10 time frames. Filament growth rates were diagrammed as plots of length versus time and the average elongation rate in subunits/sec was calculated from linear regressions of the slopes. Carboxylated 2 μm -diameter polystyrene microspheres (Polyscience, Eppelheim, Germany) were coated with 5 μM of the different VASP constructs according to Samarin et al. (2003) and the saturation of the beads was confirmed by SDS-PAGE.

Pyrene actin assays

For spontaneous assembly assays, dilution series of proteins to be assayed were prepared in VASP-storage buffer (200 mM KCl, 20 mM Hepes, 1 mM DTT, pH 7.3) and 10X polymerization buffer was added (250 mM KCl, 10 mM MgCl_2 , 10 mM EGTA, and 100 mM imidazole, pH 7.3). KCl and H_2O were added to reach final KCl concentrations of 50 or 70 mM. Anti-foam 204 (Sigma) was added to the mixture to reach a final concentration of 0.005%. 180 μl aliquots were placed in an 8-well microtiter assembly strip (Thermo scientific). 18 μl of a 20, 30 or 40 μM solution of 10% pyrene labeled G-actin (in 2 mM Tris/HCl, pH 8.0, 0.2 mM ATP, 0.1 mM CaCl_2 , and 0.5 mM DTT) were placed in another 8-well microtiter assembly strip (Thermo scientific). The assembly reaction was started by transferring 162 μl of the protein solution to 18 μl of pyrene-labeled actin. The polymerization of actin was followed by measuring the fluorescence increase of pyrene-actin (excitation at 364 nm and emission at 407 nm) in a fluorescence plate reader (Thermo scientific) for at least 1500 seconds.

For seeded polymerization assays, a 2 μM solution of F-actin in 1x polymerization buffer was vortexed for 10 sec just prior to the experiment and added to the protein solution to reach a final concentration of 50 nM F-actin seeds. The reaction was started as described above. After the measurement, the reaction mixtures were stored at 4°C over night, the steady state fluorescence was measured the next day and the kinetic data were normalized if the proteins did not sequester G-actin.

Determination of barbed end concentration:

At every time point the rate of actin polymerization (slope) is equal to $k_+ \times [\text{ends}] \times [\text{G-actin}]$, where k_+ is the association rate constant of the barbed end obtained by TIRF microscopy at the respective concentrations of VASP proteins. The concentration of ends at the maximum polymerization rate was calculated.

Actin bundling assays

50 μl of a 10 μM G-actin solution was supplemented with a mixture of 10 μl 10x polymerization buffer (500 mM KCl, 10 mM MgCl_2 , 10 mM EGTA, and 100 mM imidazole, pH 7.3), 10 μl of protein in storage buffer (200 mM KCl, 5 mM DTT, 20 mM Hepes pH 7.3) and 30 μl ddH₂O and incubated for 1h at room temperature. F-actin bundles were sedimented by centrifugation for 30 min at 15.000 rpm. 60 μl of the supernatant were mixed with 60 μl SDS-buffer and the remaining supernatant was removed. The pellet was resuspended in 100 μl H₂O and 100 μl SDS-buffer were added. Protein amounts in pellets and supernatants were quantified using SDS-PAGE and band intensities were quantified using ImageJ.

Calculation of the saturation of WH2 motifs with actin

To obtain values for the saturation of the different WH2 motifs with actin with VASP chimeras immobilized on beads, we used the equation $\Theta = [\text{actin}]/(K_d + [\text{actin}])$, assuming that $[\text{actin}] \gg [\text{WH2}]$. For experiments with VASP proteins in solution the equations $[\text{WH2-actin}] = ([\text{actin}_0] + [\text{WH2}_0] + K_d) * [\text{WH2-actin}] + [\text{actin}_0] * [\text{WH2}_0]^{1/2}$ and $\Theta = [\text{WH2-actin}]/[\text{WH2}_0]$ were used.

Analytical ultracentrifugation

Sedimentation velocity experiments were performed in a Beckman Coulter Optima XL-I analytical ultracentrifuge equipped with a fluorescence detection system (AU-FDS, Aviv Biomedical, NJ, USA) using an An50Ti rotor at 20°C and 50000 rpm.

To characterize the interaction of GFP-hGAB and G-actin the experiments were carried out in G buffer. The concentration profiles were measured with the UV/VIS absorbance optical system of the XL-I at a wavelength of 490 nm in double sector cells and filled with 100 μl sample. In case of the characterization of the interaction between GFP-DdGAB and G-actin the concentration profiles were measured using the AU-FDS with an excitation wavelength of 488 nm and emission was detected through a pair of long-pass (> 505 nm) dichroic filters. In order to prevent protein adsorption to surfaces, experiments were performed in G buffer containing 0.05% Tween20. The cells were filled with 100 μl sample.

To analyze the protein-protein interactions the measured concentration profiles were evaluated with the program package SEDFIT. A constant concentration of G-actin was titrated with increasing amounts of the respective GFP-GAB fusion protein and the

concentrations of free and bound GFP-GAB were determined from the areas under the respective peaks in the $c(s)$ distribution. The evaluation of the fluorescence data was performed on the assumption that binding of G-actin does not change the fluorescence quantum yield of GFP-DdGAB.

2.6. Contributions

Manuscript 1: Analysis of Actin Assembly by *In vitro* TIRF Microscopy.

Dennis Breitsprecher established the method “*in vitro* TIRF microscopy of single actin filament assembly” in the lab, designed the figures and wrote parts of the manuscript.

Manuscript 2: Arp2/3 complex interactions and actin network turnover in lamellipodia.

Dennis Breitsprecher performed biochemical analysis on the effect of GFP-tagged and untagged cofilin on actin assembly and disassembly using pyrene assays and TIRF microscopy.

Manuscript 3: Clustering of VASP actively drives processive, WH2 domain-mediated actin filament elongation.

Dennis Breitsprecher purified GST-WT VASP, GST-VASP mutants, His-tagged CapZ and untagged profilin isoforms, designed the experiments, performed all biochemical and TIRF assays on VASP-mediated actin assembly and wrote the manuscript.

Manuscript 4: Filopodia: Complex models for simple rods.

Dennis Breitsprecher wrote parts from the chapters “Formins” and “Ena/VASP” and designed the figures.

Manuscript 5: Affinity-based mechanism of fast Ena/VASP-mediated actin filament elongation (manuscript in preparation).

Dennis Breitsprecher purified GST-tagged Ena/VASP chimeras and performed biochemical assays, including pyrene assays, TIRF assays and F-actin sedimentation experiments, and wrote the manuscript.

3. Discussion

3.1. *In vitro* TIRF microscopy as a tool for the biochemical characterization of actin filament dynamics

The assembly and turnover of actin filaments is a key process in the development and maintenance of cell shape and motility. During the last three decades, enormous progress has been made in characterizing the kinetics of actin assembly and disassembly *in vitro*, greatly improving our understanding of the biochemical properties of actin-based processes. The pyrene assay is an excellent tool to characterize the spontaneous polymerization and depolymerization of actin. Most of our knowledge about the kinetic parameters of actin assembly goes back to seminal studies by Thomas Pollard and Marie-France Carlier who employed pyrene assays to determine the on- and off-rates for barbed end and pointed end polymerization of ADP- and ATP-actin, the equilibrium constants to the G-actin to F-actin transition and to accurately measure depolymerization kinetics. (Pollard, 1983; Pollard and Weeds, 1984; Pollard, 1984; Pantaloni et al., 1984; Carlier et al., 1984a; Carlier et al., 1984b; Carlier et al., 1985; Pantaloni et al., 1985; Pollard, 1986). Due to the ongoing improvement of pyrene assay applications, this convenient test is still a very valuable tool to analyze actin polymerization kinetics.

However, with the discovery of a growing number of proteins that alter the kinetics of actin polymerization, some drawbacks of these assays became evident: (i) Labeling of actin monomers with fluorescent dyes at Cys 374 impairs the binding of some important regulatory proteins, e.g. the ubiquitous profilins resulting a 10-fold weaker affinity of labeled actin to profilin (Schutt et al., 1993; Vinson et al., 1998). As a result, filaments that are formed mainly by profilin actin (e.g. by the action of formins) have a much lower fluorescence signal which strongly influences the outcome of pyrene assays. (ii) The addition of actin-binding proteins that influence both, nucleation and elongation kinetics of actin, leads to ambiguous results. The most prominent examples are formins, which enhance filament nucleation and alter the on-rate of barbed end assembly. Without knowing either elongation or nucleation properties of the formin used, a discrimination of these parameters is impossible (Higgs 2005). (iii) Albeit a vast number of kinetic data can be extracted from pyrene assays, it is impossible to obtain information about the overall architecture of actin filaments e.g. the formation of bundles or branches and changes in the bending flexibility. Therefore, microscopic methods are needed to address the mechanical and kinetic properties of single actin filaments.

Although the direct observation of single filaments by electron microscopy (EM) or fluorescence microscopy *in vitro* using TRITC-labeled phalloidin was early established (Pollard and Mooseker, 1981; Kron et al., 1986; Yanagida et al., 1984), the major drawback of this approach could not be eliminated for almost two decades: To use these techniques,

the polymerization process needs to be inhibited, either by fixation of the specimen for EM or by the addition of phalloidin and subsequent dilution of the reaction mixture for fluorescence microscopy. Thus, a direct observation of assembly and disassembly of single actin filaments was not possible.

This problem was subsequently solved by Pollard and colleagues, who established a novel microscopic assay allowing the direct observation of growing, fluorescently labeled actin filaments using TIRF microscopy (Amann and Pollard, 2001). This was achieved by using labeled actin monomers with fluorescent dyes covalently bound to the reactive Cys 374 and coverslips coated with NEM-treated *Heavy Mero* Myosin (HMM) (manuscript 1). This experimental setup allowed the exact measurement of the on-rates of barbed end and pointed end elongation (Kuhn and Pollard, 2005). In the following years, this technique spread rapidly and was an essential tool to analyze the biochemical properties of formins, profilin, cofilin, coronin, Arp2/3 complex, twinfilin and VASP (Moseley et al., 2005; Kovar et al., 2006; Michelot et al., 2007; Neidt et al., 2008; Paul and Pollard, 2008; Kueh et al., 2008; Pasic et al., 2008; Breitsprecher et al., 2008; Neidt et al., 2009; Gandhi et al., 2009).

In this work, *in vitro* TIRF microscopy was employed to unravel the different mechanistic aspects of Ena/VASP-mediated actin assembly.

3.2. Advantages and limitations of *in vitro* TIRF microscopy on single actin filaments

Observation of the assembly of single actin filaments allows the precise measurement of the on-rate of both, barbed end and pointed end elongation (Amann and Pollard, 2001; Kuhn and Pollard, 2005). Moreover, the biggest advantage of *in vitro* TIRF microscopy is the ability to visualize single-molecule effects directly or indirectly, either by well considered modifications of the experimental setup or by multicolor microscopy of single, fluorescently labeled molecules, which requires extremely sensitive EMCCD cameras and state-of-the-art microscopes to detect very weak fluorescence signals. However, numerous experiments from previous studies showed that it is not mandatory to detect single molecules directly in order to gain information about their modes of action. The most prominent examples are the elegant studies from Kovar and colleagues on formins leading to a plethora of information about the elongation mechanism employed by these filament elongators, merely using fluorescently labeled actin, profilin and different formin isoforms (Kovar and Pollard, 2004; Kovar et al., 2006, Neidt et al., 2008; Neidt et al., 2009). The authors immobilized formin molecules on the surface of coverslips, showing that single formins processively elongate F-actin and produce piconewton forces that result in the buckling of actin filaments. Furthermore, they showed that filaments assembled by formins were dimmer in presence of profilin-actin, allowing the clear-cut discrimination of spontaneously growing from formin-assembled actin filaments. As mentioned above, this effect is based on the lower affinity of

profilin to labeled actin, which initially complicated the analysis of pyrene assay data. However, this effect is very helpful for the *in vitro* TIRF assays allowing to accurately measuring the elongation rates of formin-mediated actin assembly as well as dissociation rates and processivity parameters.

In the present study, *in vitro* TIRF microscopy served as a very powerful tool to quantify the effects of different accessory proteins on single actin filament assembly. Numerous novel microscopic approaches have been established to characterize the effects of VASP-mediated actin assembly, showing its ability to elongate actin filaments via a mechanism that is entirely different to the one employed by formins (manuscript 3 and 5). We could also show that GFP-tagged cofilin severs actin filaments as the untagged protein, and that it preferably binds and severs aged ADP-actin filaments, while the growing barbed end consisting of ATP- and ADP+P_i actin is not severed (manuscript 2).

One approach that turned out to be critical elucidating the interactions of VASP with the growing barbed ends of single filaments was its immobilization on coverslips at different extends. While formins efficiently capture barbed ends of single filaments and subsequently elongate them resulting in filament buckling (Kovar and Pollard, 2004), such effects were not observed for VASP. Instead, filament barbed ends were frequently captured by VASP molecules attached to the coverslip surface but continued to grow freely, while the part of the filament that was initially captured remained bound to the coverslip (manuscript 3, supplementary figure 2). This finding, together with the observations that VASP in solution enhances filament elongation in a concentration dependent manner and that VASP bundles actin filaments, led to our model of a non-processive, VASP-mediated actin filament elongation in solution (manuscript 3, figures 1, 2 and 7). The most important assay developed during this study was the coating of polystyrene beads with VASP to different extends and subsequent analysis of actin filament assembly at their surface. Using this approach, we found that VASP processively elongates actin filaments upon clustering, whereas coating densities below saturation were not sufficient to trigger this effect (manuscript 3. figures 4 and 5). Under these conditions, VASP-mediated filament elongation could no longer be inhibited by CP.

Based on these data, we proposed a mechanism by which a multitude of VASP tetramers clustered on surfaces cooperate in driving processive filament elongation even in the presence of high concentrations of CP (manuscript 3, figures 4, 5 and 7). Subsequent analysis of chimeric VASP proteins bearing G-actin-binding sites with varying actin affinities finally resulted in the formulation of a general model of VASP-mediated filament elongation (manuscript 5).

Irrespective of the enormous potential of *in vitro* TIRF microscopy for analyzing the dynamics of single actin filaments, it is not suited as a stand-alone technique for extensive biochemical

characterization of actin-binding proteins. One major drawback – as for most microscopic assays – is the small viewing area. Therefore, the collection of sufficient data for statistical analysis may be time consuming and the micrographs also represent only a small part of the entire reaction volume. Although this is unproblematic when analyzing filament growth rates in solution – which can be robustly reproduced - it might falsify data of coated polystyrene beads, since the coating density of a given bead cannot be determined. Additionally, since only fluorophores at the coverslip surface are visualized in the TIRF-assays, unspecific protein-surface interactions might lead to biased results when compared to bulk assays.

A very important biochemical parameter of an actin-binding protein is its ability to nucleate actin filaments. Unfortunately, an exact determination of the nucleation activity is impossible to obtain by TIRF microscopy. Although a rough estimate of filament nucleation can be achieved by simply counting filament barbed ends, this assay does not allow quantifying the biochemical parameters. Thus, the combination of data obtained by TIRF and pyrene assay is necessary to extract the biochemical properties of proteins affecting filament nucleation. The increase in pyrenyl fluorescence is a direct measure for the overall amount of F-actin in solution. The slope of the increase at every time point can be described by the simple equation: $\text{slope} = k^+ \times [\text{ends}] \times [\text{actin}]$ (neglecting the slow pointed end growth rate) and corresponds to the polymerization rate in $\mu\text{M}\cdot\text{s}^{-1}$. For proteins that additionally modulate the elongation rate of actin filaments – like Ena/VASP and formins -, k^+ (in $\mu\text{M}^{-1}\text{s}^{-1}$) can be obtained by TIRF microscopy. Knowing this parameter, the concentration of barbed ends in solution and hence the nucleation efficiency can be easily calculated from the initial rate obtained from the pyrene assay. Unfortunately, this quantification of actin nucleation is only occasionally used, and many studies still just provide series of polymerization curves to demonstrate filament nucleation rather than nucleation efficiencies which would allow for meaningful comparison of the results with other studies.

In this work, pyrene assays were instrumental to quantify the nucleation properties of different hVASP chimeras and allowed us to draw additional conclusions on the potential role of VASP on actin assembly *in vivo* (manuscript 5). Moreover, pyrene assays are a necessary tool to determine changes in the critical concentration (the equilibrium constant) of actin polymerization, which again can not be obtained by TIRF microscopy. This analysis was particularly useful for the characterization of the chimeric VASP protein hVASP Cobl2, which mediated unexpectedly low elongation rates in solution as assessed by TIRF assay. This finding could be solved by showing that this VASP chimera strongly sequestered monomeric actin already at low concentrations, consequently resulting in a significant lower amount of free actin monomers in solution and hence impaired filament elongation (manuscript 5).

Overall, *in vitro* TIRF microscopy has proven to be a powerful method for characterizing protein-actin interactions which can be exploited to elucidate the mechanisms of proteins

regulating actin polymerization. In particular, the meaningful modification of the experimental setup, e.g. by applying coated microspheres or coverslips, greatly increases the versatility of this assay.

3.3. Analysis of VASP-mediated actin assembly – a history of controversies

Ena/VASP proteins have initially been identified as substrates for protein kinases A and G (PKA and PKG) within platelets where they participate in regulation of platelet aggregation (Halbrugge et al., 1990; Walter et al., 1993). The first biochemical characterizations of VASP revealed that VASP nucleates actin filaments in a salt-dependent manner, that it tetramerizes and that it binds G-actin, F-actin and profilin-actin by virtue of its PRD and EVH2 domain (Jonkheere et al., 1999; Bachmann et al., 1999; Huettelmaier et al., 1999). However, following biochemical studies led to a number of conflictive results on the precise effect of VASP on actin filament assembly both *in vitro* and *in vivo* (summarized in Trichet et al., 2008). The three most controversially discussed issues regarding the activity of VASP imply nucleation and elongation of filaments as well as its ability to prevent CP from barbed end binding (Table 2). In the following chapters, the dispute regarding these three activities will be highlighted on the background of the present work.

| | Yes | No |
|---|---|---|
| Ena/VASP nucleates actin filaments | Determined by pyrene assays (Huettelmaier et al., 1999; Schirenbeck et al., 2005; present work). On VASP-coated beads (present work). On ActA coated beads (Fradelizi et al., 2001; Plastino et al., 2004a). On zyxin- decorated mitochondria (Fradelizi et al., 2001). With VASP targeted to late endosomes (Schmauch et al., 2009) | Determined by pyrene assays at high salt concentrations (Barzik et al., 2005). On <i>Listeria</i> impaired of Arp2/3 complex recruitment (Skoble et al., 2000). On ActA-decorated mitochondria (Bear et al., 2000). |
| Ena/VASP enhances elongation of actin filaments | Determined by <i>in vitro</i> TIRF microscopy, non-processive in solution and processive on beads (present work). By pyrene assay using F-actin seeds (present work). By pyrene assay using monomeric actin (Skoble et al., 2001). A slight increase of filament elongation was observed by pyrene assay using F-actin seeds (Barzik et al., 2005). By pyrene assay with actin NPFs immobilized on beads (Samarin et al., | Determined by pyrene assay using F-actin seeds (Bear et al., 2002). By pyrene assay with actin NPFs free in solution (Samarin et al., 2003). By <i>in vitro</i> TIRF microscopy (Pasic et al., 2008). |

| | | |
|---------------------------------------|--|--|
| | 2003). By measuring actin incorporation into comet tails on moving beads (Plastino et al., 2004b). | |
| Ena/VASP protects barbed ends from CP | Determined by <i>in vitro</i> TIRF microscopy on VASP coated beads (present work). Determined by assay (Bear et al., 2002; Barzik et al., 2005). By <i>in vitro</i> TIRF microscopy with VASP in solution (Pasic et al., 2008). | Determined by <i>in vitro</i> TIRF microscopy with VASP in solution (present work). By pyrene assay (Samarin et al., 2003). VASP does not uncap filaments, determined by pyrene assay (Schirenbeck et al., 2006). |

Table 2: Comparison of biochemical properties of Ena/VASP determined in previous studies and this work (modified from Trichet et al., 2008).

3.3.1. Nucleation activity of Ena/VASP proteins

To date, three different classes of actin filament nucleating proteins are known: The Arp2/3 complex and its nucleation promoting factors (NPFs) such as N-WASP belong to so called class I nucleators, employing a molecular mimicry with actin related proteins (ARPs) to mimic a nucleation seed that forms the matrix for a new filament (Volkman et al., 2001). Formins comprise the class II nucleators and are thought to stabilize actin dimers and trimers via their barbed end binding FH2 domain, thereby promoting the spontaneous assembly of actin filaments (Pring et al., 2003; Otomo et al., 2005). Members of the third class of actin nucleators such as Spire, Lmod and Cobl, harbor several WH2 motifs or other G-actin-binding modules in close proximity to each other, therefore promoting the formation of nucleation seeds (Ahuja et al., 2007; Quinlan et al., 2005; Cherau et al., 2008; Chesarone and Goode, 2009).

Ena/VASP tetramers harbor in total eight WH2 or WH2-like actin-binding motifs, namely the GAB and FAB, suggesting that they might be indeed responsible for *de novo* nucleation of actin filaments. Early studies employing pyrene assays have shown that human VASP nucleates actin filaments from G-actin at low ionic strength. However, this effect was nearly abrogated at high salt concentrations of 150 mM KCl (Huettelmaier et al., 1999). The nucleation activity of VASP was confirmed in other biochemical studies (Samarin et al., 2003, Bearer et al., 2000), as well as in *in vivo* approaches where VASP was targeted to mitochondria or late endosomes (Fradelizi et al., 2001; Schmauch et al., 2009). However, several other studies found again no involvement of VASP in filament nucleation, neither in pyrene assays using 100 mM KCl (Barzik et al., 2005) nor *in vivo* after sequestration of VASP to mitochondria or on the surface of *Listeria* that were impaired of Arp2/3 complex recruitment (Bear et al., 2000; Skoble et al., 2000).

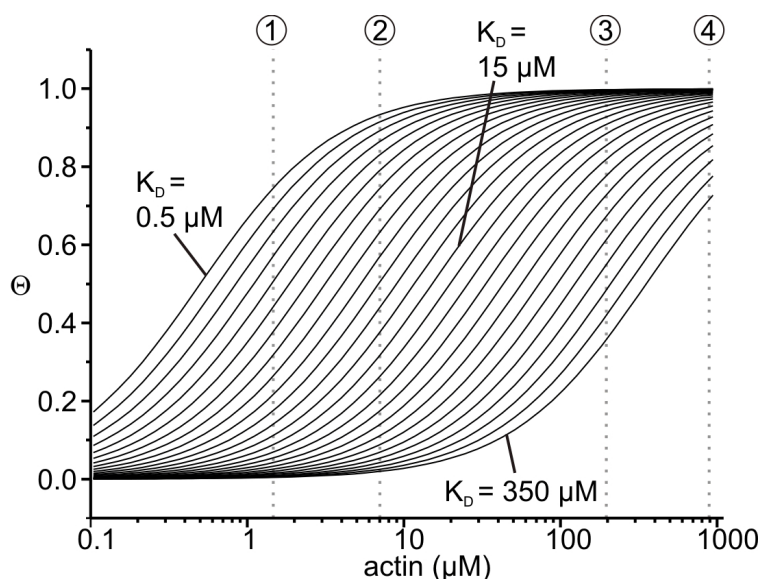


Figure 38: Saturation of the GAB with actin at different K_d s and actin concentrations.

The curves illustrate the saturation of the GAB with G-actin at different actin concentrations over a wide range of K_d s. At very high G-actin concentrations as present in cells, even GABs with weak G-actin affinities are saturated with actin to about 50%. 1) Actin concentration of the *in vitro* TIRF assay. 2) Actin concentration in biomimetic motility assays (Samarin et al., 2003; Loisel et al., 1999). 3) Average G-actin concentration in motile cells (Koestler et al., 2009; Pollard et al., 2000). 4) Estimated local G-actin concentration at the tip of the lamellipodium.

The biochemical analysis performed in the present work supports a possible role of Ena/VASP proteins in *de novo* filament nucleation both *in vitro* and *in vivo*. We analyzed the nucleation properties of hVASP and DdVASP, as well as hVASP chimeras bearing the GAB and FAB from *Dictyostelium*, either alone or in combination (manuscript 5). Since the DdGAB has a very high affinity to G-actin, we initially expected DdVASP to be a much better filament nucleator than hVASP, since the DdVASP tetramer is expected to be fully saturated with G-actin under the used actin concentrations of 1-3 μM (Figure 38). Unexpectedly, despite its lower affinity to G-actin, hVASP turned out to be a much better nucleator *in vitro* than DdVASP, which had only minor effects. We attributed the higher nucleation activity of hVASP to the hFAB motif, which is also responsible for a stronger bundling activity of hVASP, suggesting that nucleation activity by VASP depends primarily on its ability to bind to F-actin. The nucleation mechanism of VASP could therefore be comparable to the one of formins, which stabilize actin dimers or trimers, therefore promoting filament formation. Consistently, different formin isoforms showed a direct correlation of their barbed end affinities and their ability to nucleate filaments (Neidt et al., 2008). Most remarkably, the hVASP chimera hVASP DdGAB, bearing the high-affinity DdGAB and the human FAB, had the most pronounced effect on the formation of new barbed ends and showed nucleation activities as other potent filament nucleators like the Arp2/3 complex, enhancing spontaneous nucleation by a factor of 50 with a nucleation efficiency of 30 % (manuscript 5, Marchand et al., 2001).

This is most likely due to the enhanced local concentration of actin monomers by the DdGAB and the additional F-actin seed stabilization by the human FAB. Although we have shown that the hGAB is not saturated with actin monomers under our *in vitro* conditions, it is presumably fully occupied in the physiological context at high G-actin concentrations of several hundred μM in the leading edge of the cell (manuscript 5; Koestler et al., 2009). Thus it seems likely that VASP may also contribute to the nucleation of new actin filaments in lamellipodial and filopodial tips. However, this hypothesis needs to be verified in future *in vivo* studies.

3.3.2. Elongation activity of Ena/VASP proteins

After the identification of the F- and G-actin-binding sites of Ena/VASP proteins, the so called “clamped-filament elongation model” was postulated by Dickinson and colleagues, suggesting that both, proteins of the Ena/VASP family and formins might processively elongate filaments when immobilized on surfaces (Figure 39) (Dickinson and Purich, 2002; Dickinson et al., 2004, Dickinson 2008). According to this model, the growing filament barbed end is processively tracked by F-actin-binding sites while actin monomers are recruited and inserted onto the barbed end by virtue of G-actin-binding sites. Recruitment of profilin-actin complexes by the PRD will additionally enhance actin monomer delivery.

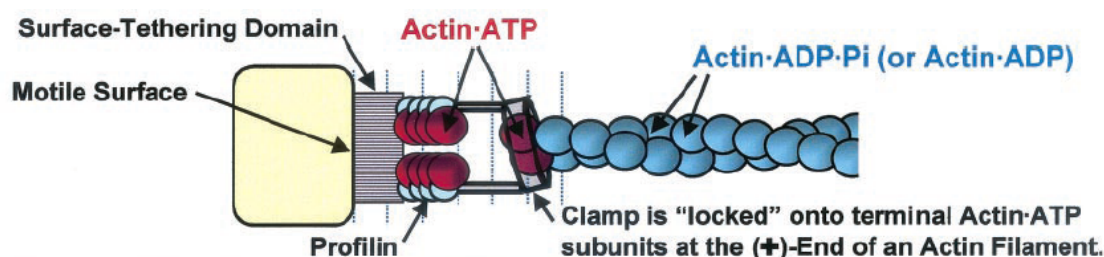


Figure 39: Clamped-filament elongation model (from Dickinson and Purich, 2002). A surface tethered filament elongator consisting of G- and F-actin-binding sites processively tracks the growing filament while actin monomers are inserted onto the barbed end.

Although this model was strongly supported by a recent crystallographic study, showing that profilin-actin can bind to a poly-proline-GAB peptide from hVASP (Ferron et al., 2007), experimental evidence for an active role of VASP in enhancing filament elongation was until very recently missing. Instead, it was proposed that VASP enhances protrusion of lamellipodia and propulsion of ActA coated beads and *Listeria* in reconstituted motility assays indirectly by preventing capping of barbed ends by CP, by lowering the number of Arp2/3 mediated branches or by mediating rapid attachment-detachment cycles of actin filaments to allow both the binding of F-actin and insertion of monomers by Brownian motion (Laurent et al., 1999; Bear et al., 2000; Bear et al., 2002; Samarin et al., 2003). Pyrene assays and *in vitro* TIRF microscopy approaches frequently failed to show a robust enhancement of

filament elongation by mammalian VASP in solution (Barzik et al., 2005; Bear et al., 2002, Samarin et al., 2003, Pasic et al., 2008).

However, our present work suggests that all three mammalian Ena/VASP isoforms, VASP, Mena and EVL, as well as the *Dictyostelium* orthologue DdVASP are able to accelerate actin filament elongation and to processively assemble actin filaments in the physiological context. We propose that all members of the Ena/VASP family are able to enhance filament elongation at least by a factor of 4 when they are saturated with actin monomers, employing a mechanism that resembles the theoretical clamped elongation model initially proposed by Dickinson and Purich remarkably well (2002). Our work also allows us to reconcile previous results into a coherent picture of a conserved mechanism of VASP-mediated actin assembly across species (manuscript 5).

Our findings showing that the low G-actin affinity of the GAB from human VASP with a K_d in the range of 20 μM explains why it was previously difficult to observe enhanced filament elongation by VASP using *in vitro* assays, because for technical reasons these can only be carried out at concentration less than 4 μM G-actin. At this concentration, the low-affinity GAB of human VASP is only saturated with actin to about 10% (Figure 38). Since Mena and EVL contain GABs highly related to human VASP, we assume that these proteins behave similarly. For some reason many studies attached great importance to using physiological salt concentrations *in vitro* but neglected the impact of the low concentrations of the reaction partners in these assays.

As VASP-mediated actin assembly was shown to be salt-dependent, and because actin nucleation and elongation also depend on parameters such as pH and viscosity of the solution, it is likely that even small variations in the experimental setups or protein activities in previous studies frequently resulted in considerable alterations in the experimental readout. Additionally, one has also to bear in mind that the effects of mammalian Ena/VASP proteins at the used actin concentrations are expected to be rather small. Moreover, in the light of our recent work, the concentrations in the range of 25 nM VASP in a number of previous *in vitro* studies seem extremely low (Pasic et al., 2008, Barzik et al., 2005). Since we have shown that the effect of VASP on actin assembly in solution is concentration dependent and maximal at a VASP to actin ratio between 0.2 and 0.5, it seems rather unlikely that such small amounts of VASP can actually cause detectable effects on filament elongation.

In contrast to previously performed pyrene and TIRF assays, biomimetic motility assays with purified proteins showed that VASP enhances the propulsion of ActA-coated beads and *Listeria* by a factor of about 2.5 (Loisel et al., 1999; Samarin et al., 2003). Due to the lack of proof for a direct enhancement of filament elongation by VASP, this effect was explained by other modes of action (see above). However, in light of the new results and based on our calculations, the actin concentrations in a range of 7-10 μM used in these assays are

expected to result in an ~50% saturation of the human VASP GAB with G-actin, and hence a approximately two-fold increase of filament elongation. Moreover, due to the usage of profilin-actin in these assays, which was shown to bind the PRD of VASP with a K_D of 7.5 μ M (Ferron et al., 2007), the local concentration of actin monomers would be raised even more, enhancing the effect of VASP on filament elongation and therefore the propulsion of the particles. Therefore, these assays perfectly resemble our model for a saturation-based filament elongation mechanism employed by Ena/VASP proteins (manuscript 5). Consistent with the model, the protrusion rate of lamellipodia was previously shown to directly correlate with the abundance of VASP in the leading edge (Rottner et al., 1999, Lacayo et al., 2007, Koestler et al., 2008), and another study using Rat2 fibroblast revealed that sequestration of VASP to the surface of mitochondria reduced the protrusion speed of lamellipodia by a factor of 3-4 (Bear et al., 2002). Taking into account that Ena/VASP proteins are powerful filament elongators, it seems therefore worthwhile to reconsider previous results on their *in vivo* function in cell motility.

3.3.3. Anti-capping activity of Ena/VASP proteins

The most controversially discussed issue concerning the different activities of Ena/VASP is its so called “anti-capping activity”, which was first postulated by Bear and colleagues (2002). They employed pyrene assays to evaluate the effect of VASP on actin assembly in the presence of CP, showing that addition of VASP restored CP-inhibited actin polymerization, which was supported by additional *in vitro* studies (Barzik et al., 2005, Pasic et al., 2008). Despite conflicting reports failing to proof such an activity (Boujemaa-Paterski et al., 2001; Samarin et al., 2003), it soon became widely accepted that VASP promotes actin based protrusion by preventing barbed end capping by CP.

The present work clearly demonstrates that immobilized, clustered Ena/VASP proteins very efficiently protect actin filament barbed ends from CP while actively delivering actin monomers for processive filament elongation, and that CP resistance is mediated by the FAB motif. The processivity of all Ena/VASP members is very high, allowing the assembly of filaments longer than 30 μ m corresponding to about 10.000 subunits even at equimolar actin and CP concentrations (manuscript 3, Figure 5). However, we have also clearly shown that such an activity cannot occur in bulk assays in solution, since VASP is not continuously associated with the barbed end under these conditions. Thus, we found no delay in barbed end capping by CP on the single filament level using TIRF microscopy (manuscript 3, Figure 3). However, the question remains why some groups detected such activities using pyrene assays? A reasonable explanation for this effect is based on our observations using TIRF assays in the presence of CP and VASP. CP inhibits filament elongation by tight interaction with the barbed end of the filament, resulting in many short, capped filaments. In the presence of VASP, not only single filaments were observed, but in addition, also

relatively large filament bundles (unpublished data). Interestingly, we observed filament growth on the sides of these bundles in presence of CP suggesting that under these conditions VASP-mediated filament elongation is resistant against CP. As soon as these growing filaments protruded beyond the bundle tip, their growth rapidly stalled indicating barbed end capping of single filaments (Figure 40). Thus, the increased pyrene fluorescence caused by VASP in bulk polymerization assays using actin and CP reported in previous studies might be primarily caused by growth of single actin filaments on the surface of rapidly forming filament bundles.

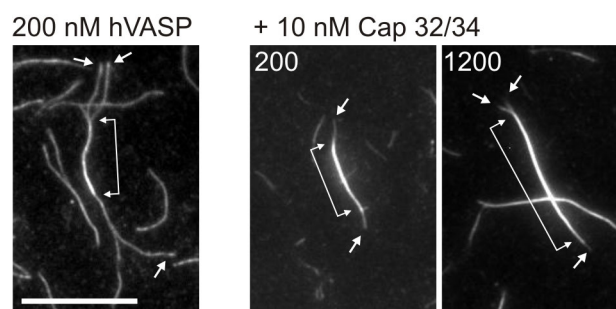


Figure 40: Polymerization of actin in the presence of VASP and CP. Time lapse micrographs showing the polymerization of $1.3 \mu\text{M}$ actin (30% Alexa-488 labeled) in presence of 200 nM hVASP alone (left) or additionally supplemented with 10 nM Cap32/34 (right). Arrows indicate barbed ends. Two headed arrows mark filament bundles. Filaments grew on hVASP-formed bundles but became rapidly capped when protruding into solution. Time is indicated in sec. Scale bar $10 \mu\text{m}$.

3.4. Conclusions and outlook

The present work demonstrates that proteins of the Ena/VASP family regulate the assembly of actin filaments by directly enhancing filament elongation in a processive manner when clustered on surfaces. Only under these conditions, they also prevent inhibition of filament growth by CP, which in turn might serve to eliminate the formation of unproductive actin filaments. Since Ena/VASP proteins are ubiquitously expressed in motile cells and accumulate at sites of actin assembly, we hypothesize that Ena/VASP proteins might be an important if not the predominant actin filament elongator in the protruding fronts of motile cells. Although the present study already uncovered many details on the mechanism of Ena/VASP mediated actin assembly, some issues still remain to be solved on the molecular level in order to build a coherent and resilient model of VASP-mediated actin assembly:

- The WH2-like FAB motif, which is able to bind both G- and F-actin and protects filament barbed ends from CP, is as yet poorly characterized actin-binding site. Since a related motif can also be found in the Arp2/3-complex activators WASP and N-WASP (Dominguez, 2007), it would be of high interest to solve its atomic structure

in complex with actin and characterize its interactions with both, G- and F-actin in more detail. A structure of an EVH2-actin complex would additionally improve our understanding of the elongation mechanism employed by Ena/VASP proteins, although it might be very difficult to obtain, as large parts of the EVH2-domain seem to be disordered. Furthermore, it is still unclear how the FAB contributes to filament elongation. Although we have shown that the FAB is able to recruit G-actin (manuscript 3), it might also well be that it is also involved in mediating interactions with the barbed end to modulate elongation by a yet unknown mechanism.

- An as yet unresolved issue is the role of ATP-hydrolysis during processive filament elongation by Ena/VASP. It was previously reported that ATP-hydrolysis is required for formin processivity (Romero et al., 2004, Romero et al., 2007). However, several studies found no involvement of ATP-hydrolysis in formin-mediated actin assembly, making this interesting hypothesis rather unlikely (Kovar et al., 2006, Paul and Pollard, 2009). The clamped elongation model from Dickinson and Purich implies that altered affinities from the FAB to ATP- and ADP-F-actin are essential for processively tracking the barbed end. If this were true for Ena/VASP-mediated actin assembly, it needs to be experimentally confirmed.
- The contribution of profilin-actin in Ena/VASP-mediated actin assembly needs to be worked out in more detail. Although we have shown that the PRD is not required for filament elongation *in vitro*, an addition of profilin-actin complexes onto the filament by the poly-proline region seems likely *in vivo* (Ferron et al., 2007). Additionally, it would be interesting to know whether profilin-actin recruited by the PRD of Ena/VASP is solely used for its own filament elongation mechanism, or if the profilin-actin complexes might also be delivered to other proteins like formins (Schirenbeck et al., 2005) or WASP, considering the fact that all these proteins do not act in isolation, but instead operate within the framework of large macromolecular assembly complexes in the tips of lamellipodia or filopodia.
- It will be important to determine the kinetic parameters for G-actin/FAB and F-actin/FAB binding and release in order to gain a comprehensive picture of the elongation process mediated by Ena/VASP. Furthermore, it is necessary to test whether actin and profilin-actin recruitment by VASP tetramers occurs in a cooperative fashion, which in turn would enhance its saturation with actin and hence promote its activity on elongation. This task could be performed with single molecule techniques like fluorescence correlation spectroscopy.
- The mechanism by which Ena/VASP proteins capture actin filament barbed ends is still elusive and needs to be worked out in more detail (manuscript 3; Pasic et al., 2008). It is conceivable that VASP either binds filament barbed ends directly by a so

far not discovered actin-binding site, or that it uses the GAB-bound (or FAB-bound) actin monomer as a kind of an adaptor for subsequent binding to the barbed end.

In addition to the knowledge of the biochemical properties of Ena/VASP proteins, *in vivo* studies can provide other valuable insights into their role in cell motility and interaction with other proteins:

- The identification of Ena/VASP proteins as ubiquitous actin filament elongators gives rise to the question whether they interact specifically with filament nucleators. Recent studies suggested a direct interaction of the formin Cappuccino with the actin nucleator spire (Quinlan et al., 2007; Dahlggaard et al., 2007). An interaction of Ena/VASP proteins with WASP was reported previously and might be worthwhile to be analyzed in more detail (Castellano et al., 2001). Another possibility is its direct interaction with formins. Yeast-two-hybrid analysis with the EVH2 domain of DdVASP and the formin dDia2 already suggested that these two proteins interact and cooperate in filopodium formation (manuscript 4; Schirenbeck et al., 2006).
- The question whether Ena/VASP proteins mediate filament nucleation of actin filaments *in vivo* still needs to be addressed. Our finding that the FAB determines the nucleation activity of Ena/VASP proteins (manuscript 5), and the finding that phosphorylated VASP displays an even higher F-actin affinity (Laurent et al., 1999) suggests that phosphorylation might alter the nucleation activity of Ena/VASP proteins *in vivo*. Consistently, Ena/VASP phosphorylation by PKA triggered filopodium formation in growth cones, whereas deletion of the FAB resulted in reduced filopodia formation in MV^{D7} and *Dictyostelium* cells (Lebrand et al., 2004; Schirenbeck et al., 2006; Applewhite et al., 2007). However, the latter effect could also be explained by altered CP resistance or a reduced localization of the protein to sites of active actin assembly (manuscript 3). In spite of these findings, the regulation of Ena/VASP by phosphorylation is still elusive and needs to be investigated in more detail in different cell types.
- One issue of particular high interest is the involvement of Ena/VASP proteins in cancer cell development and invasion. Recently, it was reported that different splice variants of Mena are important diagnostic tumor markers since they are overexpressed in invasive tumor cells (Goswami et al., 2009). Collectively, these results highlight the important role these actin-binding proteins in the regulation of cell protrusion and motility.
- As we assume that, due to the high concentration of actin *in vivo*, all members of the Ena/VASP family are fully saturated with actin monomers, consequently expected to

equally enhance filament elongation, raises the question as to why *Dictyostelium* cells have evolved a VASP protein with such a high affinity for G-actin. A possible explanation might be that, in contrast to mammalian cells, the highly motile *Dictyostelium* amoebae funnel their intracellular pool of G-actin by means of a high-affinity elongator preferentially to actin-assembly driving cell protrusion. To test this, one could for instance express mammalian VASP in *Dictyostelium* VASP-null mutants and test whether it fully restores the wild type phenotype.

- The finding that VASP processively elongates actin filaments on beads in presence of CP while the growth of filaments pointing with their barbed ends away from the bead surface is inhibited lead us to propose additional roles of CP in the leading edge of migrating cells. As yet, CP was suggested to be involved in lamellipodial protrusion by capping filaments nucleated by the Arp2/3 complex to form a dense, dendritic network of short filaments that pushes the membrane forward (Pollard and Borisy, 2003, Carlier et al., 2003). However, this model does not explain the strict localization of CP to the tip of the lamellipodium while Arp2/3 is found in the entire structure (manuscript 2). Moreover, according to our data we propose that actin filaments in the leading edge are processively elongated by Ena/VASP in the presence of high concentration of CP, questioning the role of CP in the dendritic nucleation model (Pollard and Borisy, 2003). Notwithstanding, it was shown that CP has a critical role in the formation of these structures, as depletion of CP abolished lamellipodia (Iwasa and Mullins, 2007; Mejillano et al., 2004). Collectively, our findings rather suggest that CP contributes to the regulation of lamellipodium architecture by eliminating “unproductive” filaments.

4. References

- Abercrombie M, Heaysman JE, Pegrum SM (1970a) The locomotion of fibroblasts in culture. I. Movements of the leading edge. *Exp Cell Res* 59: 393-398.
- Abercrombie M, Heaysman JE, Pegrum SM (1970b) The locomotion of fibroblasts in culture. II. "Ruffling". *Exp Cell Res* 60: 437-444.
- Aguda AH, Xue B, Irobi E, Pr eat T, Robinson RC (2006) The structural basis of actin interaction with multiple WH2/beta-thymosin motif-containing proteins. *Structure* 14: 469-76.
- Ahuja R, Pinyol R, Reichenbach N, Custer L, Klingensmith J, Kessels MM, Qualmann B (2007) Cordon-bleu is an actin nucleation factor and controls neuronal morphology. *Cell* 2007; 131: 337-50.
- Alberts AS (2001) Identification of a carboxyl-terminal diaphanous-related formin homology protein autoregulatory domain. *J Biol Chem* 276: 2824-30
- Amann KJ, Pollard TD (2001) Direct real-time observation of actin filament branching mediated by Arp2/3 complex using total internal reflection fluorescence microscopy *Proc Natl Acad Sci U S A* 98: 15009-13.
- Andrianantoandro E, Pollard TD (2006) Mechanism of actin filament turnover by severing and nucleation at different concentrations of ADF/cofilin. *Mol Cell* 24: 13-23.
- Applewhite DA, Barzik M, Kojima S, Svitkina TM, Gertler FB, et al. (2007) Ena/VASP proteins have an anti-capping independent function in filopodia formation. *Mol Biol Cell* 18: 2579-91.
- Aspenstr om P, Lindberg U, Hall A. (1996) Two GTPases, Cdc42 and Rac, bind directly to a protein implicated in the immunodeficiency disorder Wiskott-Aldrich syndrome. *Curr Biol* 6: 70-5.
- Bachmann C, Fischer L, Walter U, Reinhard M (1999) The EVH2 domain of the vasodilator-stimulated phosphoprotein mediates tetramerization, F-actin binding, and actin bundle formation. *J Biol Chem* 274: 23549-23557.
- Ball LJ, Kuhne R, Hoffmann B, Hafner A, Schmieder P, et al. (2000) Dual epitope recognition by the VASP EVH1 domain modulates polyproline ligand specificity and binding affinity. *Embo J* 19: 4903-4914.
- Bartolini F, Moseley JB, Schmoranzler J, Cassimeris L, Goode BL, Gundersen GG (2008) The formin mDia2 stabilizes microtubules independently of its actin nucleation activity. *J Cell Biol* 181: 523-536
- Barzik M, Kotova TI, Higgs HN, Hazelwood L, Hanein D, et al. (2005) Ena/VASP proteins enhance actin polymerization in the presence of barbed end capping proteins. *J Biol Chem* 280: 28653-28662.
- Basu R, Chang F (2007) Shaping the actin cytoskeleton using microtubule tips. *Curr Opin Cell Biol* 19: 88-94.
- Bear JE, Gertler FB (2009) Ena/VASP: towards resolving a pointed controversy at the barbed end. *J Cell Sci* 122: 1947-53.
- Bear JE, Loureiro JJ, Libova I, F assler R, Wehland J, Gertler FB (2000) Negative regulation of fibroblast motility by Ena/VASP proteins. *Cell* 101: 717-28.
- Bear JE, Svitkina TM, Krause M, Schafer DA, Loureiro JJ, et al. (2002) Antagonism between Ena/VASP proteins and actin filament capping regulates fibroblast motility. *Cell* 109: 509-21.
- Bearer EL, Prakash JM, Manchester RD, Allen PG (2000) VASP protects actin filaments from gelsolin: an in vitro study with implications for platelet actin reorganizations. *Cell Motil Cytoskeleton* 47: 351-64.
- Blanchoin L, Amann KJ, Higgs HN, Marchand JB, Kaiser DA, Pollard TD (2000a) Direct observation of dendritic actin filament networks nucleated by Arp2/3 complex and WASP/Scar proteins. *Nature* 404: 1007-11.
- Blanchoin L, Pollard TD (1999) Mechanism of interaction of Acanthamoeba actophorin (ADF/Cofilin) with actin filaments. *J Biol Chem* 274: 15538-146.
- Blanchoin L, Pollard TD, Mullins RD (2000b) Interactions of ADF/cofilin, Arp2/3 complex, capping protein and profilin in remodeling of branched actin filament networks. *Curr Biol* 10:1273-82.
- Block J, Stradal TE, H anisch J, Geffers R, K ostler SA, Urban E, Small JV, Rottner K, Faix J (2008) Filopodia formation induced by active mDia2/Drf3. *J Microsc* 231: 506-17.
- Bo eda B, Briggs DC, Higgins T, Garvalov BK, Fadden AJ, McDonald NQ, Way M (2007) Tes, a specific Mena interacting partner, breaks the rules for EVH1 binding. *Mol Cell* 28:1071-82.
- Bosch M, Le KH, Bugyi B, Correia JJ, Renault L, et al. (2007) Analysis of the function of Spire in actin assembly and its synergy with formin and profilin. *Mol Cell* 28: 555-568.
- Boujemaa-Paterski R, Gouin E, Hansen G, Samarin S, Le Clainche C, Didry D, Dehoux P, Cossart P, Kocks C, Carlier MF, Pantaloni D (2001) Listeria protein ActA mimics WASp family proteins: it activates filament barbed end branching by Arp2/3 complex. *Biochemistry* 40:11390-11404.

- Bowman GD, Nodelman IM, Hong Y, Chua NH, Lindberg U, Schutt CE (2000) A comparative structural analysis of the ADF/cofilin family. *Proteins* 41: 374-84.
- Brindle NP, Holt MR, Davies JE, Price CJ, Critchley DR. (1996) The focal-adhesion vasodilator-stimulated phosphoprotein (VASP) binds to the proline-rich domain in vinculin. *Biochem J*. 318: 753-757.
- Bundschu K, Walter U, Schuh K (2006) The VASP-Spred-Sprouty domain puzzle. *J Biol Chem* 281: 36477-81.
- Butt E, Abel K, Krieger M, Palm D, Hoppe V, Hoppe J, Walter U (1994) cAMP- and cGMP-dependent protein kinase phosphorylation sites of the focal adhesion vasodilator-stimulated phosphoprotein (VASP) *in vitro* and in intact human platelets. *J Biol Chem* 269: 14509-17.
- Caldwell JE, Heiss SG, Mermall V, Cooper JA (1989) Effects of CapZ, an actin capping protein of muscle, on the polymerization of actin. *Biochemistry* 28:8506-8514.
- Cao W, Goodarzi JP, De La Cruz EM (2006) Energetics and kinetics of cooperative cofilin-actin filament interactions. *J Mol Biol* 361: 257-67.
- Carlier MF, Laurent V, Santolini J, Melki R, Didry D, Xia GX, Hong Y, Chua NH, Pantaloni D (1997) Actin depolymerizing factor (ADF/cofilin) enhances the rate of filament turnover: implication in actin-based motility. *J Cell Biol* 136 :1307-22.
- Carlier MF, Le Clainche C, Wiesner S, Pantaloni D (2003) Actin-based motility: from molecules to movement. *Bioessays* 25: 336-345.
- Carlier MF, Pantaloni D (1986) Direct evidence for ADP-Pi-F-actin as the major intermediate in ATP-actin polymerization. Rate of dissociation of Pi from actin filaments. *Biochemistry* 25: 7789-92.
- Carlier MF, Pantaloni D (2007) Control of actin assembly dynamics in cell motility. *J Biol Chem* 282: 23005-23009.
- Carlier MF, Pantaloni D, Korn ED. (1984a) Evidence for an ATP cap at the ends of actin filaments and its regulation of the F-actin steady state. *J Biol Chem* 259: 9983-6.
- Carlier MF, Pantaloni D, Korn ED (1984b) Steady state length distribution of F-actin under controlled fragmentation and mechanism of length redistribution following fragmentation. *J Biol Chem* 259: 9987-91.
- Carlier MF, Pantaloni D, Korn ED (1985) Polymerization of ADP-actin and ATP-actin under sonication and characteristics of the ATP-actin equilibrium polymer. *J Biol Chem* 260: 6565-71.
- Castellano F, Le Clainche C, Patin D, Carlier MF, Chavrier P (2001) A WASp-VASP complex regulates actin polymerization at the plasma membrane. *EMBO J* 20: 5603-14.
- Chan C, Beltzner CC, Pollard TD (2009) Cofilin dissociates Arp2/3 complex and branches from actin filaments. *Curr Biol* 19: 537-45.
- Chang F, Drubin D, Nurse P (1997) cdc12p, a protein required for cytokinesis in fission yeast, is a component of the cell division ring and interacts with profilin. *J Cell Biol* 137: 169-82.
- Chereau D, Boczkowska M, Skwarek-Maruszewska A, Fujiwara I, Hayes DB, Rebowski G, Lappalainen P, Pollard TD, Dominguez R (2008) Leiomodin is an actin filament nucleator in muscle cells. *Science* 320: 239-43.
- Chereau D, Dominguez R (2006) Understanding the role of the G-actin-binding domain of Ena/VASP in actin assembly. *J Struct Biol* 155: 195-201.
- Chereau D, Kerff F, Graceffa P, Grabarek Z, Langsetmo K, Dominguez R. (2005) Actin-bound structures of Wiskott-Aldrich syndrome protein (WASP)-homology domain 2 and the implications for filament assembly. *Proc Natl Acad Sci U S A* 102: 16644-9.
- Chesarone MA, Goode BL (2009) Actin nucleation and elongation factors: mechanisms and interplay. *Curr Opin Cell Biol* 21: 28-37.
- Chhabra ES, Higgs HN (2007) The many faces of actin: matching assembly factors with cellular structures. *Nat Cell Biol* 9: 1110-21.
- Co C, Wong DT, Gierke S, Chang V, Taunton J (2007) Mechanism of actin network attachment to moving membranes: barbed end capture by N-WASP WH2 domains. *Cell* 128: 901-913.
- Cooper JA, Sept D (2008) New insights into mechanism and regulation of actin capping protein. *Int Rev Cell Mol Biol* 267: 183-206.
- Cooper JA, Walker SB, Pollard TD (1983) Pyrene actin: documentation of the validity of a sensitive assay for actin polymerization. *J Muscle Res Cell Motil* 4: 253-62.
- Dahlgaard K, Raposo AA, Niccoli T, St Johnston D. Capu and Spire assemble a cytoplasmic actin mesh that maintains microtubule organization in the Drosophila oocyte. *Dev Cell* 13: 539-53.
- De La Cruz EM, Mandinova A, Steinmetz MO, Stoffler D, Aebi U, Pollard TD (2000) Polymerization and structure of nucleotide-free actin filaments. *J Mol Biol* 295:517-526.

- Dent EW, Kwiatkowski AV, Mebane LM, Philippar U, Barzik M, et al. (2007) Filopodia are required for cortical neurite initiation. *Nat Cell Biol* 9: 1347-1359.
- DesMarais V, Ichetovkin I, Condeelis J, Hitchcock-DeGregori SE (2002) Spatial regulation of actin dynamics: a tropomyosin-free, actin-rich compartment at the leading edge. *J Cell Sci* 115: 4649-60.
- Dickinson RB (2008) Models for actin polymerization motors. *J Math Biol* 58: 81-103.
- Dickinson RB, Caro L, Purich DL (2004) Force generation by cytoskeletal filament end-tracking proteins. *Biophys J* 87: 2838-54.
- Dickinson RB, Purich DL (2002) Clamped-filament elongation model for actin-based motors. *Biophys J* 2: 605-617.
- Dickinson RB, Purich DL (2006) Diffusion rate limitations in actin-based propulsion of hard and deformable particles. *Biophys J* 91: 1548-63
- Didry D, Carlier MF, Pantaloni D (1998) Synergy between actin depolymerizing factor/cofilin and profilin in increasing actin filament turnover. *J Biol Chem* 273: 25602-11.
- Dominguez R (2007) The beta-thymosin/WH2 fold: multifunctionality and structure. *Ann N Y Acad Sci* 1112: 86-94.
- Drees B, Friederich E, Fradelizi J, Louvard D, Beckerle MC, Golsteyn RM (2000) Characterization of the interaction between zyxin and members of the Ena/vasodilator-stimulated phosphoprotein family of proteins. *J Biol Chem* 275: 22503-11.
- Drees F, Gertler FB (2008) Ena/VASP: proteins at the tip of the nervous system. *Curr Opin Neurobiol* 18:53-9.
- Edwards J (2004) Are beta-thymosins WH2 domains? *FEBS Lett* 573: 231-2;
- Evangelista M, Blundell K, Longtine MS, Chow CJ, Adames N, Pringle JR, Peter M, Boone C (1997) Bni1p, a yeast formin linking cdc42p and the actin cytoskeleton during polarized morphogenesis. *Science* 276: 118-22.
- Faix J, Breitsprecher D, Stradal TE, Rottner K (2009) Filopodia: Complex models for simple rods. *Int J Biochem Cell Bio* 41: 1656-64.
- Faix J, Grosse R (2006) Staying in shape with formins. *Dev Cell* 10: 693-706.
- Fedorov AA, Lappalainen P, Fedorov EV, Drubin DG, Almo SC (1997) Structure determination of yeast cofilin. *Nat Struct Biol* 4: 366-9.
- Ferron F, Rebowski G, Lee SH, Dominguez R (2007) Structural basis for the recruitment of profilin-actin complexes during filament elongation by Ena/VASP. *Embo J* 26: 4597-4606.
- Footer MJ, Lyo JK, Theriot JA (2008) Close packing of *Listeria monocytogenes* ActA, a natively unfolded protein, enhances F-actin assembly without dimerization. *J Biol Chem* 283: 23852-62.
- Fradelizi J, Noireaux V, Plastino J, Menichi B, Louvard D, Sykes C, Golsteyn RM, Friederich E (2001) ActA and human zyxin harbour Arp2/3-independent actin-polymerization activity. *Nat Cell Biol* 3: 699-707.
- Furman C, Sieminski AL, Kwiatkowski AV, Rubinson DA, Vasile E, Bronson RT, Fässler R, Gertler FB (2007) Ena/VASP is required for endothelial barrier function *in vivo*. *J Cell Biol* 179: 761-75.
- Galkin VE, Orlova A, VanLoock MS, Shvetsov A, Reisler E, Egelman EH (2003) ADF/cofilin use an intrinsic mode of F-actin instability to disrupt actin filaments. *J Cell Biol* 163: 1057-66.
- Gandhi M, Achard V, Blanchoin L, Goode BL. Coronin switches roles in actin disassembly depending on the nucleotide state of actin. *Mol Cell* ;34: 364-74.
- Geese M, Loureiro JJ, Bear JE, Wehland J, Gertler FB, et al. (2002) Contribution of Ena/VASP proteins to intracellular motility of *Listeria* requires phosphorylation and proline-rich core but not F-actin binding or multimerization. *Mol Biol Cell* 13: 2383-2396.
- Gertler FB, Comer AR, Juang JL, Ahern SM, Clark MJ, Liebl EC, Hoffmann FM (1995) Enabled, a dosage-sensitive suppressor of mutations in the *Drosophila* Abl tyrosine kinase, encodes an Abl substrate with SH3 domain-binding properties. *Genes Dev* 9: 521-33.
- Gertler FB, Niebuhr K, Reinhard M, Wehland J, Soriano P (1996) Mena, a relative of VASP and *Drosophila* Enabled, is implicated in the control of microfilament dynamics. *Cell* 87: 227-239.
- Ghosh M, Song X, Mouneimne G, Sidani M, Lawrence DS, Condeelis JS (2004) Cofilin promotes actin polymerization and defines the direction of cell motility. *Science* 304: 743-6.
- Gomez TS, Kumar K, Medeiros RB, Shimizu Y, Leibson PJ, Billadeau DD (2007) Formins regulate the actin-related protein 2/3 complex-independent polarization of the centrosome to the immunological synapse. *Immunity* 26: 177-90.
- Goode BL, Eck MJ (2007) Mechanism and function of formins in the control of actin assembly. *Annu Rev Biochem* 76: 593-627.

- Goswami S, Philippar U, Sun D, Patsialou A, Avraham J, Wang W, Di Modugno F, Nistico P, Gertler FB, Condeelis JS (2009) Identification of invasion specific splice variants of the cytoskeletal protein Mena present in mammary tumor cells during invasion *in vivo*. *Clin Exp Metastasis* 26:153-159.
- Halbrügge M, Friedrich C, Eigenthaler M, Schanzenbächer P, Walter U (1990) Stoichiometric and reversible phosphorylation of a 46-kDa protein in human platelets in response to cGMP- and cAMP-elevating vasodilators. *J Biol Chem* 265: 3088-93.
- Han YH, Chung CY, Wessels D, Stephens S, Titus MA, et al. (2002) Requirement of a vasodilator-stimulated phosphoprotein family member for cell adhesion, the formation of filopodia, and chemotaxis in Dictyostelium. *J Biol Chem* 277: 49877-49887.
- Harris A (1973) Behavior of cultured cells on substrata of variable adhesiveness. *Exp Cell Res* 77: 285-297.
- Harris ES, Higgs HN (2004) Actin cytoskeleton: formins lead the way. *Curr Biol* 14: 520-2.
- Hatanaka H, Ogura K, Moriyama K, Ichikawa S, Yahara I, Inagaki F (1996) Tertiary structure of destrin and structural similarity between two actin-regulating protein families. *Cell* 85: 1047-55.
- Hatano S, Oosawa F (1966) Extraction of an actin-like protein from the plasmodium of a myxomycete and its interaction with myosin A from rabbit striated muscle. *J Cell Physiol* 68:197-202.
- Haus U, Hartmann H, Trommler P, Noegel AA, Schleicher M (1991) F-actin capping by cap32/34 requires heterodimeric conformation and can be inhibited with PIP2. *Biochem Biophys Res Commun* 181: 833-9.
- Hertzog M, van Heijenoort C, Didry D, Gaudier M, Coutant J, et al. (2004) The beta-thymosin/WH2 domain; structural basis for the switch from inhibition to promotion of actin assembly. *Cell* 117: 611-623.
- Higgs HN (2005) Formin proteins: a domain-based approach. *Trends Biochem Sci* 30: 342-53.
- Holmes KC, Popp D, Gebhard W, Kabsch W (1990) Atomic model of the actin filament. *Nature* 347: 44-9.
- Hooch TC, Newcomb PM, Herman IM (1991) Beta actin and its mRNA are localized at the plasma membrane and the regions of moving cytoplasm during the cellular response to injury. *J Cell Biol* 112: 653-664.
- Hotulainen P, Paunola E, Vartiainen MK, Lappalainen P (2005) Actin-depolymerizing factor and cofilin-1 play overlapping roles in promoting rapid F-actin depolymerization in mammalian nonmuscle cells. *Mol Biol Cell* 16: 649-64.
- Huang TY, DerMardirossian C, Bokoch GM (2006) Cofilin phosphatases and regulation of actin dynamics. *Curr Opin Cell Biol* 18: 26-31.
- Huff T, Müller CS, Otto AM, Netzker R, Hannappel E (2001) beta-Thymosins, small acidic peptides with multiple functions. *Int J Biochem Cell Biol* 33: 205-20.
- Huff T, Rosorius O, Otto AM, Müller CS, Ballweber E, Hannappel E, Mannherz HG (2004) Nuclear localisation of the G-actin sequestering peptide thymosin beta4. *J Cell Sci* 117: 5333-41.
- Huettelmaier S, Harbeck B, Steffens O, Messerschmidt T, Illenberger S, et al. (1999) Characterization of the actin-binding properties of the vasodilator-stimulated phosphoprotein VASP. *FEBS Lett* 451: 68-74.
- Imamura H, Tanaka K, Hihara T, Umikawa M, Kamei T, Takahashi K, Sasaki T, Takai Y. (1997) Bni1p and Bnr1p: downstream targets of the Rho family small G-proteins which interact with profilin and regulate actin cytoskeleton in *Saccharomyces cerevisiae*. *EMBO J* 16: 2745-55.
- Ingouff M, Fitz Gerald JN, Guérin C, Robert H, Sørensen MB, Van Damme D, Geelen D, Blanchoin L, Berger F (2005) Plant formin AtFH5 is an evolutionarily conserved actin nucleator involved in cytokinesis. *Nat Cell Biol* 7: 374-80.
- Ingram VM (1969) A side view of moving fibroblasts. *Nature* 222: 641-644.
- Insall RH, Machesky LM (2009) Actin dynamics at the leading edge: from simple machinery to complex networks. *Dev Cell* 17: 310-322.
- Irobi E, Aguda AH, Larsson M, Guerin C, Yin HL, Burtnick LD, Blanchoin L, Robinson RC (2004) Structural basis of actin sequestration by thymosin-beta4: implications for WH2 proteins. *EMBO J* 23: 3599-608.
- Isambert H, Venier P, Maggs AC, Fattoum A, Kassab R, Pantaloni D, Carlier MF (1995) Flexibility of actin filaments derived from thermal fluctuations. Effect of bound nucleotide, phalloidin, and muscle regulatory proteins. *J Biol Chem* 270:11437-11444.
- Ishikawa H, Bischoff R, Holtzer H (1969) Formation of arrowhead complexes with heavy meromyosin in a variety of cell types. *J Cell Biol* 43: 312-28.
- Ishikawa, H, Bischoff, R, Holtzer, H (1969) Formation of arrowhead complexes with heavy meromyosin
- Iwasa JH, Mullins RD (2007) Spatial and temporal relationships between actin-filament nucleation, capping, and disassembly. *Curr Biol* 17: 395-406.
- Jenzora A, Behrendt B, Small JV, Wehland J, Stradal TE. (2006) PREL1 provides a link from Ras signalling to the actin cytoskeleton via Ena/VASP proteins. *FEBS Lett.* 580: 455-463.

- Jockusch BM, Murk K, Rothkegel M (2007) The profile of profilins. *Rev Physiol Biochem Pharmacol* 159: 131-49.
- Jonckheere V, Lambrechts A, Vandekerckhove J, Ampe C (1999) Dimerization of profilin II upon binding the (GP5)3 peptide from VASP overcomes the inhibition of actin nucleation by profilin II and thymosin beta4. *FEBS Lett* 447: 257-63.
- Joseph JM, Fey P, Ramalingam N, Liu XI, Rohlfis M, Noegel AA, Müller-Taubenberger A, Glöckner G, Schleicher M (2008) The actinome of *Dictyostelium discoideum* in comparison to actins and actin-related proteins from other organisms. *PLoS One* 3: e2654.
- Kabsch W, Holmes KC (1995) The actin fold. *FASEB J* 9: 167-74.
- Kang F, Laine RO, Bubb MR, Southwick FS, Purich DL (1997) Profilin interacts with the Gly-Pro-Pro-Pro-Pro sequences of vasodilator-stimulated phosphoprotein (VASP): implications for actin-based *Listeria* motility. *Biochemistry* 36: 8384-92.
- Koestler SA, Auinger S, Vinzenz M, Rottner K, Small JV (2008) Differentially oriented populations of actin filaments generated in lamellipodia collaborate in pushing and pausing at the cell front. *Nat Cell Biol* 10: 306-13
- Kovar DR, Harris ES, Mahaffy R, Higgs HN, Pollard TD (2006) Control of the assembly of ATP- and ADP-actin by formins and profilin. *Cell* 124: 423-35.
- Kovar DR, Kuhn JR, Tichy AL, Pollard TD (2003) The fission yeast cytokinesis formin Cdc12p is a barbed end actin filament capping protein gated by profilin. *J Cell Biol* 161: 875-87.
- Kovar DR, Pollard TD (2004) Insertional assembly of actin filament barbed ends in association with formins produces piconewton forces. *Proc Natl Acad Sci* 101: 14725-30.
- Krause M, Leslie JD, Stewart M, Lafuente EM, Valderrama F, Jagannathan R, Strasser GA, Rubinson DA, Liu H, Way M, Yaffe MB, Boussiotis VA, Gertler FB. (2004) Lamellipodin, an Ena/VASP ligand, is implicated in the regulation of lamellipodial dynamics. *Dev Cell*. 7:571-583.
- Kron SJ, Spudich JA (1986) Fluorescent actin filaments move on myosin fixed to a glass surface. *Proc Natl Acad Sci U S A* 83: 6272-6.
- Kueh HY, Charras GT, Mitchison TJ, Brieher WM (2008) Actin disassembly by cofilin, coronin, and Aip1 occurs in bursts and is inhibited by barbed-end cappers. *J Cell Biol* 182: 341-53.
- Kuhn JR, Pollard TD (2005) Real-time measurements of actin filament polymerization by total internal reflection fluorescence microscopy. *Biophys J* 88: 1387-1402.
- Kursula, P., Kursula, I., Massimi, M., Song, Y. H., Downer, J., Stanley, W. A., Witke, W., and Wilmanns, M. (2008). High-resolution structural analysis of mammalian profilin 2a complex formation with two physiological ligands: the formin homology 1 domain of mDia1 and the proline-rich domain of VASP. *J Mol Biol* 375: 270-290.
- Kwiatkowski AV, Rubinson DA, Dent EW, Edward van Veen J, Leslie JD, et al. (2007) Ena/VASP Is Required for neurogenesis in the developing cortex. *Neuron* 56: 441-455.
- Lacayo CI, Pincus Z, VanDuijn MM, Wilson CA, Fletcher DA, Gertler FB, Mogilner A, Theriot JA. (2007) Emergence of large-scale cell morphology and movement from local actin filament growth dynamics. *PLoS Biol* 5: e233.
- Lafuente EM, van Puijenbroek AA, Krause M, Carman CV, Freeman GJ, Berezovskaya A, Constantine E, Springer TA, Gertler FB, Boussiotis VA. (2004) RIAM, an Ena/VASP and Profilin ligand, interacts with Rap1-GTP and mediates Rap1-induced adhesion. *Dev Cell*. 7:585-595.
- Lai APL, Szczodrak M, Block J, Faix J, Breitsprecher D, et al. (2008) Arp2/3-complex interactions and actin network turnover in lamellipodia. *Embo J* 27: 982-92
- Lambrechts A, Kwiatkowski AV, Lanier LM, Bear JE, Vandekerckhove J, et al. (2000) cAMP-dependent protein kinase phosphorylation of EVL, a Mena/VASP relative, regulates its interaction with actin and SH3 domains. *J Biol Chem* 275: 36143-36151.
- Tondeleir D, Vandamme D, Vandekerckhove J, Ampe C, Lambrechts A (2009) Actin isoform expression patterns during mammalian development and in pathology: insights from mouse models. *Cell Motil Cytoskeleton* 66: 798-815.
- Lammers M, Meyer S, Kühlmann D, Wittinghofer A (2008) Specificity of interactions between mDia isoforms and Rho proteins. *J Biol Chem* 283: 35236-35246
- Lammers M, Rose R, Scrima A, Wittinghofer A (2005) The regulation of mDia1 by autoinhibition and its release by Rho*GTP. *EMBO J* 24:4176-4187.
- Lauffenburger DA, Horwitz AF (1996) Cell migration: a physically integrated molecular process. *Cell* 84:359-369.
- Laurent V, Loisel TP, Harbeck B, Wehman A, Grobe L, et al. (1999) Role of proteins of the Ena/VASP family in actin-based motility of *Listeria monocytogenes*. *J Cell Biol* 144: 1245-1258.

- Lebrand C, Dent EW, Strasser GA, Lanier LM, Krause M, Svitkina TM, Borisy GG, Gertler FB (2004) Critical role of Ena/VASP proteins for filopodia formation in neurons and in function downstream of netrin-1. *Neuron* 42: 37-49.
- Lee SH, Kerff F, Chereau D, Ferron F, Klug A, Dominguez R (2007) Structural basis for the actin-binding function of missing-in-metastasis. *Structure* 15:145-155.
- Leonard SA, Gittis AG, Petrella EC, Pollard TD, Lattman EE (1997) Crystal structure of the actin-binding protein actophorin from *Acanthamoeba*. *Nat Struct Biol* 4: 369-373.
- Li F, Higgs HN (2003) The mouse Formin mDia1 is a potent actin nucleation factor regulated by autoinhibition. *Curr Biol* 13: 1335-1340
- Liverman AD, Cheng HC, Trosky JE, Leung DW, Yarbrough ML, Burdette DL, Rosen MK, Orth K (2007) Arp2/3-independent assembly of actin by *Vibrio* type III effector VopL. *Proc Natl Acad Sci U S A* 104: 17117-22.
- Loisel TP, Boujemaa R, Pantaloni D, Carlier MF (1999) Reconstitution of actin-based motility of *Listeria* and *Shigella* using pure proteins. *Nature* 401: 613-616.
- Lorenz M, Poole KJ, Popp D, Rosenbaum G, Holmes KC (1995) An atomic model of the unregulated thin filament obtained by X-ray fiber diffraction on oriented actin-tropomyosin gels. *J Mol Biol.* 246: 108-119
- Lorenz M, Popp D, Holmes KC (1993) Refinement of the F-actin model against X-ray fiber diffraction data by the use of a directed mutation algorithm. *J Mol Biol.* 234: 826-836.
- Loureiro JJ, Rubinson DA, Bear JE, Baltus GA, Kwiatkowski AV, et al. (2002) Critical roles of phosphorylation and actin-binding motifs, but not the central proline-rich region, for Ena/vasodilator-stimulated phosphoprotein (VASP) function during cell migration. *Mol Biol Cell* 13: 2533-2546.
- Machesky LM, Mullins RD, Higgs HN, Kaiser DA, Blanchoin L, May RC, Hall ME, Pollard TD (1999) Scar, a WASP-related protein, activates nucleation of actin filaments by the Arp2/3 complex. *Proc Natl Acad Sci U S A* 96: 3739-3744.
- Machesky LM, Reeves E, Wientjes F, Mattheyse FJ, Grogan A, Totty NF, Burlingame AL, Hsuan JJ, Segal AW (1997) Mammalian actin-related protein 2/3 complex localizes to regions of lamellipodial protrusion and is composed of evolutionarily conserved proteins. *Biochem J* 328: 105-112.
- Mahaffy RE, Pollard TD (2008) Influence of phalloidin on the formation of actin filament branches by Arp2/3 complex. *Biochemistry* 47: 6460-6467.
- Marchand JB, Kaiser DA, Pollard TD, Higgs HN (2001) Interaction of WASP/Scar proteins with actin and vertebrate Arp2/3 complex. *Nat Cell Biol* 3: 76-82.
- Mattila PK, Lappalainen P (2008) Filopodia: molecular architecture and cellular functions. *Nat Rev Mol Cell Biol* 9: 446-54.
- Mattila PK, Pykäläinen A, Saarikangas J, Paavilainen VO, Vihinen H, Jokitalo E, Lappalainen P (2007) Missing-in-metastasis and IRSp53 deform PI(4,5)P₂-rich membranes by an inverse BAR domain-like mechanism. *J Cell Biol* 176: 953-964.
- Mattila PK, Salminen M, Yamashiro T, Lappalainen P (2003) Mouse MIM, a tissue-specific regulator of cytoskeletal dynamics, interacts with ATP-actin monomers through its C-terminal WH2 domain. *J Biol Chem.* 278: 8452-8459.
- McCullough BR, Blanchoin L, Martiel JL, De la Cruz EM (2008) Cofilin increases the bending flexibility of actin filaments: implications for severing and cell mechanics. *J Mol Biol* 381: 550-8.
- McGough A, Chiu W (1999) ADF/cofilin weakens lateral contacts in the actin filament. *J Mol Biol* 29:513-519.
- McGough A, Pope B, Chiu W, Weeds A (1997) Cofilin changes the twist of F-actin: implications for actin filament dynamics and cellular function. *J Cell Biol.* 138: 771-781.
- Mejillano MR, Kojima S, Applewhite DA, Gertler FB, Svitkina TM, Borisy GG (2004) Lamellipodial versus filopodial mode of the actin nanomachinery: pivotal role of the filament barbed end. *Cell* 118: 363-373.
- Michelot A, Berro J, Guérin C, Boujemaa-Paterski R, Staiger CJ, Martiel JL, Blanchoin L (2007) Actin-filament stochastic dynamics mediated by ADF/cofilin. *Curr Biol.* 17: 825-833.
- Millard TH, Dawson J, Machesky LM (2007) Characterisation of IRTKS, a novel IRSp53/MIM family actin regulator with distinct filament bundling properties. *J Cell Sci* 120: 1663-1672.
- Moeller MJ, Soofi A, Braun GS, Li X, Watzl C, Kriz W, Holzman LB (2004) Protocadherin FAT1 binds Ena/VASP proteins and is necessary for actin dynamics and cell polarization. *EMBO J* 23:3769-779.
- Mogilner, A., and Oster, G. (2003) Force generation by actin polymerization II: the elastic ratchet and tethered filaments. *Biophys J* 84: 1591-1605.
- Moseley JB, Goode BL (2005) Differential activities and regulation of *Saccharomyces cerevisiae* formin proteins Bni1 and Bnr1 by Bud6. *J Biol Chem* 280: 28023-28033.

- Moseley JB, Sagot I, Manning AL, Xu Y, Eck MJ, Pellman D, Goode BL (2004) A conserved mechanism for Bni1- and mDia1-induced actin assembly and dual regulation of Bni1 by Bud6 and profilin. *Mol Biol Cell* 15: 896-907.
- Mouneimne G, Soon L, DesMarais V, Sidani M, Song X, Yip SC, Ghosh M, Eddy R, Backer JM, Condeelis J (2004) Phospholipase C and cofilin are required for carcinoma cell directionality in response to EGF stimulation. *J Cell Biol* 166: 697-708.
- Mullins RD, Heuser JA, Pollard TD (1998) The interaction of Arp2/3 complex with actin: nucleation, high affinity pointed end capping, and formation of branching networks of filaments. *Proc Natl Acad Sci U S A* 95: 6181-6186.
- Mullins RD, Stafford WF, Pollard TD (1997) Structure, subunit topology, and actin-binding activity of the Arp2/3 complex from *Acanthamoeba*. *J Cell Biol* 136: 331-43.
- Naumanen P, Lappalainen P, Hotulainen P (2008) Mechanisms of actin stress fibre assembly. *J Microsc* 231: 446-454.
- Neidt EM, Scott BJ, Kovar DR (2009) Formin differentially utilizes profilin isoforms to rapidly assemble actin filaments. *J Biol Chem* 284: 673-84.
- Neidt EM, Skau CT, Kovar DR (2008) The cytokinesis formins from the nematode worm and fission yeast differentially mediate actin filament assembly. *J Biol Chem* 283: 23872-83.
- Nicholson-Dykstra SM, Higgs HN (2008) Arp2 depletion inhibits sheet-like protrusions but not linear protrusions of fibroblasts and lymphocytes. *Cell Motil Cytoskeleton* 65: 904-922.
- Niebuhr K, Ebel F, Frank R, Reinhard M, Domann E, Carl UD, Walter U, Gertler FB, Wehland J, Chakraborty T. (1997) A novel proline-rich motif present in ActA of *Listeria monocytogenes* and cytoskeletal proteins is the ligand for the EVH1 domain, a protein module present in the Ena/VASP family. *EMBO J* 16: 5433-44.
- Oda T, Iwasa M, Aihara T, Maéda Y, Narita A (2009) The nature of the globular- to fibrous-actin transition. *Nature* 457: 441-445.
- Otomo T, Otomo C, Tomchick DR, Machius M, Rosen MK (2005) Structural basis of Rho GTPase-mediated activation of the formin mDia1. *Mol Cell* 18: 273-281.
- Otomo T, Tomchick DR, Otomo C, Panchal SC, Machius M, Rosen MK (2005) Structural basis of actin filament nucleation and processive capping by a formin homology 2 domain. *Nature* 433: 488-494
- Pantaloni D, Carlier MF, Coué M, Lal AA, Brenner SL, Korn ED (1984) The critical concentration of actin in the presence of ATP increases with the number concentration of filaments and approaches the critical concentration of actin.ADP. *J Biol Chem* 259: 6274-6283.
- Pantaloni D, Hill TL, Carlier MF, Korn ED (1985) A model for actin polymerization and the kinetic effects of ATP hydrolysis. *Proc Natl Acad Sci U S A* 82: 7207-72011.
- Pantaloni D, Le Clairche C, Carlier MF (2001) Mechanism of actin-based motility. *Science* 292: 1502-1506.
- Pasic L, Kotova TI, Schafer DA (2008) Ena/VASP proteins capture actin filament barbed ends. *J Biol Chem* 283: 9814-9
- Paul AS, Pollard TD (2008) The role of the FH1 domain and profilin in formin-mediated actin-filament elongation and nucleation. *Curr Biol* 18: 9-19.
- Paul AS, Pollard TD (2009) Review of the mechanism of processive actin filament elongation by formins. *Cell Motil Cytoskeleton* 66: 606-617.
- Paunola E, Mattila PK, Lappalainen P (2002) WH2 domain: a small, versatile adapter for actin monomers. *FEBS Lett* 513: 92-97.
- Pavlov D, Muhlrad A, Cooper J, Wear M, Reisler E (2007) Actin filament severing by cofilin. *J Mol Biol* 365:1350-1358.
- Peng J, Wallar BJ, Flanders A, Swiatek PJ, Alberts AS (2003) Disruption of the Diaphanous-related formin Drf1 gene encoding mDia1 reveals a role for Drf3 as an effector for Cdc42. *Curr Biol* 13: 534-545.
- Plastino J, Olivier S, Sykes C (2004) Actin filaments align into hollow comets for rapid VASP-mediated propulsion. *Curr Biol* 14: 1766-1771.
- Pollard TD (1983) Measurement of rate constants for actin filament elongation in solution. *Anal Biochem* 134: 406-412.
- Pollard TD (1984) Polymerization of ADP-actin. *J Cell Biol* 99:769-777
- Pollard TD (1986) Rate constants for the reactions of ATP- and ADP-actin with the ends of actin filaments. *J Cell Biol* 103: 2747-2754.
- Pollard TD (2007) Regulation of actin filament assembly by Arp2/3 complex and formins. *Annu Rev Biophys Biomol Struct* 36: 451-477.

- Pollard TD, Blanchoin L, Mullins RD (2000) Molecular mechanisms controlling actin filament dynamics in nonmuscle cells. *Annu Rev Biophys Biomol Struct* 29: 545-576.
- Pollard TD, Borisy GG (2003) Cellular motility driven by assembly and disassembly of actin filaments. *Cell* 112: 453-465.
- Pollard TD, Mooseker MS (1981) Direct measurement of actin polymerization rate constants by electron microscopy of actin filaments nucleated by isolated microvillus cores. *J Cell Biol*. 88: 654-659.
- Pollard TD, Weeds AG (1984) The rate constant for ATP hydrolysis by polymerized actin. *FEBS Lett* 170:94-98.
- Pope BJ, Zierler-Gould KM, Kühne R, Weeds AG, Ball LJ (2004) Solution structure of human cofilin: actin binding, pH sensitivity, and relationship to actin-depolymerizing factor. *J Biol Chem* 279: 4840-4848.
- Popp D, Yamamoto A, Iwasa M, Maéda Y (2006) Direct visualization of actin nematic network formation and dynamics. *Biochem Biophys Res Commun* 351: 348-353
- Pring M, Evangelista M, Boone C, Yang C, Zigmund SH (2003) Mechanism of formin-induced nucleation of actin filaments. *Biochemistry* 42: 486-496.
- Prochniewicz E, Janson N, Thomas DD, De la Cruz EM (2005) Cofilin increases the torsional flexibility and dynamics of actin filaments. *J Mol Biol* 353:990-1000.
- Pruyne D, Evangelista M, Yang C, Bi E, Zigmund S, Bretscher A, Boone C (2002) Role of formins in actin assembly: nucleation and barbed-end association. *Science* 26:297612-297615.
- Qualmann B, Kessels MM (2009) New players in actin polymerization--WH2-domain-containing actin nucleators. *Trends Cell Biol* 19: 276-285.
- Quinlan ME, Heuser JE, Kerkhoff E, Mullins RD (2005) Drosophila Spire is an actin nucleation factor. *Nature*. 43:382-388.
- Quinlan ME, Hilgert S, Bedrossian A, Mullins RD, Kerkhoff E (2007) Regulatory interactions between two actin nucleators, Spire and Cappuccino. *J Cell Biol* 179: 117-128.
- Quinlan ME, Kerkhoff E (2008) Actin nucleation: bacteria get in-Spired. *Nat Cell Biol* 10:13-5.
- Rebowski G, Boczkowska M, Hayes DB, Guo L, Irving TC, Dominguez R (2008) X-ray scattering study of actin polymerization nuclei assembled by tandem W domains. *Proc Natl Acad Sci U S A*. 105: 10785-10790.
- Reinhard M, Giehl K, Abel K, Haffner C, Jarchau T, et al. (1995) The proline-rich focal adhesion and microfilament protein VASP is a ligand for profilins. *Embo J* 14: 1583-1589.
- Reinhard M, Halbrugge M, Scheer U, Wiegand C, Jockusch BM, et al. (1992) The 46/50 kDa phosphoprotein VASP purified from human platelets is a novel protein associated with actin filaments and focal contacts. *Embo J* 11: 2063-2070.
- Resch GP, Goldie KN, Hoenger A, Small JV (2002) Pure F-actin networks are distorted and branched by steps in the critical-point drying method. *J Struct Biol* 137: 305-312.
- Robinson RC, Turbedsky K, Kaiser DA, Marchand JB, Higgs HN, Choe S, Pollard TD (2001) Crystal structure of Arp2/3 complex. *Science* 294: 1679-1684.
- Rodal AA, Tetreault JW, Lappalainen P, Drubin DG, Amberg DC (1999) Aip1p interacts with cofilin to disassemble actin filaments. *J Cell Biol* 145: 1251-1264.
- Romero S, Didry D, Larquet E, Boisset N, Pantaloni D, Carlier MF (2007) How ATP hydrolysis controls filament assembly from profilin-actin: implication for formin processivity. *J Biol Chem* 282: 8435-8445.
- Romero S, Le Clainche C, Didry D, Egile C, Pantaloni D, et al. (2004) Formin is a processive motor that requires profilin to accelerate actin assembly and associated ATP hydrolysis. *Cell* 119: 419-429.
- Rose R, Weyand M, Lammers M, Ishizaki T, Ahmadian MR, Wittinghofer A (2005) Structural and mechanistic insights into the interaction between Rho and mammalian Dia. *Nature* 435:513-518.
- Rottner K, Behrendt B, Small JV, Wehland J (1999) VASP dynamics during lamellipodia protrusion. *Nat Cell Biol* 1: 321-322.
- Rottner K, Stradal TE, Wehland J (2005) Bacteria-host-cell interactions at the plasma membrane: stories on actin cytoskeleton subversion. *Dev Cell* 9: 3-17.
- Sagot I, Rodal AA, Moseley J, Goode BL, Pellman D (2002) An actin nucleation mechanism mediated by Bni1 and profilin. *Nat Cell Biol* 4: 626-631.
- Samarin S, Romero S, Kocks C, Didry D, Pantaloni D, et al. (2003) How VASP enhances actin-based motility. *J Cell Biol* 163: 131-142.
- Sarmiento C, Wang W, Dovas A, Yamaguchi H, Sidani M, El-Sibai M, Desmarais V, Holman HA, Kitchen S, Backer JM, Alberts A, Condeelis J (2008) WASP family members and formin proteins coordinate regulation of cell protrusions in carcinoma cells. *J Cell Biol* 180: 1245-1260.

- Schafer DA, Jennings PB, Cooper JA (1996) Dynamics of capping protein and actin assembly *in vitro*: uncapping barbed ends by polyphosphoinositides. *J Cell Biol* 135: 169-179.
- Schirenbeck A, Arasada R, Bretschneider T, Schleicher M, Faix J (2005b) Formins and VASPs may cooperate in the formation of filopodia. *Biochem Soc Trans* 33: 1256-1259.
- Schirenbeck A, Arasada R, Bretschneider T, Stradal TE, Schleicher M, et al. (2006) The bundling activity of vasodilator-stimulated phosphoprotein is required for filopodium formation. *Proc Natl Acad Sci U S A* 103: 7694-7699.
- Schirenbeck A, Bretschneider T, Arasada R, Schleicher M, Faix J (2005a) The Diaphanous-related formin dDia2 is required for the formation and maintenance of filopodia. *Nat Cell Bio* 7:619-625.
- Schleicher M, Jockusch BM (2008) Actin: its cumbersome pilgrimage through cellular compartments. *Histochem Cell Biol* 129:695-704.
- Schmauch C, Claussner S, Zöltzer H, Maniak M (2009) Targeting the actin-binding protein VASP to late endosomes induces the formation of giant actin aggregates. *Eur J Cell Bio* 88: 385-396.
- Schutt CE, Myslik JC, Rozycki MD, Goonesekere NC, Lindberg U (1993) The structure of crystalline profilin-beta-actin. *Nature* 365: 810-816.
- Scott RW, Olson MF (2007) LIM kinases: function, regulation and association with human disease. *J Mol Med* 85: 555-568.
- Sechi AS, Wehland J (2004) Ena/VASP proteins: multifunctional regulators of actin cytoskeleton dynamics. *Front Biosci* 9: 1294-1310.
- Skoble J, Auerbuch V, Goley ED, Welch MD, Portnoy DA (2001) Pivotal role of VASP in Arp2/3 complex-mediated actin nucleation, actin branch-formation, and *Listeria monocytogenes* motility. *J Cell Biol* 155: 89-100.
- Skoble J, Portnoy DA, Welch MD (2000) Three regions within ActA promote Arp2/3 complex-mediated actin nucleation and *Listeria monocytogenes* motility. *J Cell Biol* 150: 527-538.
- Small JV (1988) The actin cytoskeleton. *Electron Microsc Rev* 1: 155-174.
- Small JV, Auinger S, Nemethova M, Koestler S, Goldie KN, Hoenger A, Resch GP (2008) Unravelling the structure of the lamellipodium. *J Microsc* 231: 479-485.
- Small JV, Stradal T, Vignal E, Rottner K (2002) The lamellipodium: where motility begins. *Trends Cell Biol* 12: 112-120.
- Steffen A, Faix J, Resch GP, Linkner J, Wehland J, Small JV, Rottner K, Stradal TE (2006) Filopodia formation in the absence of functional WAVE- and Arp2/3-complexes. *Mol Biol Cell* 17: 2581-2591.
- Sutherland JD, Way M (2002) Looking over the edge: a new role for Ena/VASP proteins in lamellipodial dynamics. *Dev Cell* 2: 692-694.
- Svitkina TM, Borisy GG (1999) Arp2/3 complex and actin depolymerizing factor/cofilin in dendritic organization and treadmilling of actin filament array in lamellipodia. *J Cell Biol* 145: 1009-1026.
- Svitkina TM, Bulanova EA, Chaga OY, Vignjevic DM, Kojima S, et al. (2003) Mechanism of filopodia initiation by reorganization of a dendritic network. *J Cell Biol* 160: 409-421.
- Swan KA, Severson AF, Carter JC, Martin PR, Schnabel H, Schnabel R, Bowerman B (1998) *cyk-1*: a *C. elegans* FH gene required for a late step in embryonic cytokinesis. *J Cell Sci* 111: 2017-2027.
- Tam VC, Serruto D, Dziejman M, Briehner W, Mekalanos JJ (2007) A type III secretion system in *Vibrio cholerae* translocates a formin/spire hybrid-like actin nucleator to promote intestinal colonization. *Cell Host Microbe* 1: 95-107.
- Tolliday N, VerPlank L, Li R (2002) Rho1 directs formin-mediated actin ring assembly during budding yeast cytokinesis. *Curr Biol* 12: 1864-1870
- Tominaga T, Sahai E, Chardin P, McCormick F, Courtneidge SA, Alberts AS (2000) Diaphanous-related formins bridge Rho GTPase and Src tyrosine kinase signaling. *Mol Cell* 5:13-25.
- Trichet L, Sykes C, Plastino J. (2008) Relaxing the actin cytoskeleton for adhesion and movement with Ena/VASP. *J Cell Biol* 181: 19-25.
- Uruno T, Remmert K, Hammer JA 3rd (2006) CARMIL is a potent capping protein antagonist: identification of a conserved CARMIL domain that inhibits the activity of capping protein and uncaps capped actin filaments. *J Biol Chem* 281: 10635-10660.
- Van Troys M, Huyck L, Leyman S, Dhaese S, Vandekerckhove J, Ampe C (2008) Ins and outs of ADF/cofilin activity and regulation. *Eur J Cell Biol* 87: 649-667.
- Vandekerckhove J, Weber K (1978) Mammalian cytoplasmic actins are the products of at least two genes and differ in primary structure in at least 25 identified positions from skeletal muscle actins. *Proc Natl Acad Sci U S A* 75: 1106-1110.

- Vasioukhin V, Bauer C, Yin M, Fuchs E (2000) Directed actin polymerization is the driving force for epithelial cell-cell adhesion. *Cell* 100: 209-219.
- Vavylonis D, Kovar DR, O'Shaughnessy B, Pollard TD (2006) Model of formin-associated actin filament elongation. *Mol Cell* 21: 455-466.
- Vinson VK, De La Cruz EM, Higgs HN, Pollard TD (1998) Interactions of Acanthamoeba profilin with actin and nucleotides bound to actin. *Biochemistry* 37: 10871-10880.
- Volkman N, Amann KJ, Stoilova-McPhie S, Egile C, Winter DC, Hazelwood L, Heuser JE, Li R, Pollard TD, Hanein D (2001) Structure of Arp2/3 complex in its activated state and in actin filament branch junctions. *Science* 293: 2456-2459.
- Walders-Harbeck B, Khaitlina SY, Hinssen H, Jockusch BM, Illenberger S (2002) The vasodilator-stimulated phosphoprotein promotes actin polymerisation through direct binding to monomeric actin. *FEBS Lett* 529: 275-280.
- Walter U, Eigenthaler M, Geiger J, Reinhard M (1993) Role of cyclic nucleotide-dependent protein kinases and their common substrate VASP in the regulation of human platelets. *Adv Exp Med Biol* 344: 237-249.
- Watanabe N, Kato T, Fujita A, Ishizaki T, Narumiya S (1999) Cooperation between mDia1 and ROCK in Rho-induced actin reorganization. *Nat Cell Biol* 1: 136-143.
- Watanabe N, Madaule P, Reid T, Ishizaki T, Watanabe G, et al. (1997) p140mDia, a mammalian homolog of Drosophila diaphanous, is a target protein for Rho small GTPase and is a ligand for profilin. *Embo J* 16: 3044-3056.
- Welch MD, DePace AH, Verma S, Iwamatsu A, Mitchison TJ (1997a) The human Arp2/3 complex is composed of evolutionarily conserved subunits and is localized to cellular regions of dynamic actin filament assembly. *J Cell Biol* 138: 375-384.
- Welch MD, Iwamatsu A, Mitchison TJ (1997b) Actin polymerization is induced by Arp2/3 protein complex at the surface of Listeria monocytogenes. *Nature* 385: 265-269.
- Welch MD, Rosenblatt J, Skoble J, Portnoy DA, Mitchison TJ (1998) Interaction of human Arp2/3 complex and the Listeria monocytogenes ActA protein in actin filament nucleation. *Science* 281: 105-108.
- Wiesner S, Helfer E, Didry D, Ducouret G, Lafuma F, Carlier MF, Pantaloni D (2003) A biomimetic motility assay provides insight into the mechanism of actin-based motility. *J Cell Biol* 160: 387-398.
- Xu Y, Moseley JB, Sagot I, Poy F, Pellman D, Goode BL, Eck MJ (2004) Crystal structures of a Formin Homology-2 domain reveal a tethered dimer architecture. *Cell* 116: 711-723.
- Yanagida T, Nakase M, Nishiyama K, Oosawa F (1984) Direct observation of motion of single F-actin filaments in the presence of myosin. *Nature* 307: 58-60.
- Yang C, Czech L, Gerboth S, Kojima S, Scita G, Svitkina T (2007) Novel roles of formin mDia2 in lamellipodia and filopodia formation in motile cells. *PLoS Biol* 5: e317.
- Zaidel-Bar R, Ballestrem C, Kam Z, Geiger B (2003) Early molecular events in the assembly of matrix adhesions at the leading edge of migrating cells. *J Cell Sci* 116:4605-4613.
- Zigmond SH, Evangelista M, Boone C, Yang C, Dar AC, Sicheri F, Forkey J, Pring M (2003) Formin leaky cap allows elongation in the presence of tight capping proteins. *Curr Biol* 13: 1820-1823.
- Zuchero JB, Coutts AS, Quinlan ME, Thangue NB, Mullins RD (2009) p53-cofactor JMY is a multifunctional actin nucleation factor. *Nat Cell Biol* 11: 451-459.

Curriculum vitae

Persönliche Daten:

Name: Dennis Breitsprecher
Adresse: Sporlederweg 7
30449 Hannover
Geburtstag und -ort: 01.03.1981 in Einbeck
Familienstand: verheiratet, 1 Sohn (0)

Schulische Ausbildung:

1987-1991 Grundschule Dassel
1991-1993 Wilhelm-Busch Schule Dassel
1993-2000 Paul-Gerhardt Gymnasium Dassel
01.07.2000 Abitur

Zivildienst:

08.2000-07.2001 Kreisjugenddienst Einbeck

Studium:

2001-2007 Biochemie, Leibniz-Universität Hannover,
Abschluss Diplom-Biochemiker.
10.2006-03.2007 Diplomarbeit „Einzelmolekülmessung Formin-
vermittelter Aktinpolymerisation durch TIRF Mikroskopie“ in der AG
Faix am Institut für Biophysikalische Chemie, Medizinische
Hochschule Hannover.
03.2007 – 05.2010 Promotion zum Thema „Molecular mechanism of
actin filament elongation by Ena/VASP proteins“ in der AG Faix am
Institut für Biophysikalische Chemie, Medizinische Hochschule
Hannover.

Publications and presentations

Publications:

Breitsprecher, D., Kieseletter, A.K., Linkner, J., Urbanke, C., Resch, G. P., Small, J. V. & Faix, J. (2008). Clustering of VASP actively drives processive, WH2 domain-mediated actin filament elongation. *Embo J.*

Lai, F. P., Szczodrak, M., Block, J., Faix, J., **Breitsprecher, D.**, Mannherz, H. G., Stradal, T. E., Dunn, G. A., Small, J. V. & Rottner, K. (2008). Arp2/3 complex interactions and actin network turnover in lamellipodia. *Embo J.*

Faix, J., **Breitsprecher, D.**, Stradal, T.E.B., Rottner, K. (2009). Filopodia: Complex models for simple rods. *International Journal of Biochemistry and Cell Biology.*

Breitsprecher, D., Kieseletter, A.K., Linkner J., Faix J. (2009). Analysis of actin assembly by *in vitro* TIRF microscopy. *Methods in Molecular Biology. Humana Press.*

Breitsprecher, D., Faix J. (2010). The inverted formin INF2 sorts it out. *Dev Cell.*

Ramalingam, N., Zhao, H., **Breitsprecher, D.**, Lappalainen, P., Faix, J., Schleicher, M. (2010) Phospholipids regulate localization and activity of mDia1 formin. *European Journal of Cell Biology* (in press).

Breitsprecher, D., Kieseletter, A.K., Linkner, J., Vinzenz, M., Stradal, T.E.B., Small, J.V., Curth U., Faix J. (2010). Affinity-based mechanism of Ena/VASP-mediated actin filament elongation (manuscript in preparation).

Talks and Poster presentations:

Poster: "Clustering of VASP Actively Promotes Processive, WH2-Domain-mediated Actin Filament Elongation." **D.Breitsprecher**, , A. K. Kieseletter, J. Linkner, C. Urbanke, G. P. Resch, J. V. Small and J. Faix,. *ASCB meeting 2008.*

Poster: "High affinity WH2 domain/G-actin interactions reveal the molecular basis for fast VASP-mediated actin assembly." **D. Breitsprecher**, A.K. Kieseletter, U. Curth, and J. Faix *ASCB meeting 2009.*

Poster: "Differential Regulation of mDia Formins by Phospholipids." N. Ramalingam, **D. Breitsprecher**, J. Faix, M. Schleicher. *ASCB meeting 2008.*

Talk: "Dissection of VASP-mediated actin assembly". 22.06.2009. MPI for Biochemistry Martinsried, Cell Dynamics and Cell Patterning group, Roland Wedlich-Söldner.

Talk: "Molecular mechanism of VASP-mediated actin assembly." 13.12.2009. Brandeis University, Waltham (MA). Cytoskeletal Assembly and Dynamics group, Bruce L. Goode.